Summer 8-11-2011

Assessment of Watershed Model Simplification and Potential Application in Small Ungaged Watersheds: A Case Study of Big Creek, Atlanta, GA

Zoia A. Comarova Ms
Georgia State University

ASSESSMENT OF WATERSHED MODEL SIMPLIFICATION AND POTENTIAL APPLICATION IN SMALL UNGAGED WATERSHEDS: A CASE STUDY OF BIG CREEK, ATLANTA, GA

by

ZOIA COMAROVA

Under the Direction of Jordan A. Clayton

ABSTRACT

Technological and methodological advances of the past few decades have provided hydrologists with advanced and increasingly complex hydrological models. These models improve our ability to simulate hydrological systems, but they also require a lot of detailed input data and, therefore, have a limited applicability in locations with poor data availability. From a case study of Big Creek watershed, a 186.4 km^2 urbanizing watershed in Atlanta, GA, for which continuous flow data are available since 1960, this project investigates the relationship between model complexity, data availability and predictive performance in order to provide reliability factors for the use of reduced complexity models in areas with limited data availability, such as small ungaged

watersheds in similar environments. My hope is to identify ways to increase model efficiency without sacrificing significant model reliability that will be transferable to ungaged watersheds.

INDEX WORDS: Hydrological model, Ungaged watershed, Sensitivity, Model complexity

ASSESSMENT OF WATERSHED MODEL SIMPLIFICATION AND POTENTIAL APPLICATION IN SMALL UNGAGED WATERSHEDS: A CASE STUDY OF BIG CREEK, ATLANTA, GA

by

ZOIA COMAROVA

A Thesis Submitted in Partial Fulfillment of the Requirements for the Degree of

Master of Arts

in the College of Arts and Sciences

Georgia State University

2011

ASSESSMENT OF WATERSHED MODEL SIMPLIFICATION AND POTENTIAL APPLICATION IN SMALL UNGAGED WATERSHEDS: A CASE STUDY OF BIG CREEK, ATLANTA, GA

by

ZOIA COMAROVA

Committee Chair: Jordan A. Clayton

Committee: Jeremy Diem

Dajun Dai

Brian Watson

Electronic Version Approved:

Office of Graduate Studies

College of Arts and Sciences

Georgia State University

August 2011

To Comarov Family

ACKNOWLEDGEMENTS

I would like to thank my advisor Jordan Clayton for his encouragement and constant support over the past three years of my graduate studies at Georgia State University (GSU). This thesis would not have done without his guidelines, patience and motivation. For helping to guide this research and provide exceptional feedback and encouragement, I thank my graduate committee members: Brian Watson, Jeremy Diem and Dajun Dai. Thank you to the great Tetra Tech office in Atlanta for teaching me the science in practice, help with running my experiments and providing an exceptional moral support through my 'academic journey'.

To all my colleagues and professors in the department of Geosciences of GSU: thank you for making this department my second home and a greatest working environment ever.

My friends in the US and back home in Moldova are a part of energy that has fueled this research. Helen Mayoral has been one of my devoted companions from the coffee breaks and homework assignments, through the maze of field work, and on the dance floor. Thank you for keeping me balanced.

Finally I shout out to my adorable family: to my husband for his endless love, patience and support while starting our new life in the US, being students; for cooking, taking care of the house, making me smile and never doubting commitment to my completion of this degree. Thank you to my Mama and Papa, for raising me to be a woman with honesty, persistence, love and creativity; I feel your love and care being on the other side of the ocean.

Last, but not the least, I would like to thank the Lord who brought me to the tropics of Atlanta and told to survive. I did, and became stronger, and He has always been in my heart.

TABLE OF CONTENTS

LIST OF TABLES

LIST OF FIGURES

LIST OF ACRONYMS

CN – Curve Number

DEM – Digital Elevation Model

EPA – Environmental Protection Agency

GIS – Geographic Information Systems

HecHMS - Hydrologic Engineering Center Hydrologic Modeling System

HRU - Hydrological Response Units

HSPF - Hydrologic Simulation Program FORTRAN

HUC 12 - USGS 12 digit hydrological cataloging unit data layer

LSPC - Loading Simulation Program in C++

L-THIA - Long – Term Hydrologic Impact Assessment Model

NCGC - National Cartography and Geospatial Center

NED - National Elevation Dataset

NHD - National Hydrography Dataset

SCS – Soils Conservation Service

SHE - European Hydrological System model

SSURGO – Soil Survey Geographic Database

SWAT – Soil and Water Assessment Tool

TOPMODEL - TOPography-based hydrological MODEL

TR-55 – Technical Report 55

USACE – United States Army Corps of Engineers

USGS – United States Geological Survey

1 INTRODUCTION

Methodological and technological progress of the past two decades strongly facilitated observational and computational abilities of hydrological models (Sivakumar 2004; McDonnell et al. 2007; Wood et al. 2011). Remote sensing (RS) imagery of a higher resolution, advanced geographical informational tools (e.g., ARC Hydro tool in GIS) and more powerful computers have provided more accurate data collection, more efficient data processing, and better data sharing that overall facilitate a greater ability to imitate the real world and to model complete pathways of hydrological systems than was previously possible (Vieux 2004; Chen et al. 2007; McDonnell et al. 2007). Commonly-employed hydrological models such as TOPMODEL (Beven and Kirkby 1979) and the Soil Water Assessment Tool (SWAT) (Arnold et al.1998) use straightforward RS and GIS tools to translate historical satellite images into a land cover time series and to produce hydrological variables with a sense of realism in the land cover change.

While these developments are indeed encouraging, recent studies demonstrate that there are certain challenges related to hydrologic distributed models. For instance, Weiler and McDonnell (2007) argue that the current generation of detailed models produce results that may be in contradiction with known hydrological laws, such as Darcy or Richards equations. Sivakumar (2008) claims that comprehensive models require enormous amounts of data, which are often not available in data poor environments (e.g. Africa, south-east Asia). In McDonnell et al. (2007) it is hypothesized that landscape change over time due to climate change further exacerbates the rate of model error and is related to the uncertainty of the input parameters. All these remarks reveal interesting difficulties facing the current generation of sophisticated hydrological models and underscore the question raised by many hydrologists since the 1990s (Jakeman and

Hornberger 1993; Grayson and Blöschl 2001; Sivapalan et al. 2003; McDonnell et al. 2007), which is: *How much complexity is warranted in a hydrological model so that it does not require enormous amounts of generally unavailable data and is still realistic and useful in conditions of changing landscape and climate*? In this study the term "model complexity" indicates the degree of detailed real-world representation of simulated hydrologic processes and therefore, of the modeling input parameters. A complex model has more parameters in the input data set and/or has data of a higher density (resolution). To answer the question stated above, one should first critically examine the existing modeling practices and the model complexity associated with each type of model.

1.1 Lumped vs. Distributed Models

Most hydrologic models that are used by industry and science nowadays (Soil and Water Assessment Tool (SWAT), Hydrologic Simulation Program Fortran (HSPF), Loading Simulation Program in C++ (LSPC)) are based on the conceptual mathematical or physical equations that relate processes and phases of the hydrological cycle. These models belong to the group of the deterministic models (Fig. 1.1).

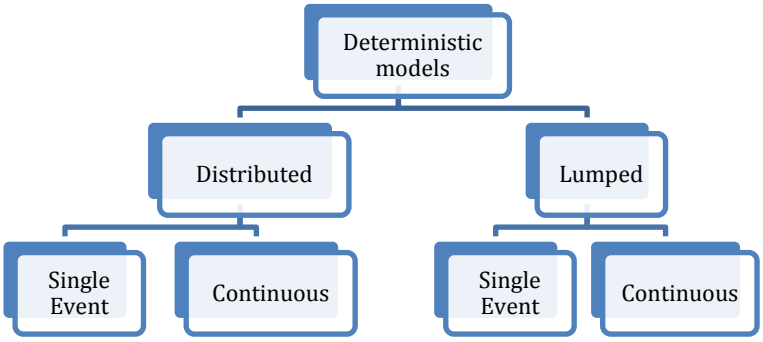

Figure 1.1 Classification of deterministic models according to distributed versus lumped treatment (modified from Vieux, 2004).

There is a well-known hydrologic tradeoff between simple lumped models that do not describe watershed characteristics in detail, and more complex distributed conceptual models that have a stronger theoretical foundation and require the input of detailed data sets (Jakeman and Hornberger 1993; Grayson and Blöschl 2001; Tague and Pohl-Costello 2008). Lumped models suggest that spatial variability of the watershed characteristics and hydrological processes are not significant enough to warrant explicit inclusion in the model and therefore imply that average values of the watershed elements are uniformly distributed throughout the watershed and provide sufficient precision (Vieux 2004). Simulation of the water budget is linked to the topographical, geological, and meteorological characteristics through the lumped coefficients. For example, the Soil Conservation Service (SCS) method uses Curve Numbers (CN) that quantitatively describe soil and land cover classes and link runoff with land use characteristics (Weng 2001; Zhan and Huang 2004). Hence, the model's accuracy depends directly on how well the available data reflects the field conditions, and how close the lumped values (i.e., CN's) are to the average values of the watershed characteristics. However, lumped models calculate the water balance by the equation of continuity that does not account for the within-watershed interactions between important hydrological controls of runoff generation; such as topography, antecedent moisture, and vegetation within the spatially heterogeneous watersheds (Beven 2000; Tague and Pohl-Costello 2008). Despite these limitations, the coefficient-based approach is attractive to the users because of its simplicity and flexibility. A wide range of lumped models such as TR-55, HecHMS (U.S. Army Corp of Engineers 2006), L-THIA (Bhaduri et al. 2000) are used in both science and industry to assess water resources in small watersheds, analyze water balances, and fill in historically missing data. Lumped hydrological models have become particularly popular during the last decade by being integrated with geographi-

cal informational systems and remote sensing that reduce the processing time for calculation of the hydrologic variables; such as surface runoff, from days, if not weeks, to hours (Mendoza et al. 2002; Zhan and Huang 2004). The ArcCN Runoff tool, an extension of the ESRI ArcGIS software, finds curve numbers based on the land use input file and automatically calculates the runoff or infiltration for any storm event (Zhan and Huang 2004). This approach is conceptually simple (e.g., the percentage of the rainfall contributing to the runoff is solely a function of the land-use type), easy to use, available for free on the web, and does not require a sophisticated understanding of hydrological processes, all of which make it an attractive tool for watershed managers and planners. Overall, the fact that lumped models such as L-THIA (Bhaduri et al. 2000) and hydrologic tools as ARC-Hydro (Maidment 2002) and CN Runoff (Zhan and Huang 2004) are broadly promoted by such agencies as Environmental Protection Agency (USEPA), the U.S. Geological Survey (USGS) and the U.S. Army Corp of Engineers (USACE), means that they will continue to be in use.

On the other hand, there are distributed hydrological models that take into account the spatial variability of the watershed characteristics, hydrologic variables, and boundary conditions (Grayson and Blöschl 2001; Vieux 2004) and, therefore, are considered more complex than lumped models. These typically subdivide the watershed into a series of hydrologically-similar zones, termed Hydrological Response Units (HRUs) (Blöschl et al. 1995). HRUs, similar to watersheds in the lumped models, are homogeneous subareas of the watershed with an individual hydrologic response based on combinations of the watershed characteristics; such as soil type, land cover, and topography. Given the uniqueness of the HRUs characteristics, a separate set of parameters is assigned to each unit and a water balance is calculated. The runoff in each HRU is then routed one to another based on the HRUs slope, and the total hydrologic yield

is presented in the output. Due to the spatial variability of the parameters, the hydrologic processes in the distributed models also vary according to the land use, climate and other drivers that, overall, results in a greater ability to mimic hydrologic systems and to monitor the effects of the watershed characteristics changing in space and time. Models that are topographically-based, e.g. TOPOG and TOPMODEL (Beven 2000), simulate spatially variable hydrological processes in water balance: storage and transport of water at the surface and subsurface level of the watershed. Limitations of the distributed models include both the need for large and detailed data that may not be fully available in data poor regions (Sivakumar 2008), and sophisticated skills and tools required to run the models (Abbott and Refsgaard 1996; Bertrand-Krajewski et al. 2000). For example, the new version of the European Hydrological System model (SHE) involves substantial input requirements and computational processes that limit application on machines other than mainframe computers.

In order to overcome difficulties faced with both types of the models, researchers combine lumped model parameters with the distributed computational principles. As a result, there are semi-distributed models (e.g. Hydrological Model Application System (Hughes and Sami 1994)) that require lumped input data (such as the consideration of only one precipitation gage in a watershed), and treat rainfall-runoff processes in a distributed way (according to the HRUs distinct characteristics) (Beven 2000; Vieux 2004). Solomatine and Wagener (2011) suggested that the hydrological processes related to surface water are more complex than those for subsurface water, and therefore semi-distributed models may be better suited for groundwater simulations. It is also unclear whether lumped input parameters of the semi-distributed models provide enough heterogeneity for the hydrologic variables at the catchment scale (small, medium, large).

Another way to overcome the problem of over-parameterization of the distributed hydrologic models is to explore what input data and at what resolution can predict runoff with the least error. In order to identify the minimum quantitative and qualitative requirements for the input data, the basic relation between the complexity, data availability, and performance of the distributed models has to be explored. The term "data availability" is used in this study to imply both quality and quantity of the available data. Thus, having an incomplete dataset or data of lower resolution is equivalent to limited data availability, whereas having data of the full pattern implies ''large'' availability of the data.

1.2 On the discussion of model complexity

"Something is better than nothing,
but nothing is better than nonsense"
Sivakumar, 2008

One conceptual relationship between model complexity, data availability and predictive performance is illustrated in Figure 1.2. It reveals that model performance, in general, increases with data availability and that complex models require large amounts of data (Grayson and Blöschl 2001); as well as demonstrates that for limited data availability the models with moderate complexity may perform better than very complex models. The reason for this is that the uncertainty of model predictions (the opposite of the predictive performance axis in Figure 1.2) consists of two terms: (1) the parameter uncertainty which increases with model complexity because of an increasing number of parameters; and (2) the model structure uncertainty which decreases with model complexity. Therefore, for a model of given complexity (dotted line) an increasing data availability (bold line) leads to a better model performance up to a certain point, where more data would not improve the accuracy of prediction. Therefore, every model has its maximum performance and adding more input data or increasing spatial density of the input parameters, does not necessarily improve the accuracy of prediction (Grayson and Blöschl 2001;

Fisher and Tate 2006). For example, Watson et al (1998) demonstrated that use of Digital Elevation Models (DEMs) of coarser resolution does not necessarily degrade the modeling accuracy at scales of small catchments. Hypothetically the relation between the accuracy of model performance and the resolution of available data, as addressed in this study, can be illustrated by Figure 1.3. The model uncertainty is decreasing with the increase in data density up to point of optimal data density, which is the minimum data that is required for a defined accuracy of model performance. Collection of data at the point of optimal density, as opposed to data of higher densities, may help to efficiently allocate the data resources and to apply the model in data poor regions of the world.

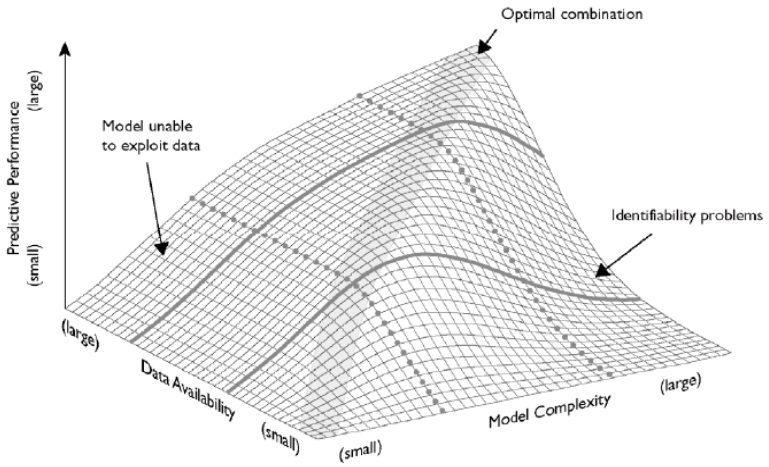

Figure 1.2 Schematic diagram of the relationship between model complexity, data availability and predictive performance (from Grayson and Blöschl, 2000)

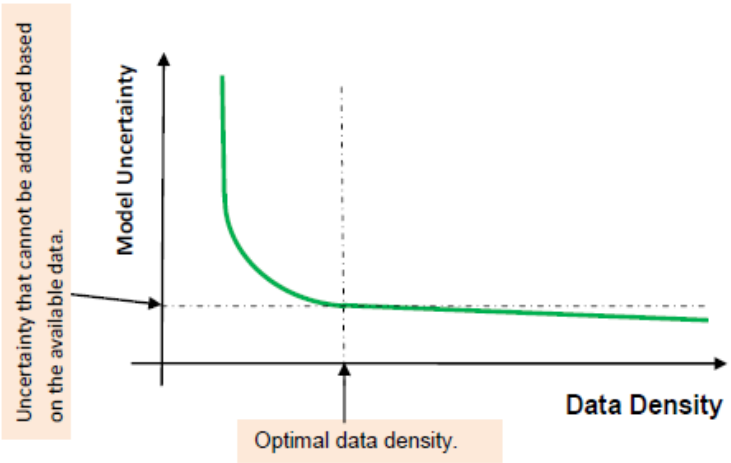

Figure 1.3 Hypothetical relationship between density of the input data and uncertainty of the output data (from Zajac, 2010)

1.3 Problem statement

Regardless of technological advances and our better ability to mimic the real world, as discussed in Chapter 1.1, the major difficulties that hydrological modelers face nowadays are related to applying distributed models to ungaged watersheds. The problem is analogous to an ancient Indian legend, where people were trying to reproduce an image of the entire elephant by approaching it from different sides (Saxe 1963; Sivapalan et al.2003). They could not create a true representation of the elephant with incomplete data that was available from different perspectives (Figure 1.4).

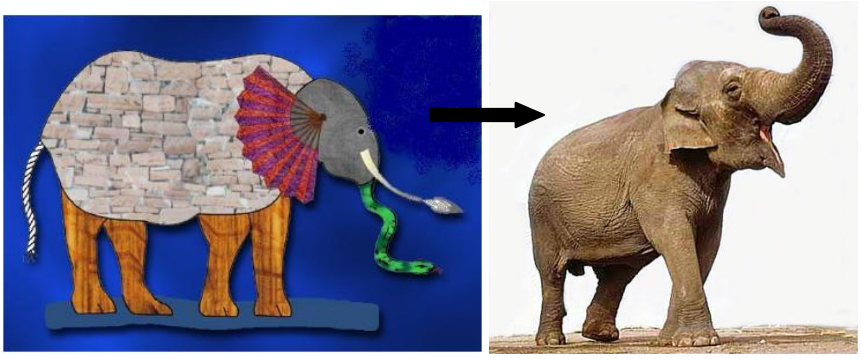

Figure 1.4 Uncertain representation of the elephant due to incomplete data available from different perspectives is analogous to incomplete/inadequate input data from ungaged watersheds (modified from Sivapalan et al. 2003)

The problem of the elephant representation is analogous to the ungaged watersheds where incomplete climatic, geologic, topographic records preclude hydrologic modeling at the required spatial and temporal scales (Sivapalan et al. 2003). If input variables do not provide the level of detail required by the model, the data density decreases and according to the hypothetical relation between data density and model predictive uncertainty (illustrated in Figure 1.3), the model predictive uncertainty increases. Thus, analogous to the elephant's representation, distributed hydrological models demand multiple input variables and in conditions of limited data availability (ungaged watersheds), a true representation of reality is possible only if the point of

optimal data density is reached (Figure 1.3). One could argue that incomplete/inadequate records in ungaged watersheds could be managed by transferring data from a similar gaged environment, or by extrapolating the available data. However, due to spatial and temporal variability of topographic, geologic and climatic properties of the watersheds, these traditional methods face significant uncertainties (Sivapalan 2003). Metaphorically speaking, the assumption that the elephant of interest can be represented by an elephant from a similar environment implies uncertainties related to the uniqueness of each of the elephants. Therefore, when reproducing an image of the entire elephant (hydrologic modeling of a watershed) by approaching it from different sides (ungaged conditions), one would find the best perspective (model complexity) from where the most important elements are available (data of the optimal density), instead of focusing on data transfer or data extrapolation. Hence, accurate modeling in ungaged watersheds demands a careful analysis of how much complexity is warranted in a distributed model so that it does not require enormous amounts of (often unavailable) data, while still remaining realistic and useful for both current conditions and for future landscape and climatic changes. The question remaining to be answered is how to simplify distributed models so that they are still complex enough to explain the spatial variability of the environment and provide users with accurate hydrologic predictions, but not overly complex in terms of the number and resolution of the input data usually available in ungaged conditions.

Despite the fact that uncertainty of hydrologic predictions in ungaged watersheds is a major concern in contemporary hydrological modeling (Sivakumar 2004), little work has been done to determine the optimal data density of distributed hydrological models without sacrificing significant model accuracy in the data poor environments. Former studies have mostly considered the uncertainty of each input parameter on their own and have, overall, insufficiently

examined the combined effects of several variables with decreased density within distributed models (Fisher and Tate, 2006).

1.4 Goal and objectives of the study

The goal of this study is to apply a distributed hydrological model to a small urbanizing watershed in the Atlanta metropolitan area where all model input data are available and to perform sensitivity analysis of the model's performance to the changing spatial scale of input parameters for a period of 10 years (1998-2007), in order to determine a minimum resolution required to reasonably match the simulated and the observed runoff.

Specific objectives are:

- To apply a distributed model (Loading Simulation Program in C++) that explicitly considers spatial variability of the topographical, meteorological, land use, and soils characteristics of an urbanizing watershed in order to better understand the contribution of the surface and subsurface flows to the water balance in the Big Creek watershed, Atlanta, Georgia (GA);
- To evaluate the effects of simplifying or eliminating the potentially influential input variables (land use coverage, watershed segmentation, soils coverage, meteorological data resolution, and complexity of the stream reach characteristics) on the predictive accuracy of the LSPC model;
- To determine what kind of rescaling/reduction of input variables most successfully predicts runoff with the least error.

Based on the objectives, the research question is stated as follows: *How can a distributed hydrologic model make use of the readily available meteorological and topographic data to si-*

mulate spatially distributed hydrological variables for the purpose of management of water resources in small urbanizing watersheds in environments similar to Atlanta?

The null hypothesis to be tested is that the model efficiency can be achieved by applying input spatial data of the reduced resolution without sacrificing significant model reliability.

2 LOADING SIMULATION PROGRAM C++ (LSPC)

2.1 Overview

Loading Simulation Program in C++ (LSPC) is a complex watershed model that estimates changes in hydrology, sediment transport, and general water quality based on rainfall-runoff simulation algorithms of the Hydrologic Simulation Program FORTRAN (HSPF) model (Bicknell et al. 1997). In order to improve the LSPC´s efficiency and flexibility, the original HSPF algorithms were implemented in the C++ programming language, incorporated with geographical information systems, enhanced with the data storage capacity, provided with a post processing analysis tool, and integrated in a user-friendly interface (USEPA and Tetra Tech, Inc. 2007). The LSPC combines simulation algorithms analogous to the ones in the HSPF model, technologically advanced management features, and highly adaptable user's design that overall ranks the model as one of "the most advanced hydrologic and watershed loading model tools available" (USEPA and Tetra Tech, Inc. 2007). Since this research is focused on a hydrologic mass balance simulation, the water quality components of the LSPC will be omitted, although the ability to model biogeochemical and ecological responses provides a great possibility for further studies of using LSPC for the evaluation of environmental management practices.

LSPC modeling processes have been applied to a number of catchments worldwide to examine the effects of spatial variability of land-use change (Mishra et al. 2007), rainfall (Ryu 2009), and climate change on streamflow and reservoir storage (Göncü and Albek 2009). These studies acknowledged the benefits of the LSPC simulating algorithms to be:

1) a cell-based representation of the land use segments and drainage channels;

2) ability to compute long-term streamflow hydrographs for the large watersheds, while maintaining a high level of detail (e.g. outputs of 1 minute to 1 day time scale);

3) ability to dynamically simulate flow for pervious and impervious land and water bodies of varying network orders.

However, no study has been performed dealing with streamflow simulations in the LSPC model where landscape and climate data are varying in spatial resolution (Ryu 2009). In order to explore how the input data density affects the simulated streamflow, a brief overview of the hydrologic portion of the LSPC model is provided below; a complete discussion of the LSPC parameters and processes may be found in the HSPF User's Manual (Bicknell et al. 1997).

2.2 Input requirements

The hydrologic components of the LSPC are based on the rainfall-runoff processes developed for the Stanford Watershed Model (Crawford and Linsley 1966). However, unlike other "pioneering" watershed models of that time that do not account for spatial variations of input parameters, the LSPC model considers the heterogeneity of rainfall and basin characteristics by dividing the watershed into a set of subbasins (Bicknell et al., 1997) and assigning water flows into a modular format (Chen et al. 2007; US EPA and Tetra Tech, Inc. 2007; Göncü and Albek

2009). Due to detailed spatial and temporal representation of hydrologic variables by LSPC, the demand for complete and continuous input data is substantial (e.g., continuous meterological files). The input data required by the LSPC are illustrated in Figure 2.1 and can be grouped in two categories (Göncü and Albek 2009):

(1) physical data (basin topography, stream reach dimensions, soils, land use), and

(2) meteorological data (precipitation, air temperature).

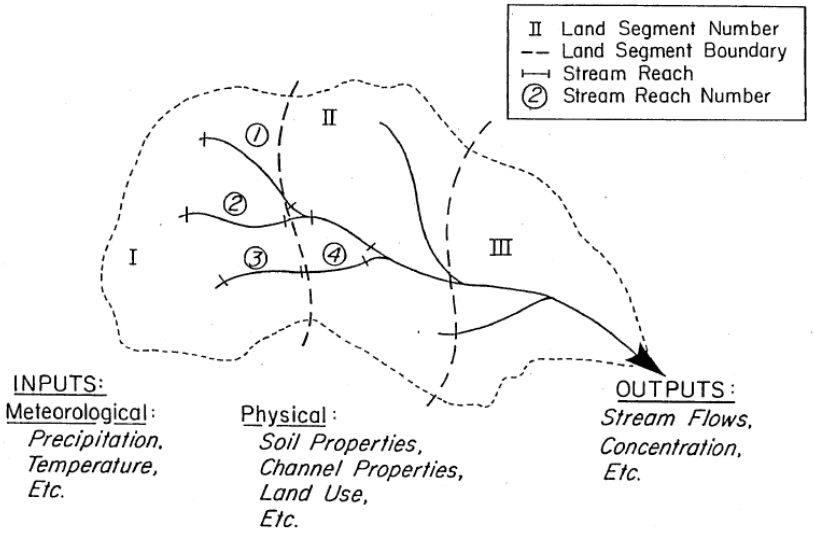

Figure 2.1 LSPC setup requirements for runoff simulation (from Aqua Terra Consultance, 2005)

Given the focus of this research on the sensitivity of the model to variations in scaling of input parameters available in ungaged environments, the following model input parameters are considered: (1) subbasin delineation; (2) meteorological records (precipitation, air temperature); (3) land use characteristics; (4) soils; and (5) stream channel cross-section geometry. A detailed discussion of these parameters from both physical and meteorological categories is further elaborated upon in Chapter 3 – Methods. The physical background of the simulated hydrologic components and their dependence on the input data is given more attention in the overview of the modeling approach (below). Numerical background of the parameters and processes in-

volved in the modeling may be found in more detail in the HSPF User's Manual (Bicknell et al. 1997).

2.3 LSPC Modeling Approach

The watershed of study is first spatially divided into a set of subbasins based on the topography, hydrography and availability of the gage stations (Figure 2.1), so that each subbasin represents the drainage area that contributes to a given reach (Figure 2.2). In order to account for spatial variability of natural watershed characteristics (topography, land use, and soil properties) each subbasin is refined into a series of hydrological response units (HRUs), which are the areas of homogeneous topography (elevation, slope), land use and soil characteristics, as discussed in Chapter 1.1. The hydraulic behavior is calculated in each HRU to generate subbasin and then watershed response. The calculation is done according to the water balance equation:

$$R = P - ET - IG - S \quad (1)$$

where: R is runoff (mm), P is precipitation (mm), ET is evapotranspiration (mm), IG is inactive groundwater(mm), and S is the change in soil water storage (mm).

After the hydrologic balance is simulated in each HRU, the water is transported via a reach network in order to generate a watershed response at the outlet of each subbasin. The hydrologic simulation has a modular structure (Mishra et al. 2007) with three major components: 1) PERLND - for modeling watershed processes on the pervious land areas; 2) IMPLND - for simulating hydrology on the impervious land areas; and 3) RCHRES - for estimating processes in the streams. The hydrologic budget of each HRU is simulated simultaneously in two modules: pervious (PWATER) and impervious (IWATER) components of the land surface and the soil columns. Each module includes a series of hydrologic processes (evaporation, transpiration, inflow, and outflow) and storage zones (vegetative, surface, shallow subsurface, and deep sub-

surface). Due to the more complex hydrologic nature of the pervious cover, the hydrologic behavior of PWATER is governed by a larger number of hydrologic processes and parameters than IWATER .The major processes and storages of the PWATER modeling components are schematically demonstrated in the Figure 2.3, and are summarized in the Table 2.1.

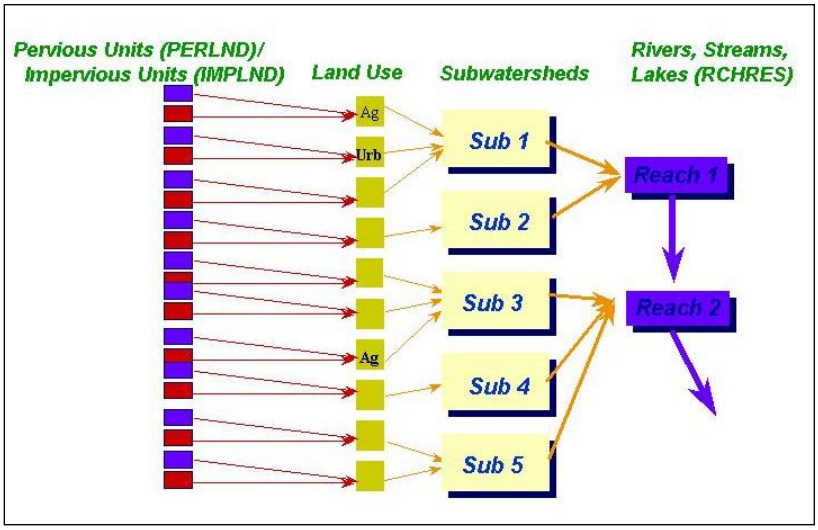

Figure 2.2 Model segmentation in LSPC (from USEPA, 2007)

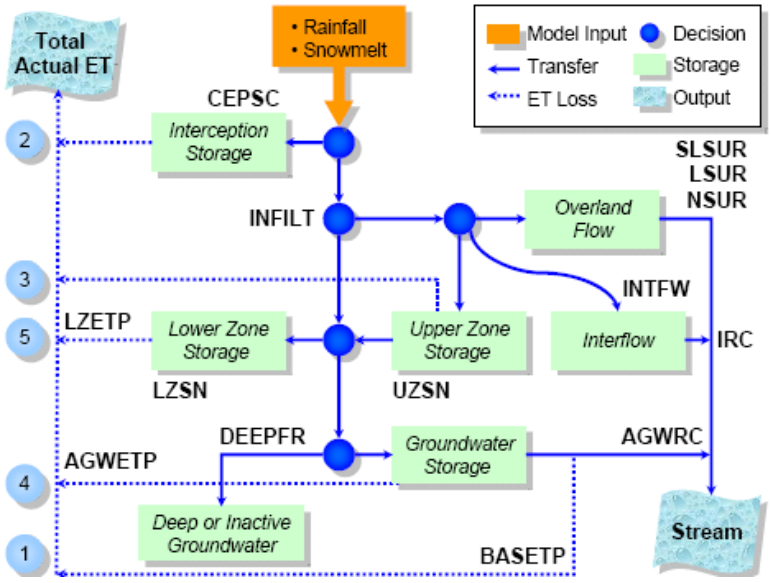

Figure 2.3 Schematic of water budget of the pervious land component (PWATER) according to the LSPC (from USEPA, 2007)

Precipitation, supplied to the upper-zone soil layer, first is subjected to interception (CEPSC). The rate of the vegetation-retained rainfall depends on the type of the vegetation present on a parcel of land and is provided by the user. After a portion of the incoming precipitation is intercepted, the water infiltration parameter (INFILT) gives the distribution of the remaining water. The water may infiltrate into the lower storage zone (LZSN), may be directed to the upper zone storage (UZSN), or distributed among the active groundwater storage (AGWRS), and inactive groundwater storage (DEEPFR). It may also remain in the surface detention storage as overland flow or runoff, or be routed to an interflow. Interflow pathways are activated when both the groundwater storage is saturated and the rate of precipitation equals the rate of infiltration. Water from the interflow storage is released to the stream using interflow recession constants (IRCs). The water from surface detention storage becomes overland flow when all the subsurface storages (LZETP, UZSN, AGWETP and DEEPFR) are saturated and/or when the rainfall rate exceeds the infiltration capacity of the soils. Slope (SLSUR), length (LSUR), and roughness (NSUR) of the overland flow paths determine the amount of the overland flow directed to the stream. Stored water in the upper-zone (UZSN) is first subjected to evapotranspiration and then is transported to the deeper subsurface through a delayed infiltration process. Water that was directed to the deeper ground is distributed among the lower-zone storage (LZSN), inactive groundwater storage, and active groundwater storage (AGWS). Water from the lower zone becomes subject to evapotranspiration (LZETP). Water is further allocated to the inactive groundwater storage based on the DEEPFR parameter and is lost from the simulated basin. The active ground water storage receives the infiltrated water from the UZSN or from the surface storage. Water in the active ground zone is either evaporated through the AGWETP parameter and/or transported to the stream through the active groundwater recession

constant AGWRC. Finally, the base flow is subjected to evapotranspiration (BASETP) prior to entering the stream channel.

The component that calculates the water budget of the impervious land segment (IMPLND) is the module IWATER. Similar to PWATER, the IWATER module has storage parameters (impervious surface and rooftop) and processes (evaporation and runoff) of the water cycle, which are assigned to each impervious HRU. However since there is no infiltration, which means the subsurface processes do not exist in this module, IWATER is less sophisticated than the PWATER module. The routing principles of the IWATER module are similar to the ones described in the PERLND module: rainfall is first intercepted by the impervious surfaces that are elevated above the land level (building tops, urban vegetation) through the impervious retention storage – RETS. This water is lost to the atmosphere through evaporation. The remaining water is directed into the surface-detention storage (SURS) and then is transported to the stream reach as a surface runoff. The overland flow is controlled by the length (LSUR), slope (SLSUR), and roughness (NSUR) of the overland flow path.

Overall, the hydrologic balance in LSPC is governed by storage and transport of precipitation along the overland flow, interflow and ground flow paths in PWATER, and the overland flow – in IWATER component. Given that water balance is simulated based on the HRUs response, the variables of the water budget are sensitive to spatial resolution of the input parameters (e.g. the ones that are more related to characteristics of the soils and land cover, etc). A summary of hydrologic variables that are used in the simulation of streamflow for pervious and impervious land cover and their relation to the input parameters is presented in Table 2.1.

Table 2.1 Hydrologic parameters used in the simulation of streamflow for pervious and impervious land cover components; (modified from Tetra Tech, 2010)
[ET - evapotranspiration; PET - potential evapotranspiration]

Parameter	Description	Unit
AGWETP	Active groundwater ET. Represents the fraction of stored ground water that is subject to direct evaporation and transpiration by plants whose roots extend below the active groundwater table. Accounts for the fraction of available PET that can be met from active groundwater storage.	none
AGWRC	Active groundwater recession rate. Represents the ratio of current groundwater discharge to that from 24 hours earlier.	1 per day
BASETP	Base flow ET. ET by riparian vegetation from active ground water entering the stream channel. Represents the fraction of PET that is fulfilled only as groundwater discharge is present.	none
CEPSC	Interception storage capacity of vegetation. Is related to type of vegetation present on a parcel of land.	inches
DEEPFR	Fraction of infiltrating water that is lost to deep aquifers. Represents the fraction of ground water that becomes inactive ground water and does not discharge to the modeled stream channel. Is related to geology and groundwater recharge.	none
INFEXP	Infiltration equation exponent. Is related to variability in soils.	none
INFILD	Ratio of maximum and mean soil-infiltration capacities. Is related to soils variability.	none
INFILT	Index to mean soil infiltration rate. INFILT governs the overall division of available moisture between surface and subsurface flow paths. High values of INFILT divert more water to the subsurface flow paths. Is a function of soil characteristics and land use.	inches per hour
INTFW	Interflow coefficient that governs the amount of water that enters the ground from surface detention storage. Is related to soils, topography and land use.	none
IRC	Interflow retention coefficient. Rate at which interflow is discharged from the upper-zone storage. Is related to soils topography and land use.	1 per day
KVARY	Groundwater recession flow parameter; describes nonlinear groundwater recession rate. Varies with season and groundwater levels.	1 per inch
LSUR	Length of the overland flow plane. Is related to the size of HRU.	feet
LZETP	Lower-zone evapotranspiration ET. Percentage of moisture in lower-zone storage that is subject to ET. Is related to vegetation type and root depth.	none
LZSN	Lower-zone nominal storage. Defines the storage capacity of the lower-unsaturated zone. Is related to both precipitation patterns and soil characteristics.	inches
NSUR	Surface roughness (Manning's n) of the overland flow plane. Is related to surface soil conditions.	none
RETS	Retention-storage capacity of impervious surfaces. Depends on land use.	inches
SLSUR	Average slope of the overland flow path. Is related to topography.	none
UZSN	Upper-zone normal storage. Defines the storage capacity of the upper-unsaturated zone. Is related to surface soil conditions and land use.	inches

From the hydraulic point of view, LSPC is a relatively simple water routing model, governing overland and channel flow by the kinematic wave form of St. Venant equations. These equations represent simplified forms of the continuity and momentum equation, with the assumption of one dimensional uniform flow.

The equation for continuity is:

$$\frac{\partial y}{\partial t} + \frac{\partial Q}{\partial x} = q \ (2)$$

where Q is the discharge per unit width of channel (m^3/s), A is the cross-sectional area (m^2), q is the lateral inflow per unit length (m^3/s per m), x is the space coordinate (m), and t is the time (s) (Singh 1996).

The equation of momentum:

$$g\frac{\partial y}{\partial x} + v\frac{\partial v}{\partial x} + \frac{\partial v}{\partial t} = g(i - j) \ (3)$$

Where, y is mean depth (m), v is x-component of mean velocity (m/s), i is average bottom slope (m/m), j is friction slope defined by the Manning equation (US Army Corp of Enginners 1993).

The overland and channel flows are routed according to equations 2 and 3 separately and then are combined, in order to preserve continuity of the system. The kinematic approach assumes that the dynamic portion in the momentum equation is neglected and the bed slope of the channel is equal to the friction slope:

$$i = j \ (4)$$

Under these conditions there is no significant backwater effect and so the discharge can be defined as a function of the depth of flow alone rather than the difference between bottom slope and friction slope. The discharge per unit length is therefore calculated as:

$$q = ay^b \ (5)$$

where q is discharge per unit length (cfs), y is flow depth (m), a and b - are kinematic waver routing parameters related to the channel cross-section shape and flow. Additionally, both over-land and channel flow are simplified by assigning homogeneous properties to the surfaces and reaches (for example, unique roughness parameter for a reach).

It is assumed that the overland flow is distributed over the area of each subbasin at a shallow depth until it reaches the stream reach and hence, overland portion of the flow is calculated combining equations 2, 3 and Manning's equation:

$$Q = \frac{k}{n} R^{\frac{2}{3}} S^{\frac{1}{3}} A \quad (6)$$

where: Q is discharge (m^s/s), n is Manning's coefficient of roughness, k is a conversion constant equal to 1.486 for U.S. customary units or 1.0 for SI units, R is hydraulic radius (m), S is the slope of the water surface (m/m), A is the cross-section area (m^2). Assuming a very shallow flow that has depth y_0, the hydraulic radius (R) and the area (A) are $(y_0 * 1)/1$ and $y_0 * 1$ respectively. Substituting the R and A values in equation 6, defines the original Manning's equation as function of Manning's n coefficient, flow depth and bed slope:

$$Q = \frac{k}{n} y_0^{\frac{5}{3}} S^{\frac{1}{3}} \quad (7)$$

where: Q is discharge (m^s/s), n is Manning's coefficient of roughness, k is a conversion constant equal to 1.486 for U.S. customary units or 1.0 for SI units, y_0 is depth of a shallow flow (m), S is the slope of the water surface (m/m).

The mechanics for overland flow from both pervious (PWATER) and impervious (IWATER) model components is governed by equation 7; but slope, and surface roughness differ between land use types. Thus, percent of imperviousness of the land types is an important factor for overland portion of the model. Impervious land uses are treated by LSPC as hydrolog-

ically effective areas and drain directly to the stream; pervious land use components are hydrologically ineffective and drain into pervious land types. For example, if rain falls on the impermeable road and then is routed to the lawn, the area is hydrologically ineffective.

After the overland flow is routed to the reach, it becomes part of the streamflow. LSPC represents reaches in RCHRES module as one dimensional, completely mixed, dynamic flow units. Each unit has an inflow from an upstream subbasin that includes components of water balance for both pervious (overland flow, interflow, and baseflow) and impervious (overland flow) portions of the watershed, as well as point sources entering through a single point; the outflows may leave the reach in multiple pathways. Given the details of the channel transect (width, depth, cross-sectional area, slope, and roughness), the relations among water depth, surface area, volume, and streamflow are developed for each reach. Surface area, volume, and streamflow information at given water depths are summarized in a function table (FTABLE) and are further used to simulate discharge in each reach for a given inflow. The streamflow is routed according to kinematic wave equations that combine continuity equation (equation 2) and simplified form of momentum equation (equation 3) so that the discharge is directly related to cross sectional area of the flow:

$$Q = aA^b \quad (8)$$

where Q is discharge (m^s/s), y is flow depth (m), A is cross-sectional area of flow (m^2), a and b are kinematic wave routing parameters related to the channel cross-section shape and flow.

.

3 STUDY AREA

The LSPC model was developed for watersheds of various scales: small, medium, or large (USEPA, 2007). However, certain hydrologic processes dominate at different watershed scales. In small drainage areas, infiltration and overland flow predominate and channel flow is less important. Small watersheds are also more sensitive to high-intensity, short-duration precipitation events than are large ones (Beven 2000). Since this research explores the sensitivity of the model to variations in spatial and temporal scales of the input data, it was decided to perform model runs on a small scale watershed. The selected basin for this research, Big Creek watershed located north of Atlanta, GA, has an area of 186 km^2 and continuous flow data since 1960. The watershed is located within the Piedmont physiographic province and is characterized by moderate hilly terrain underlain by crystalline, metamorphic rock (Rose and Peters 2001). The watershed straddles three counties — Cherokee, Forsyth and Fulton — with about 50 percent of the area sitting within Forsyth County. The area above the Roswell intake is located within the Georgia 400 Corridor, which is one of the most rapidly developing areas of Atlanta and the entire state of Georgia (Brashear et al. 2001). The watershed is experiencing intense, continuing growth pressures associated with land use changes that significantly impact water quality and water budgets of the area. According to Smucygz et al. (2010), impermeable cover in Big Creek watershed increased by 19.24 percent between 1984 and 2005 resulting in an 11.65 percent increase in event runoff in the watershed during that period. An urbanizing basin was deliberately selected to explore the sensitivity of the model to temporal variations in land use change. In addition to the goals of this research, finding the ideal data resolution for hydrologic modeling of the Big Creek watershed may be of interest to local governments in the state of Georgia that are seeking to address issues concerning watershed and stream protection with

regards to projected urbanization of the watershed, for example, by 2020 the developed area in the Big Creek watershed is projected to increase from 45 to 87 percent (Brashear et al. 2001).

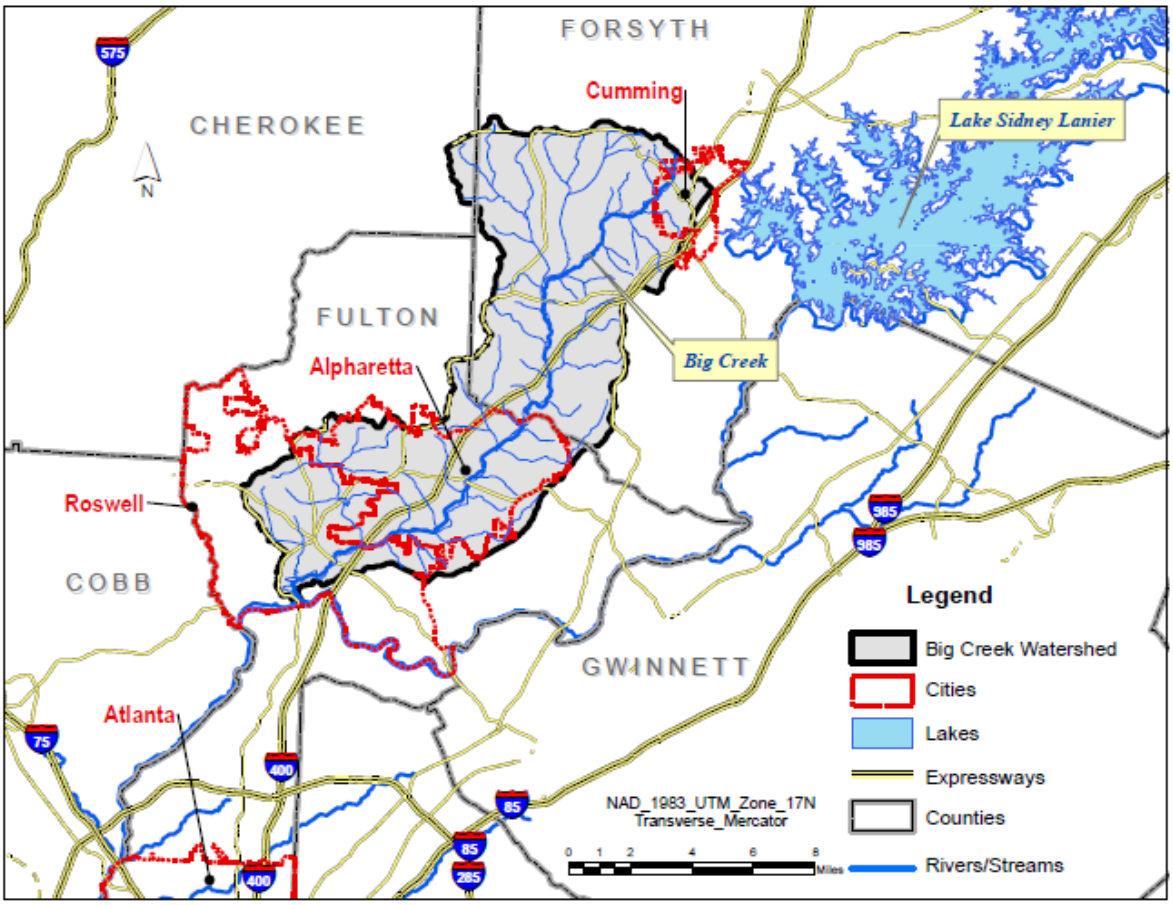

Figure 3.1 Big Creek Watershed, Location Map

4 METHODS

The LSPC model has been previously tested for its sensitivity to ranges of values of hydrological indexes and for uncertainties related to the calculation of nutrient loads (Tetra Tech, 2010). However, the assessment of minimum data requirements for land use coverage, watershed segmentation, soils coverage, meteorological data resolution, and complexity of stream reach characteristics, has not yet been addressed. In an effort to explore the relationship between

data availability, model complexity and predictive performance, this research attempts to determine the optimal data density for each of the parameters listed above. The optimal data density of these parameters are of specific interest since they may provide reliability factors for the use of LSPC with reduced complexity in areas with limited data availability.

In order to achieve the objectives listed in Section 1.4, the LSPC model was run for the Big Creek watershed for a 10 year period (1998-2007), using the following steps:

1. Both (a) the full range of available input parameters (land use coverage, watershed segmentation, soils coverage, meteorological data resolution, and complexity of stream reach characteristics) for the time period of interest, and (b) the measured event stream discharges at the USGS 02335700 Big Creek near Alpharetta, GA gage station were used to establish baseline conditions, defined herein as the baseline scenario.

2. For each input parameter, a reduced resolution of data, meant to replicate the data resolution that may be typical in ungaged watersheds, was defined (experimental scenarios). The LSPC was run for each combination of the reduced resolutions input parameters. Overall, given the five major input variables of LSPC listed above, and two variations (baseline and experimental) of each of the input parameters, $2^5=32$ permutations (runs) were required to evaluate the effect of input parameters on modeling accuracy.

3. To identify which combined reduction of input variable(s) predicts runoff with the least error, a sensitivity analysis was performed using dimensionless statistics, absolute error statistics, and graphical residual and outlier analysis (Arnold et al. 2007). After the sensitivity to each variable was compared, optimal data density for each of the parameters and a simpler model, transferrable to ungaged watersheds, was identified.

4.1 Watershed Segmentation

Topography is recognized to be a major control of the rainfall–runoff relation in a catchment (Brasington and Richards, 1998). In order to account for the spatial heterogeneity of Big Creek watershed's morphology, the basin was segmented into a series of subbasins homogenous from the topographic prospective: elevation and slope, in particular. The Digital Elevation Model (DEM) for the basin was downloaded from National Elevation Dataset (NED) in 1/3-arc-second resolution (30 m). It was observed that elevation of the northern part of Big Creek watershed is approximately 60 m higher than of the ones in the center and south of the watershed (Figure 4.1). To account for this topographic difference, a subbasin with the unique mean elevation of 345.4 m was delineated at the northern portion of the watershed (SWS nr 11 on Figure 4.1), while elevations of the central and southern subbasins varied from 262.2 m to 304.5 m. The subbasins delineated based on NED data were cross checked with the USGS 12-digit hydrologic cataloging units. According to USGS, the study area consisted of four (4) 12-digit Hydrologic Unit Codes (HUC's), as opposed to six (6) subbasins delineated because of the topographic differences observed from the NED. The stream network obtained from the National Hydrography Dataset (NHD) was used further as a guideline for delineations. It was observed, that the stream network is denser in the southern portions and, therefore, some smaller subbasins were delineated in that portion of the watershed, to capture the details stream channel network (Figure 4.1). The subbasins were finally checked with the location of three (3) US Geological Survey (USGS) flow gauge stations available in the catchment (Table 4.1), in order to obtain modeling output at the reaches' outlets. Overall, eleven (11) subbasin were delineated within the Big Creek watershed on the basis of variations in land-surface elevation, stream network and USGS flow gages (Figure 4.1).

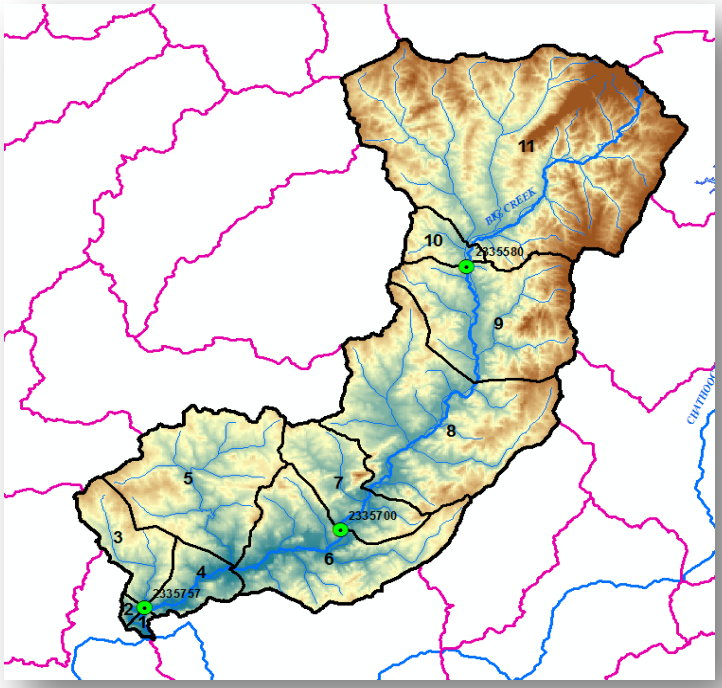

Figure 4.1 Subbasin delineation at Big Creek watershed

Table 4.1 USGS gage stations available within Big Creek Watershed

USGS Gage Nr	Gage Name	Drainage Area, sq mi	Start Date	End Date
02335580	BIG CREEK AT GA 9, NEAR CUM-MING, GA	36.4	2007-03-08	2011-03-23
02335757	BIG CREEK BELOW HOG WALLOW CREEK AT ROSWELL, GA	103.16	2004-03-27	2010-09-30
02335700	BIG CREEK NEAR ALPHARETTA, GA	72.0	1960-05-01	2010-09-30

However, high resolution elevation data (i.e. 5 m, 10 m, 30 m) is not publically and freely accessible in many parts of the world. For example, the Digital Line Graph (a 5 m resolution DEM), is used as standard data in China, but is the property of the National Bureau of Surveying and Mapping of China, and therefore is not available free of charge (Lin et al. 2010). More-

over, according to the hypothesis presented in Figure 1.3, increased resolution of DEM does not necessarily result in more accurate hydrologic prediction. Therefore, sensitivity of LSPC outputs to a coarser DEM that is similar to the resolution that would be available to most populated regions of the world and is publically and freely available, was performed. A 3 arc DEM (90 m) from the Shuttle Radar Topography Mission (STRM) is a result of collaboration of American National Aeronautics and Space Administration (NASA), the National Imagery and Mapping Agency (NIMA), and German and Italian space agencies, covers most land regions between 60°N and 56 ° S and is freely available online. For the experimental scenario, the STRM coverage for Big Creek watershed was downloaded from the website http://srtm.csi.cgiar.org/ (accessed on April 2, 2011). The shaped terrain of 30 m resolution NED from the baseline scenario and 90 m resolution STRM from the experimental scenario, are illustrated in Figure 4.2. Since the study aims to explore how sensitive the model is to DEM resolution and to geomorphic characteristics of the modeled watershed in particular, the identical subbasin delineation was used in both baseline and experimental scenario.

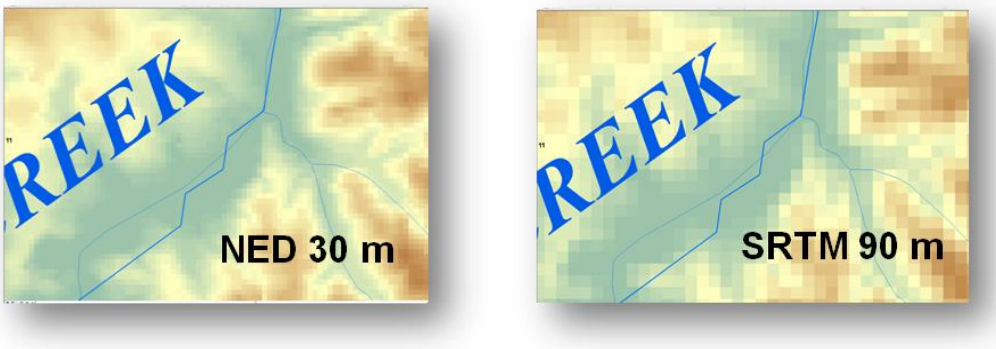

Figure 4.2 The DEMs of 30m and 90m resolution were used in the baseline and experimental scenarios.

4.2 Land Use Representation

To represent the spatial variability of land use, LSPC uses a GIS grid-based coverage, which is converted into a table format, with the columns being the land use numeric categories and the rows, the subbasin IDs. For the baseline scenario, the 2005 land use and impervious cover raster sets of 30x30 m resolution were downloaded from the Natural Resources Spatial Analysis Laboratory Georgia Land Use Trends (GLUT) database (http://narsal.uga.edu/projects/glut, accessed on February 10, 2011). The LSPC model requires division of land uses into separate pervious and impervious model land units. The GLUT data-set provides separate coverages of land use and percent impervious cover with a detailed classification, so the layers were first overlain. This geoprocessing enabled greater resolution of the spatial representation of imperviousness by the model land units. Two urban land units (22 and 24) were adopted to capture low- and high-developed urban areas identified by the GLUT land use coverage. The remaining GLUT impervious areas, representing thirteen GLUT land use categories, were grouped into a category encompassing all other impervious areas (All Other Imperv). The model land units, or LSPC land use categories, and their corresponding geoprocessed GLUT classifications are summarized in Table 4.2.

Due to the fact that similarly classified land cover data are rarely available throughout the world, it was assumed that only the Landsat imagery of 2005 would be available and the corresponding land use classification (supervised or unsupervised) would be performed. Since impervious surfaces of low, medium and high intensity have similar spectral reflectance properties, these classes are often classified into the same category (IDRISI Klimanjaro 2004). Therefore, a classification scheme that neglects the range of development intensity for both impervious and pervious developed land use classes was used for the experimental scenario. Specifi-

cally, low, medium and high- intensity developed land use for both pervious and impervious components were reclassified into a single low intensity developed land use (Table 4.2).

Table 4.2 Land Use classifications in the LSPC model and GLUT database (from Tetra Tech 2009)

LSPC Model Land Use Category Baseline Scenario	LSPC Model Land Use Category Experimental Scenario	Geoprocessed GLUT Land Use Category
Beach	Beach	Beaches/Dunes/mud
Water	Water	Open Water
LowIntDevPerv	LowIntDevPerv	LowIntDeveleoped Perv
LowIntDevImperv	LowIntDevPerv	LowIntDeveleoped Imperv
HighIntDevPerv	LowIntDevPerv	HighIntDevelopedPerv
HighIntDevImperv	LowIntDevPerv	HighIntDevelopedImperv
Barren	Barren	Clearcut/sparse
Barren	Barren	Quarries/strip mines/ Rock Outcrop
Forest	Forest	Deciduous Forest
Forest	Forest	Evergreen Forest
Forest	Forest	Mixed Forest
Pasture	Pasture	Row Crops/Pasture
Wetland	Wetland	Forested Wetlands
Wetland	Wetland	Non-forested Wetland (Salt/Brackish)
Wetland	Wetland	Non-forested Wetland (Freshwater)
AllOtherImperv	AllOtherImperv	Catch-All for remaining Impervious

Given the 30 m resolution of publicly available satellite imagery, estimation of the percent of impervious land per each land use class from standard land use classification techniques is problematic. In these cases, the readily available impervious surface coefficients are commonly used. For the experimental land use scenario, the 100% pervious area recommended by TR-55 (SCS 1986) was used for the reclassified low developed land use class.

4.3 Reach Characteristics

Each delineated sub-watershed in LSPC is represented by a single stream reach and is assumed to be a completely mixed, one-dimensional segment. Cross-section characteristics for each reach are summarized in functional tables (FTABLEs) and include the length and slope of the reach and the channel geometry that is described by bankfull width and depth (the main channel), a bottom width factor, a floodplain width factor, the slope of the floodplain, and the Manning's roughness coefficient for the stream channel (Figure 4.3). Physical characteristics of

each stream are determined using Rosgen's approach (Rosgen 1994), taking into account size of the drainage basin and location to estimate the bankfull depth and the bankfull width of a stream. Based on information on the stage, cross-sectional area, storage, and discharge information at the headwaters and the outlet, the runoff is routed within the subbasins.

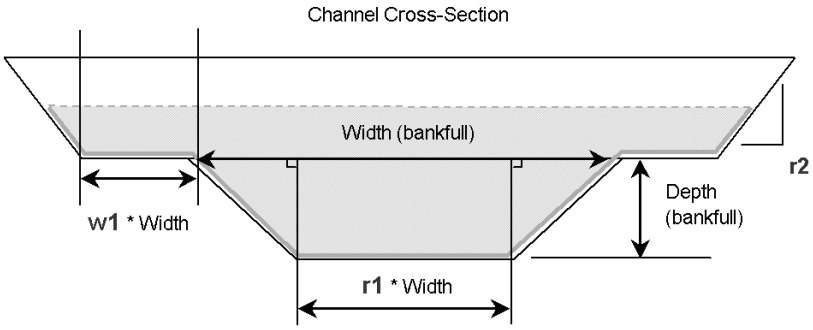

Figure 4.3 Stream channel representation in the LSPC model (from USEPA, 2007)

The baseline scenario cross-section scenario assumed that surveyed cross-section data for a representative reach was available and, therefore, field-based reach geometry from a cross-section of Big Creek was applied for the entire stream. Field measurements, including surveying the stream-channel cross sections (transects), identifying bankfull elevation, and channel slope were performed for the representative reach at Oxbo Rd in Roswell, located in subbasin 3 (Figure 4.1). This reach was selected because of the ease of accessibility and the cross-section dimensions, which are comparable with the other ten (10) reaches. In the field, the cross-section was surveyed by establishing transects and measuring bed surface elevations at pronounced changes in slope. Accuracy in measuring bankfull elevations with respect to the streambed was crucial in producing accurate estimates of bankfull flow conditions; therefore, a verification of the controlling benchmark was regularly performed. Although various definitions of "bankfull" exist in the literature, bankfull width and depth were determined primarily based upon geomorphic features, identified by an abrupt change in bank slope from near vertical to near horizontal (Parrett et al., 1983), or the lower edge of permanent vegetation and the elevation of point bars

(Olsen et al. 1997). Channel slope was calculated by dividing the upstream-downstream change in elevation by reach length. Channel roughness (Manning's n) was estimated based on channel median grain size, channel irregularity (width to depth ratio), and vegetation (instream and bank vegetation) (Arcement and Schneider, 1989; Coon 1998). With the assumption of a trapezoid cross section, the surveyed cross-section parameters were used to compute the stage, wetted perimeter, cross sectional area and total widths for 60 stages, for of each profile using basic geometry. The reach length, previously measured from NHD, was used to obtain the reach volume. Finally, the discharge for each stage was calculated using Manning's equation:

$$Q = \frac{k}{n} R^{\frac{2}{3}} S^{\frac{1}{3}} \quad (9)$$

where: Q is discharge (m^s/s), n is Manning's coefficient of roughness, k is a conversion constant equal to 1.486 for U.S. customary units or 1.0 for SI units, R is hydraulic radius (m), S is the slope of the water surface (m/m). Thus the stage, surface area, volume and discharge required for the FTABLE of reach 3 were calculated. Assuming that one representative stream is surveyed for the entire stream, the FTABLE generated for the surveyed reach was applied for all the eleven (11) reaches of Big Creek watershed in the baseline scenario.

For the experiment scenario, a trapezoidal cross-section was assumed for each delineated subbasin. The reach slope was calculated based on the upstream and downstream elevations that were extracted manually from the Digital Elevation Maps (30 m), and the reach length was digitally calculated from the National Hydrography Dataset (NHD). Geomorphic cross-section characteristics were determined using Rosgen's approach previously described. The surface area, volume and discharge for each reach then were calculated using methods and equations from the baseline scenario.

4.4 Soil Characteristics

Rainfall-runoff modeling is highly dependent on the estimation of infiltration because rainfall rates exceeding infiltration produce runoff. Given that a point by point measurement of infiltration over the watersheds of study is impractical and impossible, soil-mapping units are generally used to estimate infiltration rates from the hydrologic properties of the soils (Vieux 2004). The basis for watershed groups in LSPC is defined by the Natural Resources Conservation Service (NRCS) hydrologic soils groups. Soil data for the study area was obtained from the Soil Survey Geographic Database (SSURGO, available online at http://soildatamart.nrcs.usda.gov; accessed January 24, 2011) and the total area that each hydrologic soil group covered within each subbasin was determined. The subbasins were represented by the hydrologic soil group that had the highest percent of coverage (Figure 4.4). There was one dominant hydrologic soil group B in all subbasins of the Big Creek watershed. The soil group B consists chiefly of soils that are moderately deep to deep, moderately to well drained, with moderately coarse textures, and therefore have a moderate to low runoff potential. Due to homogeneity of the watershed from a hydrogeologic point of view, no variation of soil input parameter was possible and the experimental scenario was omitted. The use of a single baseline scenario for soil characteristics reduced the total number of model permutations from 32 to 16.

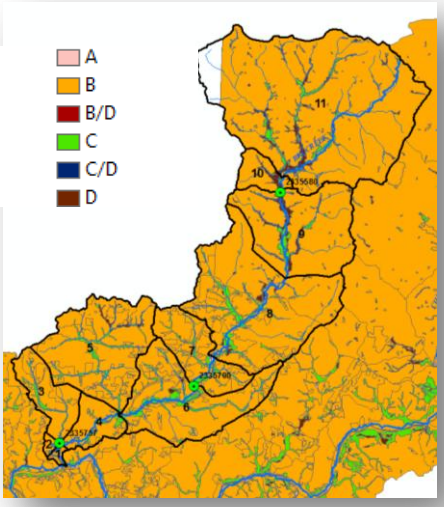

Figure 4.4 Hydrologic soil groups in Big Creek watershed

4.5 Meteorological data

The LSPC model is driven by precipitation and other meteorological data (e.g. temperature, cloud cover, wind speed) and therefore it is a critical component of watershed modeling efforts. Historically, meteorological data for hydrological applications have been obtained from the network of meteorological station and rain gages available (e.g. National Climate Data Center). According to the US Army Corp of Engineers (1993), the number of gages required for hydraulical modeling correlates to the watershed area as following:

$$Ng = A^{0.33} \quad (10)$$

where: Ng refers to the number of gages and A is the watershed area (km^2). The number of gages recommended by this equation for the area of Big Creek watershed (186.4 km^2) is 6, with a density of one gage per 31 km^2. Unfortunately, weather gages near the Big Creek watershed are sparse - there were no stations within the boundary of the watershed and only 3 stations were within close proximity (Figure 4.5). Due to the limited station availability, the USACE recommended number of weather stations had to be neglected and the 3 available meteorological stations were used for the baseline scenario (Table 4.3).

Table 4.3 Meteorological stations used in the study

Station ID	Station Name	County	Elevation, m	Start date
GEMN270	Johns Creek	Fulton	283 m	5/27/1994
092408	Cumming 1	Forsyth	398	8/1/1948
090451	Atlanta Hartsfield AP	Fulton	308	1/1/1930

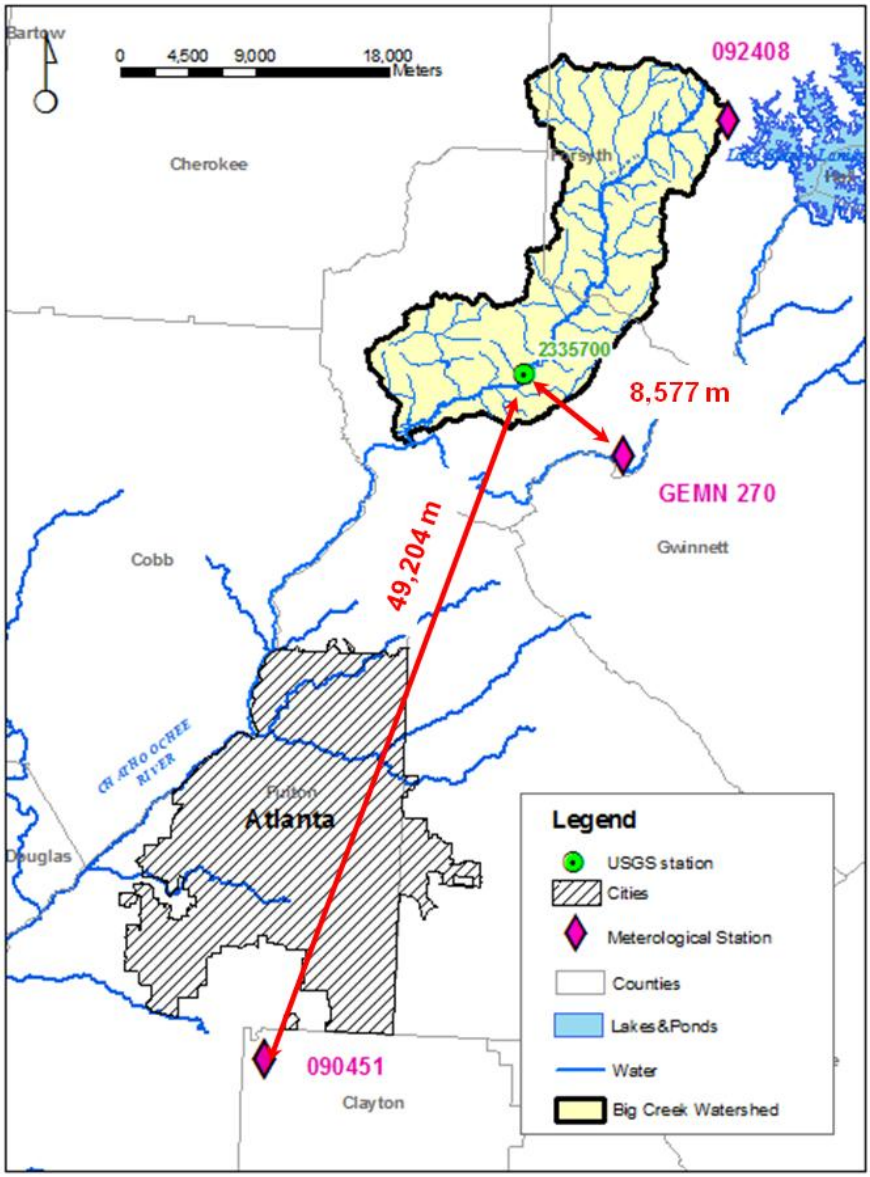

Figure 4.5 Meteorological stations in proximity to the Big Creek watershed

The first station was the Georgia Automated Environmental Monitoring Network station (GEMN270), which is maintained and operated by the College of Agricultural and Environmental Sciences of the University of Georgia and provides precipitation data at 15-minute intervals. The other two stations station were the National Climate Data Center station (092408) and Atlanta Hartsfield Airport station (090451) which provide daily observations for precipitation. The rainfall data from three stations were aggregated and disaggregated to hourly totals and an ASCII file was generated for each meteorological station. The meteorological stations were assigned to model subbasins through the use of Thiessen polygons, which are created by joining the perpendicular bisectors of the lines between the 3 meteorological stations available. This method essentially assigns each subbasin to the nearest weather station, not to the most representative station, which would take into account the local knowledge and characteristics of the subbasin, such as topography, that may impact rainfall-runoff response. Due to the limited station availability, the most representative meteorological stations coincided with the nearest: the northern subbasins got assigned to the station 092408, located on the northeast of the watershed, while subbasins from the central and southern portions were assigned to the GEMN270 station, located in the southeast (Figure 4.6). The Atlanta Airport station was not assigned to any subbasins due to its distant location from the subbasins.

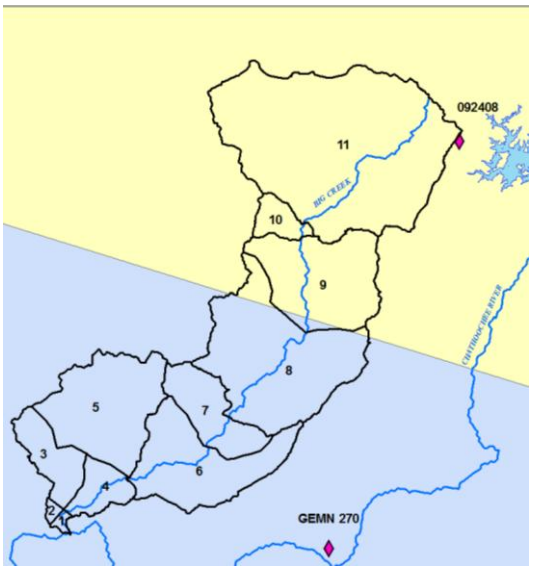

Figure 4.6 Assignment of meteorological stations according to the Thiessen polygons in the baseline scenario.

Although the spatial variability of the rainfall is an important factor in the process of runoff generation, scarcity of rainfall measurements often requires the use of data from a single meteorological station. In many countries, the automated airport weather stations become the backbone of weather observing due to their efficiency and cost-savings. For the experimental scenario, hourly precipitation records from the airport weather station were assumed and the entire watershed was assigned to the Atlanta Hartsfield Airport station. The weather stations used for both baseline and experimental scenario are summarized in Table 4.3 and their locations are shown in Figure 4.5.

4.6 Sensitivity analysis

In order to determine the minimum and/or threshold resolution of input data required to reasonably match runoff observations with the model predictions, a sensitivity analysis of LSPC runs to variations in input variables, in accordance with baseline and experimental scenarios, was performed. The baseline scenario was calibrated to the flow records at the USGS 02335700 Big Creek near Alpharetta, GA station over the period of study and therefore served as the "control" for the experiment. Hydrologic calibration followed the operating procedures and the tolerance targets for hydrologic models described in Donigian et al. (1984) and Lumb et al. (1994) (Table 4.4). Modeling parameters were adjusted within the bounds for parameter values set out in BASINS Technical Note 6 (USEPA 2000) and in accordance with observed temporal trends and soil and land cover characteristics. In order to explore the sensitivity of the model outputs to variations in input parameters, the experimental scenarios were not calibrated individually, but the modeling parameters from the calibrated baseline scenario were used.

Table 4.4 Recommended criteria for model calibration
(modified from Donigian et al. (1984) and Lumb et al. (1994)

Category	Recommended Criteria (%)
Error in total volume:	±10
Error in the mean of the 10% lowest flows:	±10
Error in the mean of the 10% highest flows:	±15
Error in Monthly Volumes:	±30
Error in Growing Season Volumes:	±30
Error in Nongrowing Season Volumes:	±30

Sensitivity of the model in this study indicates that the predicted flows, from experimental and baseline scenarios, are compared to the observed flow records at the USGS gage for the entire calibration period. Multiple quantitative and qualitative evaluation techniques of the model performance are used in hydrologic studies: standard regression, correlation coefficient, coefficient of determination, prediction efficiency, RMSE-observations standard deviation ratio, daily root-mean square percent exceedence probability curves (Gupta et al. 1999, Santhi et al. 2001, Van Liew et al. 2007; Arnold et al. 2007). In addition, these studies reveal that every evaluation technique faces limitations and therefore the selection of a technique depends on the purpose of the project and the type of model used. For example, a traditional statistical measure for evaluating the goodness-of-fit of modeled and observed values in test theory is the error variance, which provides a greater weight to the prediction of peak discharges, and tends to have the higher residuals than to predictions of low flows. To avoid limitations of specific evaluation techniques, complex metrics that would assess different aspects of similarity/dissimilarity between the observed and the predicted results have to be used (Saltelli et al. 2000, Arnold et al. 2007). Following a study by Arnold et al (2007), a combination of Nash and Sutcliffe coefficient, absolute error statistic, and graphical techniques was employed to judge the adequacy of the experimental and baseline scenarios fit to the observed data.

The efficiency of model performance was estimated by modeling efficiency coefficient of Nash and Sutcliffe (1970). This is a widely used dimensionless measure of fit based on the error variance, defined as:

$$E = 1 - \frac{\sum_{t=1}^{T}(Q_o^t - Q_m^t)^2}{\sum_{t=1}^{T}(Q_o^t - \overline{Q_o})^2} \quad (11)$$

where: Q_o is the observed discharge (, Q_m is the modeled discharge, Q_{ot} is the observed discharge at time t.

The coefficient can range from $-\infty$ to 1, with an efficiency of E = 1 corresponding to a perfect match of modeled discharge to the observed data, and an efficiency of E = 0 indicates that the model predictions are as accurate as the mean of the observed data, which gives a prediction of the mean of all observations for all time steps (Beven 2000). An efficiency E < 0 occurs when the observed mean is a better predictor than the model or, in other words, when the residual variance, is larger than the data variance. Essentially, the closer the model efficiency is to 1, the more accurate the model is. Such error variance–based measures have some practical and theoretical limitations, such as the fact that they are only suitable if the errors between observed and modeled data are normally distributed with constant variance and are not correlated. These assumptions are not always met in rainfall-runoff modeling, where the errors of predicting discharge are not necessarily normally-distributed, and the variance of predicted high flows may be different to the variance of predicted low flows. This may be especially true when the model does not get the timing of the hydrograph prediction correct (e.g. the shape of hydrograph is perfect but there is a large sum of correlated squared errors due to delayed lag time).

In order to consider the residuals along peaks and for low flow portions of the hydrograph, daily, monthly, seasonal, and total modeled flows were compared to the observed data, and error statistics were calculated for the percent difference according to equation:

$$Error = \frac{|simulated\ runoff\ -\ observed\ runoff\ |}{observed\ runoff}\ 100\%\ (12)$$

The percent errors were compared to the tolerance targets that were previously used for calibration (Table 4.6).

In order to provide a visual comparison of simulated and measured constituent data, hydrographs, flow duration curves, bar graphs and box plots were used. Hydrographs helped to identify how well the model predicted the magnitude of peak flows, timing and the shape of recession curves. Percent exceedence probability curves, or daily flow duration curves, were used to illustrate how well the model reproduces the frequency of measured daily flows throughout the calibration and validation periods (Van Liew et al., 2007). Bar graphs and box plots examined annual and seasonal data distributions.

4.7 Scenario coding

Once the model performance for the conditions of gaged and ungaged watersheds for each of the four input parameters was reviewed, the 16 possible permutations of all the experimental and the baseline scenarios were run. Given the large number of permutations a coding scheme based on variation of input parameters was used (Figure 4.7). Each code consists of 4 digits with the first position being assigned to the watershed DEM resolution, the second to the reach characteristics, the third to the land use schemes, and the fourth to permutations in meteorological stations. The experimental scenario is coded as 1 and the baseline as 0. For example a scenario with the code "0011" indicates that watershed DEM resolution and the reach characteristics are assigned to the baseline conditions ("0"), while land use classification and meteorological stations use conditions of the experimental scenarios ("1").

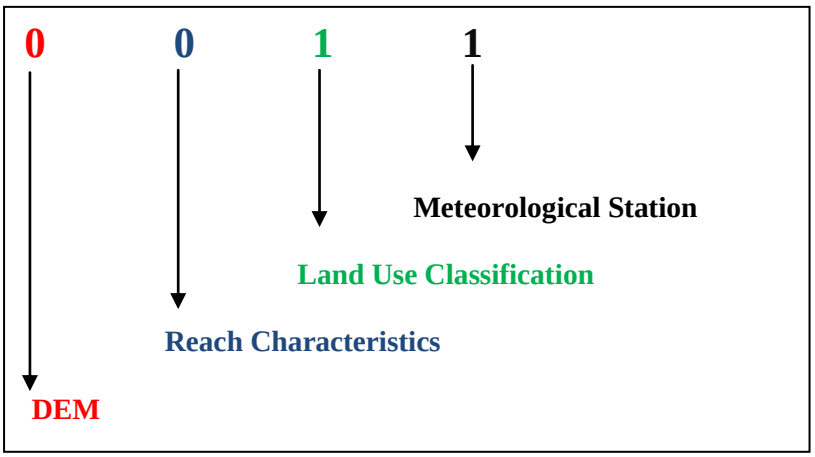

Figure 4.7 Scenario coding

5 RESULTS AND DISCUSSION

5.1 Watershed Segmentation

Comparison of input parameters

The DEM was used to segment the watershed into subbasins and their topographic characteristics in the LSPC model. The original 30 x 30 m DEM resulted in eleven subbasins with the area varying from 1 km^2 to 90 km^2, mean reach elevation ranging from 810 m to 1133 m, and the average slope values from 0.001m/m to 0.039 m/m. Given the fact that this study was focused on the sensitivity of the modeled discharge to DEM resolution and to topographic characteristics of the subbasins in particular, the variation in individual subbasin areas was neglected. Comparison of the input parameters for the NED 30 m and STRM 90 m scenarios demonstrated that as the resolution of DEM decreased, the average watershed and reach slope also decreased (Table 5.1).

The mean elevation of the subbasins increased by 15.53 percent with the decrease in DEM resolution from 30 m to 90 m. The mean slope of the hillslope terrain calculated from STRM 90 m was lower than calculated from NED 30 m by 0.2 percent. The average reach slope

derived from the STRM 90 m was lower by 28.39 percent. Significant slope reduction is a consequence of losing topographic detail at coarser DEM resolutions. Due to the slope being derived from the coarser STRM 90 m, the steeper slopes decreased in areal extent. Therefore, a coarser DEM does not properly reproduce the topographic variability in the watershed, cutting off the hilltops in the northern portion of the watershed and filling in valleys in the southern portion. Studies performed for the other distributed models: TOPMODEL (Zhang and Montgomery 1994), SWAT (Chaubey et al. 2005) reported a similar decrease in watershed slope (15 - 22 percent) with a decrease in DEM resolution from 30 m to 100 m.

LSPC Output Comparison

The 10-year streamflow predictions from the experimental scenario (STRM 90 m), were compared to the predictions of the calibrated baseline scenario (NED 30 m). Table 5.2 shows the average annual simulated flow volumes and its components for the two scenarios, and the error statistics for these scenarios are summarized in Table 5.3.

The total in-stream flow simulated for the NED 30 m and STRM 90 m were very similar (22.60 inches/year). The seasonal and storm runoff volumes were also close despite differences in DEM resolution (Table 5.2), so the total predicted accuracy was insignificantly affected by coarsening of DEM (Table 5.3). The difference in error for all of the components of flow volume for the baseline and experimental scenarios was less than 0.5 percent, with the maximum difference of 0.22 percent for the summer storm volumes. The overall predicting accuracy expressed by Nash-Sutcliffe Coefficient increased by 0.002 for the experimental scenario at the 10-year time scale. In general, the volumetric and statistic results indicate that as the DEM resolution became coarser, the predicted streamflow volume did not significantly change.

Table 5.1 Comparison of the input parameters for the NED30m and STRM90m scenarios exhibit that as the resolution of DEM decreased, the average watershed and reach slope also decreased.

Variable	Scenario 0000 (NED30m)	Scenario 1000 (STRM90m)	Relative difference%
Mean SWS Elevation (m)	285.75	330.13	15.53
Mean SWS Slope (m/m)	0.05	0.04	-0.20
Area (m^2)	the same	the same	0.00
Reach Length (m)	the same	the same	0.00
Mean Reach Elevation (m)	298.55	304.39	1.96
Average Reach Slope (m/m)	0.0057	0.0048	-28.39

Table 5.2 The average annual simulated flow volumes and its components for the NED30m and STRM90m scenarios. Model Outlet 7 vs. USGS 02335700 Big Creek near Alpharetta, GA.10-Year
Analysis Period: 1/1/1998 - 12/31/2007.

Flow volumes inches/year	LSPC Simulated Flow	
	Scenario 0000 NED30m	Scenario 1000 STRM90m
Total In-stream Flow:	22.60	22.60
Highest 10% flows:	9.47	9.47
Lowest 50% flows:	3.57	3.58
Summer Flow Volume	5.08	5.08
Fall Flow Volume	4.63	4.63
Winter Flow Volume	7.47	7.47
Spring Flow Volume	5.41	5.41
Storm Volume:	9.73	9.72
Summer Storm Volume	*2.53*	2.52

Table 5.3 Comparative summary statistics for the NED30m and STRM90m scenarios. Model Outlet 7 vs. USGS 02335700 Big Creek near Alpharetta, GA.10-Year
Analysis Period: 1/1/1998 - 12/31/2007.

Errors in flow volumes (percent) ((Simulated-Observed)/Observed)*100	LSPC Simulated Flow	
	Scenario 0000 NED30m	Scenario 1000 STRM90m
Error in total volume:	8.76	8.75
Error in 50% lowest flows:	9.23	9.27
Error in 10% highest flows:	-3.13	-3.22
Seasonal volume error - Summer:	28.29	28.26
Seasonal volume error - Fall:	10.51	10.49
Seasonal volume error - Winter:	-1.75	-1.76
Seasonal volume error - Spring:	7.80	7.81
Error in storm volumes:	2.77	2.63
Error in summer storm volumes:	19.81	19.59
Nash-Sutcliffe Coefficient of Efficiency	0.655	0.657

In order to evaluate the impact of changed DEM resolution on flow volume for a range of climatic conditions, a comparison of model output for representative wet and dry years from the study period was performed (2005 and 2007). The time series of predicted and observed daily mean flow for wet and dry years, for the baseline and experimental scenarios, are shown in Figures 5.1, 5.2 and 5.3, 5.4 respectively. A statistic interpretation of model performance at these annual time scales for the baseline and experimental scenarios is given below the hydrographs in Tables 5.4 and 5.5 for wet and dry years, respectively. Comparison with the USGS stream gage information revealed that the model predictions of average flow were generally good for the annual time scales. The exceptions were summer months with error for the summer (wet and dry year) flow volumes varying from 48 percent to 96 percent. In visually comparing the hydrographs of the baseline and experimental scenarios for wet (Figures 5.1 and 5.3) and dry (Figures 5.2 and 5.4) years, no significant difference in timing or flow scaling of the hydrographs was observed. Comparison of the error statistics (Tables 5.4 and 5.5) confirmed that flow volume for the years was not significantly affected by the change in DEM resolution - the degree of error for flow volume was the same for dry year and less by 0.01 percent for wet year. The storm volume was not very sensitive to the coarser DEM resolution, evidenced by the reduction in error for the summer of the dry year by 0.008.

Overall, no significant differences between the predicted daily mean flow for the experimental and baseline scenarios were observed from qualitative (hydrograph) and quantitative (error) evaluations. Line graphs and more detailed statistics comparing predicted to observed values for the baseline and experimental scenario are presented in Appendices A and B, to facilitate more detailed qualitative and quantitative evaluations.

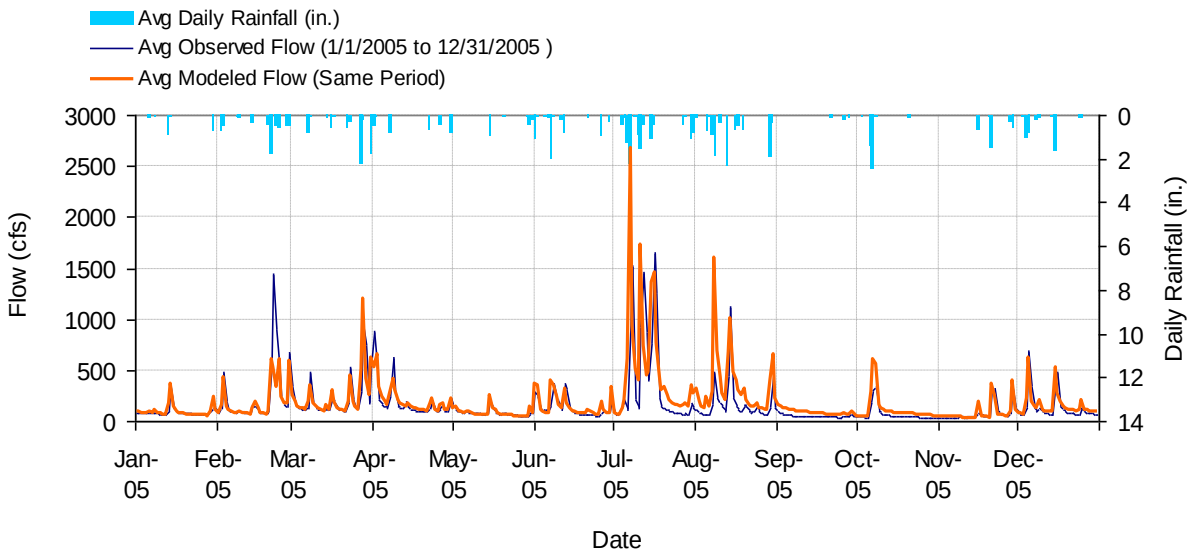

Figure 5.1 Mean daily flow for a wet year (2005): model outlet 7 vs. USGS 02335700 Big Creek near Alpharetta, GA. Baseline scenario 0000: NED30m, digital-based FTABLES, complete land use classification and GEMN270 meteorological station.

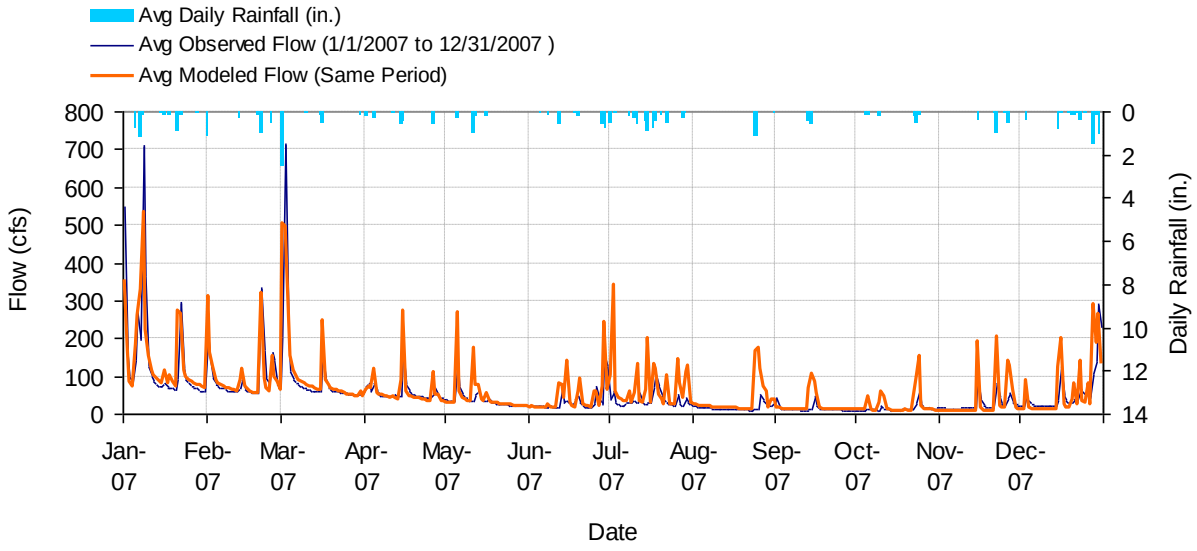

Figure 5.2 Mean daily flow for a dry year (2007): model outlet 7 vs. USGS 02335700 Big Creek near Alpharetta, GA. Baseline scenario 0000: NED30m, digital-based FTABLES, complete land use classification and GEMN270 meteorological station.

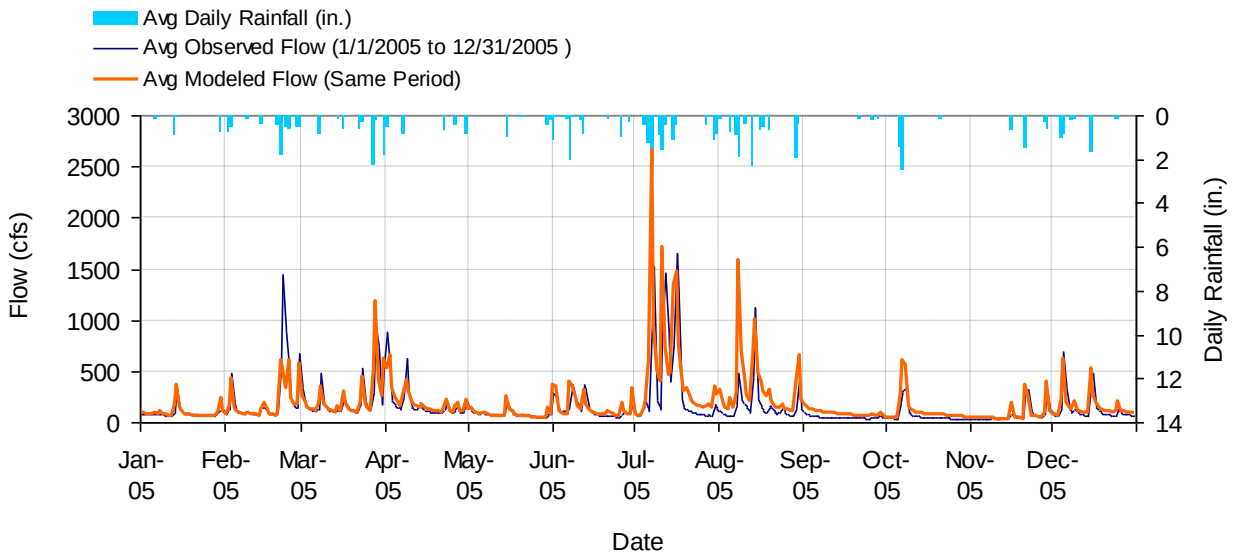

Figure 5.3 Mean daily flow for a wet year (2005): model outlet 7 vs. USGS 02335700 Big Creek near Alpharetta, GA Experimental scenario 1000: STRM90m, digital-based FTABLEs, complete land use classification and GEMN270 meteorological station.

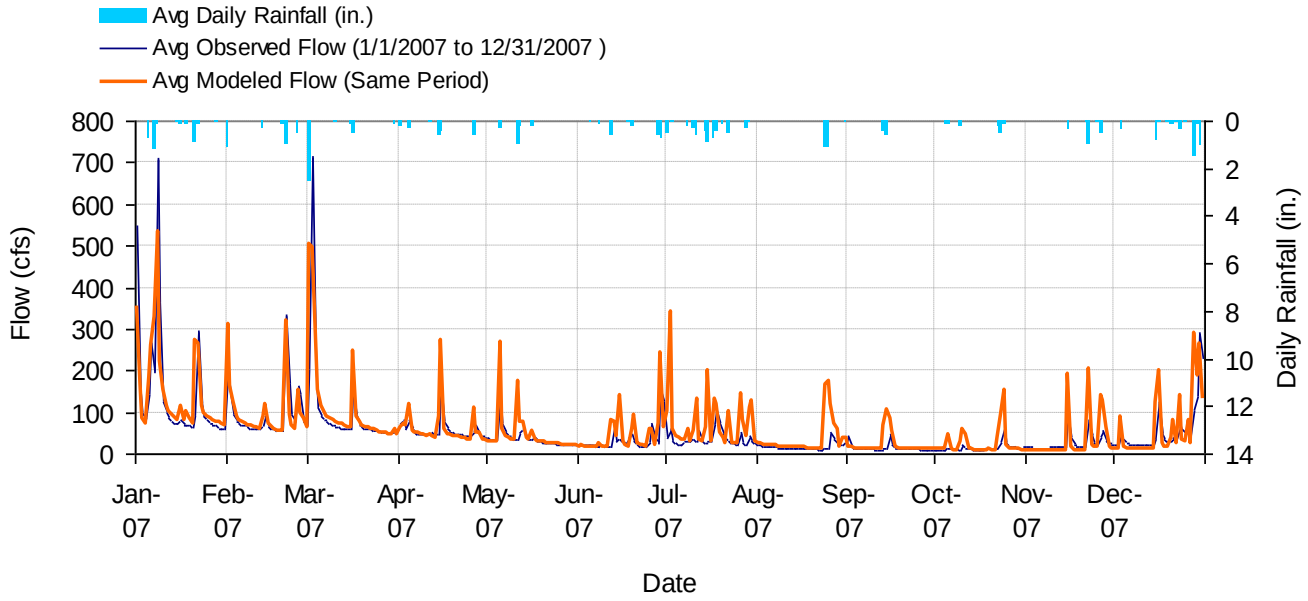

Figure 5.4 Mean daily flow for a dry year (2007): model outlet 7 vs. USGS 02335700 Big Creek near Alpharetta, GA Experimental scenario 1000: STRM90m, digital-based FTABLEs, complete land use classification and GEMN270 meteorological station.

Table 5.4 Comparative summary statistics for the NED30m and STRM90m scenarios for a wet year (2005). Model Outlet 7 vs. USGS 02335700 Big Creek near Alpharetta, GA.

Errors in flow volumes (percent) (Simulated-Observed)/Observed)*100	LSPC Simulated Flow	
	Scenario 0000 NED30m	Scenario 1000 STRM90m
Error in total volume:	20.10	20.09
Error in 50% lowest flows:	21.46	21.52
Error in 10% highest flows:	6.90	6.78
Seasonal volume error - Summer:	48.75	48.72
Seasonal volume error - Fall:	23.88	23.90
Seasonal volume error - Winter:	-5.72	-5.75
Seasonal volume error - Spring:	7.64	7.67
Error in storm volumes:	7.16	6.95
Error in summer storm volumes:	21.27	20.94
Nash-Sutcliffe Coefficient of Efficiency	0.453	0.459

Table 5.5 Comparative summary statistics for the NED30m and STRM90m scenarios for a dry year (2007). Model Outlet 7 vs. USGS 02335700 Big Creek near Alpharetta, GA.

Errors in flow volumes (percent) (Simulated-Observed)/Observed)*100	LSPC Simulated Flow	
	Scenario 0000 NED30m	Scenario 1000 STRM90m
Error in total volume:	21.09	21.09
Error in 50% lowest flows:	1.72	1.75
Error in 10% highest flows:	19.51	19.48
Seasonal volume error - Summer:	95.85	95.87
Seasonal volume error - Fall:	24.14	24.13
Seasonal volume error - Winter:	6.03	6.04
Seasonal volume error - Spring:	17.85	17.87
Error in storm volumes:	59.25	59.17
Error in summer storm volumes:	283.84	283.75
Nash-Sutcliffe Coefficient of Efficiency	0.606	0.606

Regardless of the obtained results, the resolution-induced topographic flattening in the basin was expected to have an impact on the shape of the hydrograph, and specifically, to attenuate them. The fact that the impact of the reduced DEM resolution on the flow volume was minor may be explained by the overall flat relief of Big Creek watershed (the average slope is 0.005), and by the fact that variations in subbasin area due to the changes in DEM resolution

were neglected. Because of the preserved areas, the results of this study are somewhat dissimilar to the results reported for other distributed hydrologic models which found that coarsening DEM resolution from 30 m to 90 m results in lower runoff (TOPMODEL -Wolock and Price (1994), SWAT - Cho and Lee (2001)). However, the results of this study are consistent with the findings of the previously mentioned authors in regards to the decrease of mean slope with a coarsening DEM resolution from 30 m to 90 m, and the overall minor role the mean slope plays in simulation of runoff by distributed hydrologic models. Overall, the STRM 90 m, relative to the NED 30 m scenarios, had good model performance at time scales ranging from 10 years to annual. Therefore, one may conclude, at least for the Big Creek watershed, that mean slope plays a minor role in runoff output for the LSPC model, and that smoothing the DEM from 30 m to 90 m resolution does not substantively affect the hydrological simulations.

5.2 Land Use Representation

Comparison of input parameters

The GLUT 2005 land use breakdown for the Big Creek watershed for both baseline and experimental scenarios is summarized in Figure 5.5. The developed land use in both scenarios covered about 80 percent of the watershed. In the baseline scenario, the 80 percent of developed land use consisted of: 10 percent of high intensity impervious, 10 percent medium intensity impervious and 7 percent of low intensity impervious land use; which overall brings the percent of imperviousness for the baseline scenario to 27 percent. In order to determine the impact of simplified land use classification for the experimental scenario, the entire 27 percent of imperviousness for developed land use types was set to zero percent, such that the 80 percent of developed land resulted in 100% perviousness (Figure 5.5).

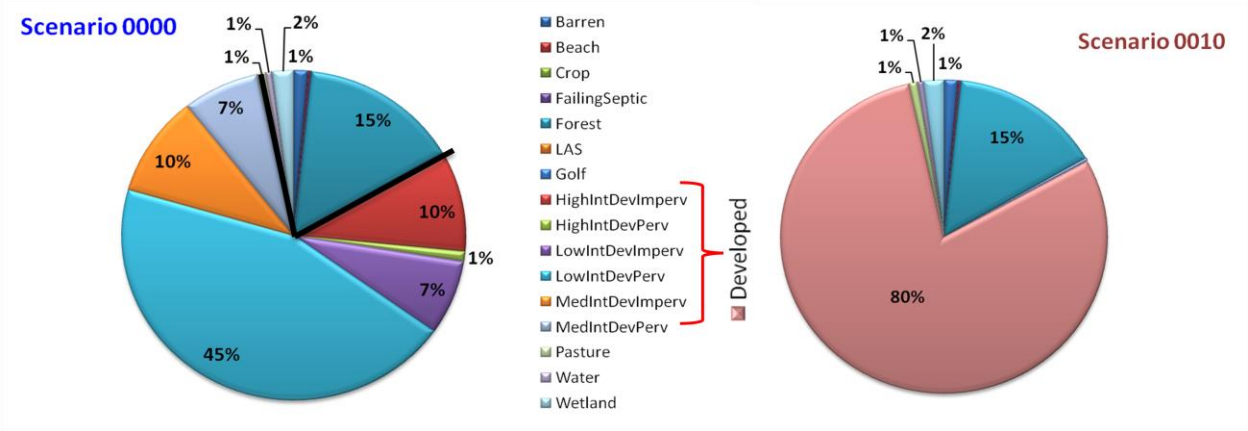

Figure 5.5 Comparison of the input data for the scenarios of complete and simplified land use classification scenario 0000 and 0010 correspondingly.

LSPC Output Comparison

The 10-year model predictions of flow volume, for the land use classification scheme with reduced complexity (experimental scenario), were compared to the predictions from the calibrated complete land use classification (baseline scenario) in Table 5.6; error results for the baseline and the experimental scenarios are summarized in Table 5.7. For the experimental scenario, the total flow volume decreased by 2 inches per year. The error in simulation of the total flow volume in the experimental scenario was 8 percent lower than in the calibrated baseline scenario and therefore resulted in better estimation of total flow. Instead, errors in low and high flows were most significant in the experimental scenario, in which the error in '50 percent lowest flows' decreased by 26.25 percent. A much larger difference in percent error for the 10-year period was observed for storm volumes, where the error in summer storm volumes for model runs assuming reduced imperviousness, decreased by 85.39 percent. Regardless of the observed changes in flow volume, the difference in the overall predictive accuracy of the model (Nash Sutcliff coefficient) for the experimental and baseline scenarios was low: 0.099; indicating that, similar to the reduced resolution DEM, the predicted flow was not substantially affected by the simplified land use classification scheme at the decadal time scale. Insignificant

changes in total flow volume due to decreased imperviousness in the experimental scenario are analogous to previous studies. For example, Choi and Deal (2008) and White and Greer (2006) showed that total runoff changed by only 2-5 percent in spite of an increase in imperviousness of up to 25 percent for urbanizing basins in Illinois and California.

Table 5.6 The average annual simulated flow volumes and its components for the scenarios of complete and simplified land use classification - 0000 and 0010 correspondingly. Model Outlet 7 vs. USGS 02335700 Big Creek near Alpharetta, GA.10-Year Analysis Period: 1/1/1998 - 12/31/2007.

Flow volumes inches/year	LSPC Simulated Flow	
	Scenario 0000 Complete LU	Scenario 0010 Simplified LU
Total In-stream Flow:	22.60	20.65
Highest 10% flows:	9.47	7.83
Lowest 50% flows:	3.57	2.71
Summer Flow Volume	5.08	2.78
Fall Flow Volume	4.63	4.84
Winter Flow Volume	7.47	8.54
Spring Flow Volume	5.41	4.50
Storm Volume:	9.73	5.13
Summer Storm Volume	2.53	0.73

Table 5.7 Comparative summary statistics for the scenarios of complete and simplified land use classification. Model Outlet 7 vs. USGS 02335700 Big Creek near Alpharetta, GA.10-Year Analysis Period: 1/1/1998 - 12/31/2007.

Errors in flow volumes (percent) (Simulated-Observed)/Observed)*100	LSPC Simulated Flow	
	Scenario 0000 Complete LU	Scenario 0010 Simplified LU
Error in total volume:	8.76	-0.62
Error in 50% lowest flows:	9.23	-17.02
Error in 10% highest flows:	-3.13	-19.98
Seasonal volume error - Summer:	28.29	-29.80
Seasonal volume error - Fall:	10.51	15.51
Seasonal volume error - Winter:	-1.75	12.22
Seasonal volume error - Spring:	7.80	-10.48
Error in storm volumes:	2.77	-45.85
Error in summer storm volumes:	19.81	-65.58
Nash-Sutcliffe Coefficient of Efficiency	0.655	0.556

In order to explore the sensitivity of the model to the simplified land use classification at finer time scales, a comparison of model output for the wet (2005) and dry (2007) years from

the study period was performed. The hydrographs of predicted and observed daily mean flow for both scenarios are shown in Figures 5.1 and 5.6 for the wet year, and in Figures 5.2 and 5.7 for the dry year; errors for these simulations are summarized and compared with the baseline scenario in Tables 5.8 and 5.9 for wet and dry years, respectively. A visual comparison of the hydrographs showed that predicted flow in the experimental scenario consistently underpredicted the observed values. The error in annual flow data illustrate that there was a substantial reduction in the total annual volume for the experimental scenario. For same precipitation levels, the error in total flow volume for the experimental scenario was reduced by over 25 percent and 100 percent compared to the baseline scenario for wet and dry years, respectively. These trends are further supported by differences in modeling error for the 'lowest 50 percent' and the 'highest 10 percent' flow volume. The error for the 'lowest 50 percent flow' in the baseline scenario during the dry season exceeds the same error in the experimental scenario by over 10 times (1.72 vs. -47.17 percent), and the error in the 'highest 10 percent flow' in the baseline scenario is greater than the error for the experimental scenario by over 5 times (19.51 vs. -2.87 percent) (Table 5.9). The 'highest 10 percent flow' category is representative of major storm events, and 'the lowest 50 percent' is representative of base-flow conditions. Visual analysis indicated that the median streamflow for each of the scenarios is nearly identical, but that the storm and baseflow volumes differ significantly (Figures 5.2 and 5.7). For the dry year (Figure 5.2), the storm event of July 7, 2005 resulted in a 47.62% increased peak flow for the baseline scenario, and the baseflow for the baseline scenario was lower by 20 percent compared to the output from the experimental scenario (Figure 5.7). These results confirm the widely accepted view that a higher degree of imperviousness leads to increased storm runoff (Walsh et al. 2005; Gregory 2006) and decreased base flow (Rose and Peters 2001). Twenty-seven (27) percent of

impermeable surface, as was included in the baseline scenario, provides a more efficient routing of stormwater via sewer systems and strongly influenced the modeled stormflow volume and higher peak discharge. Concurrently, the 27 percent imperviousness decreased the groundwater recharge, producing the decrease in observed low flow. Visual comparisons of the flow recession trends illustrated that storm runoff rates for the baseline scenario increased sharply during each rain event and fell back rapidly after the rain ceased, whereas the recession rate in the experimental scenario was less flashy and was more gradual (Figure 5.2 and 5.7). These sharp increases in storm flow in the baseline scenario indicate how much runoff was quickly routed through the basin as surface flow, with reduced groundwater recharge, when the watershed had 27 percent more impervious cover.

Statistically insignificant changes in total flow volume, due to decreased imperviousness for the experimental scenario at the 10-year time scale (expressed by Nash-Sutcliff coefficient) suggest that to estimate the total flow volume, simplification of the land use classification input data may be appropriate, even for an urbanizing watershed with percent of impervious cover of up to 27 percent. However, model results are extremely sensitive for storm and baseflow volumes at the annual time scale, that suggests the necessity for preserving the percent of imperviousness for developed land use types, especially when modeling annual flow volumes in the watersheds with the land use breakdowns similar to Big Creek watershed. The study did not consider land use change over the time – a factor that may be important in urbanizing watersheds, as Big Creek. Since the model demonstrated a high sensitivity to representation of imperviousness at the annual level, and impermeable cover in Big Creek watershed increased by 19.24 percent between 1984 and 2005, change of land use (and impervious land cover in particular) over the time could be an important factor to consider when running LSPC model over a

long period of time. Line graphs, seasonal medians, ranges, and regressions comparing predicted to observed values during wet and dry seasons for the scenario with the simplified land use classification are presented in Appendix C to facilitate more detailed qualitative and quantitative evaluations.

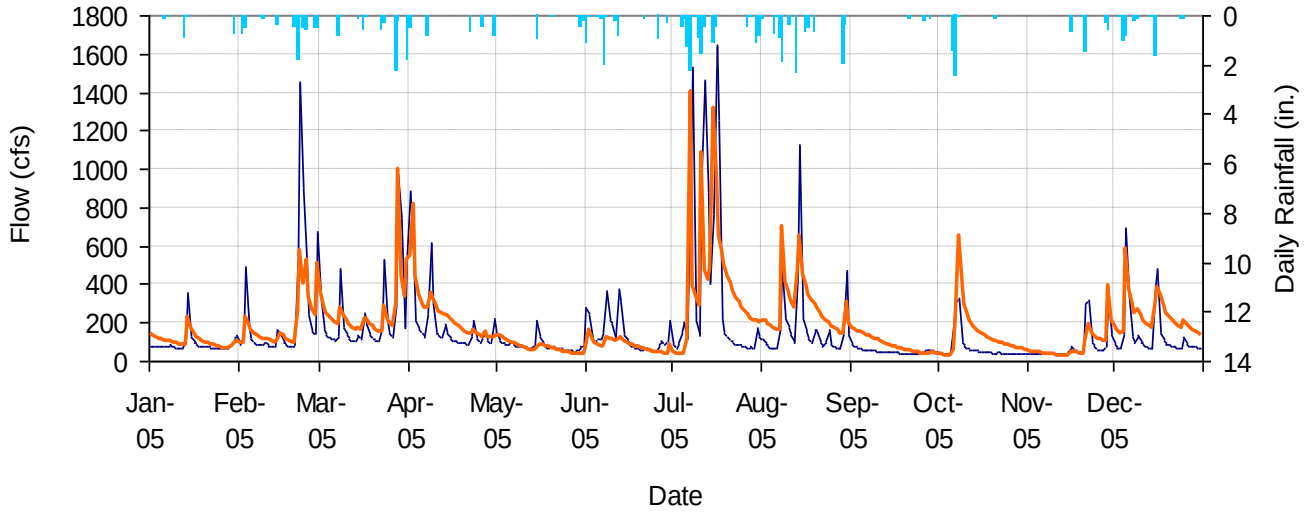

Figure 5.6 Mean daily flow for a wet year (2005): model outlet 7 vs. USGS 02335700 Big Creek near Alpharetta, GA Experimental scenario 0010: STRM30m, digital-based FTABLEs, simplified land use classification and GEMN270 meteorological station.

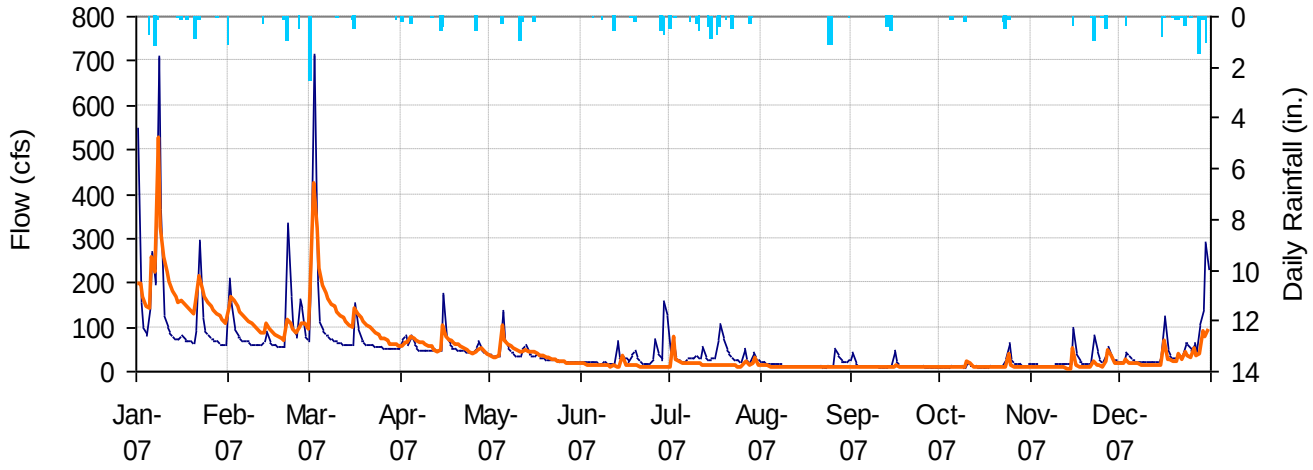

Figure 5.7 Mean daily flow for a dry year (2007): model outlet 7 vs. USGS 02335700 Big Creek near Alpharetta, GA Experimental scenario 0010: STRM30m, digital-based FTABLEs, simplified land use classification and GEMN270 meteorological station.

Table 5.8 Comparative summary statistics for the scenarios with complete and simplified land use classification (scenarios 0000 and 0010, respectively) for a wet year (2005). Model Outlet 7 vs. USGS 02335700 Big Creek near Alpharetta, GA.

Errors in flow volumes (percent) (Simulated-Observed)/Observed)*100)	LSPC Simulated Flow	
	Scenario 0000 complete LU classification	Scenario 0010 simplified LU classification
Error in total volume:	20.10	15.19
Error in 50% lowest flows:	21.46	28.33
Error in 10% highest flows:	6.90	18.00
Seasonal volume error - Summer:	48.75	21.71
Seasonal volume error - Fall:	23.88	56.39
Seasonal volume error - Winter:	-5.72	-0.33
Seasonal volume error - Spring:	7.64	-2.88
Error in storm volumes:	7.16	40.08
Error in summer storm volumes:	21.27	39.42
Nash-Sutcliffe Coefficient of Efficiency	0.453	0.514

Table 5.9 Comparative summary statistics for the scenarios with complete and simplified land use classification (scenarios 0000 and 0010, respectively) for a dry year (2007). Model Outlet 7 vs. USGS 02335700 Big Creek near Alpharetta, GA.

Errors in flow volumes (percent) (Simulated-Observed)/Observed)*100	LSPC Simulated Flow	
	Scenario 0000 complete LU classification	Scenario 0010 simplified LU classification
Error in total volume:	21.09	-3.46
Error in 50% lowest flows:	1.72	-47.17
Error in 10% highest flows:	19.51	-2.87
Seasonal volume error - Summer:	95.85	-52.60
Seasonal volume error - Fall:	24.14	-46.42
Seasonal volume error - Winter:	6.03	24.75
Seasonal volume error - Spring:	17.85	-17.70
Error in storm volumes:	59.25	-46.62
Error in summer storm volumes:	283.84	-69.96
Nash-Sutcliffe Coefficient of Efficiency	0.606	0.610

5.3 Reach Characteristics

Comparison of input parameters

Surface area, volume, and streamflow information at the given water stages are summarized in a function table for each reach (FTABLE), which are then used to simulate discharge for inflow of each subbasin. Given the fact that FTABLE depends on the shape of the cross section, the FTABLE stage discharge curves for the baseline and experimental scenarios were compared prior to considering the effect the two FTABLE scenarios had on the flow volumes. Visual comparison of the digital-based (baseline scenario) and field-based (experimental scenario) stage discharge relationship at the reach at Oxbo Road in Roswell, GA (sub-basin 3 on Figure 4.1), indicated that there is a minor difference in the bankfull flow range, and a major difference at stages above bankfull (Figure 5.8).

The minor difference in stage-discharge relationships below bankfull can be explained by a higher resolution of the field-based FTABLES. As described in the Methods (Chapter 4), the detailed stream cross-section surveys with multiple stages were used to develop the field-based FTABLES, while only 2 points extracted from the 30 m DEM were used to interpolate discharges at stages less than bankfull for the digital-based FTABLES. The agreement between field-based and digital-based stage discharge relationships improved at bankfull, which may be explained by the overall agreeable fit between bankfull width and depth measured from the survey and extracted from 30m-DEM. The cross-sections and bankfull width and depth values obtained using field measurements and digital-based calculations are shown on Figure 5.9. The percent difference between the measured and calculated bankfull width and depth were 15.2 and 7.17 percent, respectively. Visual comparison of the digital-based and field-based stage dis-

charge relationships exhibited a separation in predicted discharge rates for stages above bankfull (approximately 2.07 m in Figure 5.9).

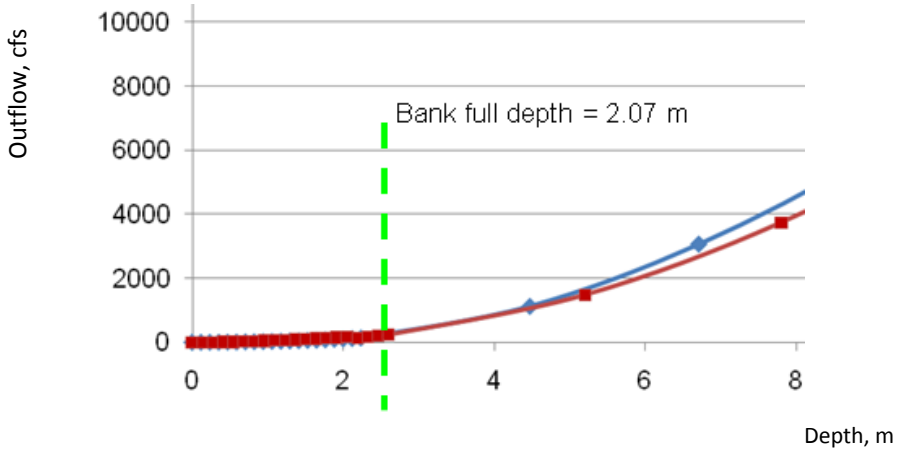

Figure 5.8 Stage discharge curves for the field-based and digital-based FTABLE scenarios FTABLEs generated using digital data are a viable option when simulating stream discharge with LSPC.

a)

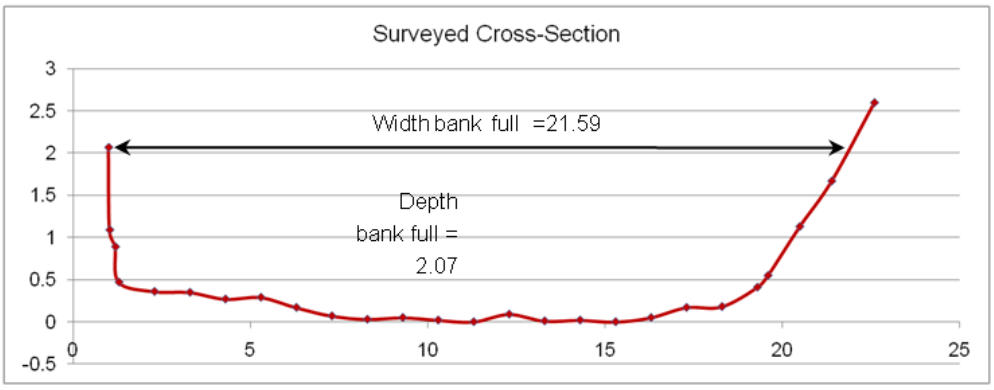

b)

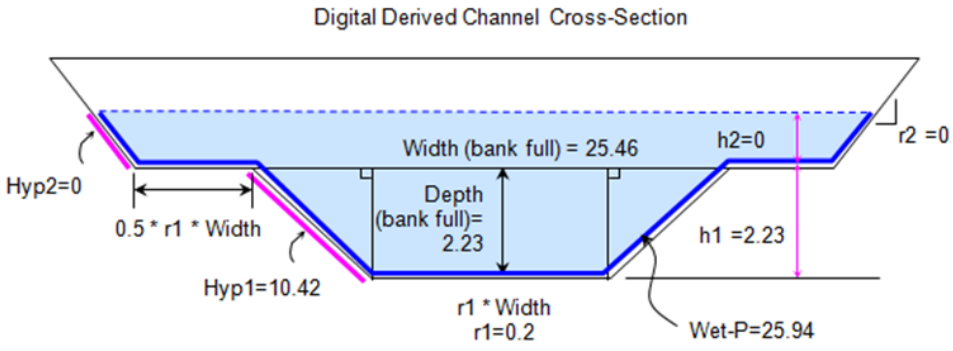

Figure 5.9 Stream cross-sectional profile used for the for the a) field-based and b)digital-derived FTABLE scenarios. All the dimensions are given in meters.

The difference increases with higher stage and is likely due to the fact that the dimensions of the floodplain for the field-based scenario were not measured, but calculated based on the stage discharge relations below bankfull. Still, the overall lack of significant differences between the bankfull characteristics of the channel below bankfull suggests that digital data and Digital derived cross-section parameters may be a viable option for representation of (fairly simple) channel cross sections in small watersheds where field surveying is not possible.

LSPC Output Comparison

The 10-year streamflow predictions from the experimental scenario (digital-based cross-section topography) were compared to the predictions for the baseline scenario (field-based topography). Table 5.10 shows the average annual simulated flow for the 10-year period for the two scenarios; in table 5.11 a comparative statistics for the scenarios of digital- and field-based FTABLES is summarized. The total in-stream flow simulated for the 10-year period (1998-2007), based on digital-based and field-based FTABLES, correspond to 22.58 and 22.60 inches/year. Error results suggest that there were no significant differences in simulated stream discharge between the two scenarios. The experimental scenario increased the error of total simulated flow volume by 0.09 percent, but decreased the error of the storm volumes by 2.11 percent. According to the Nash Sutcliff coefficient, the overall model performance of the experimental scenario relative to the baseline scenario increased by only 0.011.

A more detailed statistical analysis comparing predicted and observed values for the experimental scenario are presented in Appendix D to facilitate more detailed qualitative and quantitative evaluations.

Table 5.10 The average annual simulated flow volumes and its components for the scenarios of digital- and field-based FTABLEs - 0000 and 0100 correspondingly. Model Outlet 7 vs. USGS 02335700 Big Creek near Alpharetta, GA.10-Year Analysis Period: 1/1/1998 - 12/31/2007.

Flow volumes inches/year	LSPC Simulated Flow	
	Scenario 0000 Digital–based FTABLE	Scenario 0100 Field FTABLE
Total In-stream Flow:	22.58	22.60
Highest 10% flows:	9.59	9.47
Lowest 50% flows:	3.50	3.57
Summer Flow Volume	5.08	5.08
Fall Flow Volume	4.62	4.63
Winter Flow Volume	7.47	7.47
Spring Flow Volume	5.02	5.41
Storm Volume:	9.93	9.73
Summer Storm Volume	2.57	2.53

Table 5.11 Comparative statistics for the scenarios of digital- and field-based FTABLEs - 0000 and 0100 correspondingly. Model Outlet 7 vs. USGS 02335700 Big Creek near Alpharetta, GA.10-Year Analysis Period: 1/1/1998 - 12/31/2007.

Errors in flow volumes (percent) ((Simulated-Observed)/Observed)*100)	LSPC Simulated Flow	
	Scenario 0000 Digital–based FTABLE	Scenario 0100 Field-based FTABLE
Error in total volume:	8.67	8.76
Error in 50% lowest flows:	6.93	9.23
Error in 10% highest flows:	-2.00	-3.13
Seasonal volume error - Summer:	28.20	28.29
Seasonal volume error - Fall:	10.38	10.51
Seasonal volume error - Winter:	-1.81	-1.75
Seasonal volume error - Spring:	7.69	7.80
Error in storm volumes:	4.88	2.77
Error in summer storm volumes:	21.68	19.81
Nash-Sutcliffe Coefficient of Efficiency	0.644	0.655

Accuracy of flow simulation was then assessed at the annual scale. Hydrographs of predicted and observed daily mean flows, for the digital-based and field-based scenarios, are shown in Figures 5.1 and 5.10 for the wet year, in Figures 5.2 and 5.11 for the dry year; the associated error for these simulations is summarized in Tables 5.12 and 5.13 for wet and dry years, respectively. Comparison of Figures 5.1 and 5.10, 5.2 and 5.11 illustrates a minor difference in the average daily flow rate output from LSPC using the two FTABLE scenarios at the

annual time scale. The error for wet and dry years for both field-based and digital-based was less than 1 percent. Storm runoff error decreased by almost 15 percent during the dry year for the summer season (Figure 5.11). In order to compare the prediction ability of the experimental and baseline scenarios at stages greater than bankfull (2.07 m) the hydrological response for the storm on March 1, 2007 was explored. A rainfall event of 2.57 in/day resulted in a peak flow that was 5.8 percent lower in the baseline than in the experimental scenario. This may be explained by the fact that the field-based scenario has a smaller cross-section area, and the same amount of outflow would result in higher peak discharges during intense or long-term precipitation events than in the digital based scenario. Overall, a greater error in total storm volume supports the suggestion stated previously that for stages above bankfull, a higher error in hydrologic response may have occurred due to the fact that cross-sectional areas were not measured but extrapolated based on the cross sectional measurements below bankfull.

The minor difference in model performance at both decadal and annual time scales with the increase of cross-section resolution suggests that details of channel cross-section do not have a significant effect on model prediction on streamflow volume or timing. This is likely due to the fact that channel routing is simulated through the kinematic wave equation in LSPC. As discussed in Chapter 2, the kinematic wave equation is one of the most basic forms of hydraulic routing which assumes that the friction slope is equal to the bed slope, and ultimately means that a unique roughness value from the bed slope was assigned to the entire reach. Since the reach slope and Manning's n values are unique for each reach, the discharge is calculated based on hydraulic radius which varies with the size of the cross-section and not with its shape. Therefore, the size of the cross-section and the reach slope drive the flow, however the shape of the transect is largely irrelevant.

Regardless of whether field-surveyed or digital-derived shapes of cross sections are employed in the modeling, no lateral (secondary flow) circulation occurs. Therefore, the simulated stream velocity and the timing of the streamflow, does not change. Finally, since the kinematic wave equation assumes a single stage-discharge relationship for the entire basin, the discharge does not vary in space. Model outputs were not sensitive to the field data used in the experimental scenario where data from a single surveyed cross-section was applied to all the reaches; this suggests that if surveyed transects are used, the number of cross-sections may have little effect on simulated streamflow in the LSPC model.

Overall, the results suggest that digitally-based cross sections can be a good alternative to using field surveys. If surveyed cross sections are used, apparently fewer cross-sections will not significantly impact the model flow predictions. These results are consistent with the results reported by Staley et al (2006) in which the authors found that, for 14 stream reaches in Virginia, the average daily discharge produced by HSPF model was not significantly sensitive to the use of surveyed cross sections versus digitally-derived topographic data, nor to the number of surveyed cross sections included in the model.

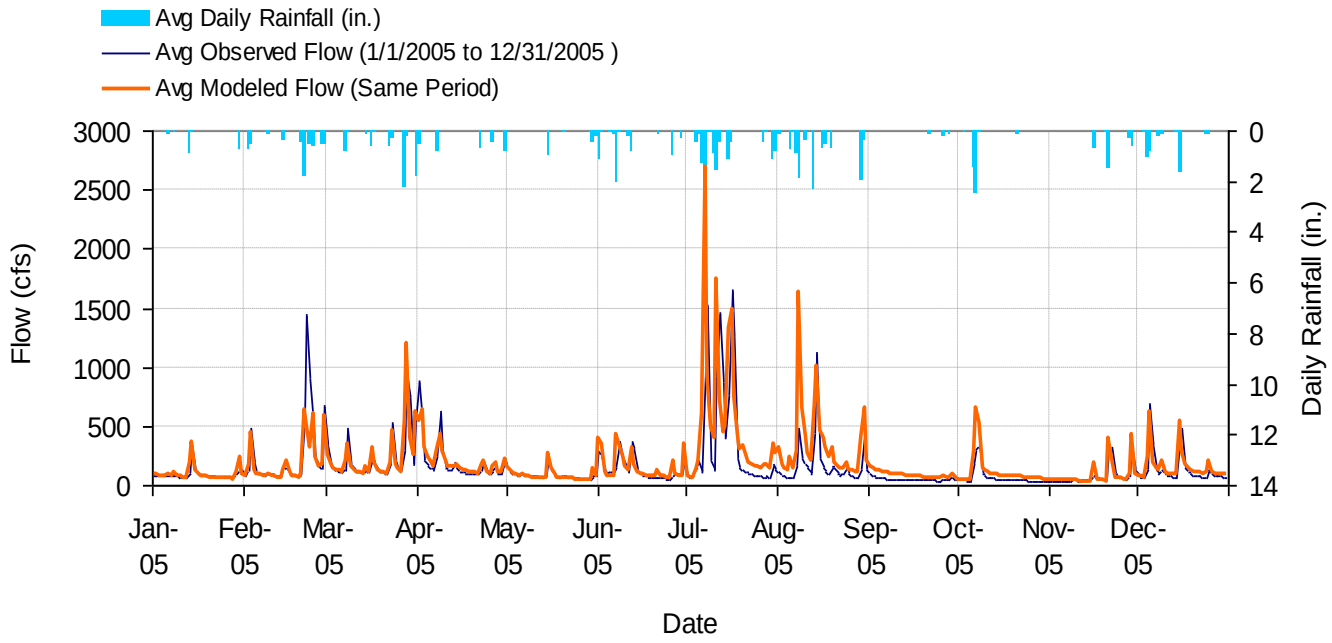

Figure 5.10 Mean daily flow for a wet year (2005): model outlet 7 vs. USGS 02335700 Big Creek near Alpharetta, GA Experimental scenario 0100: STRM30m, field-based FTABLEs, complete land use classification and GEMN270 meteorological station.

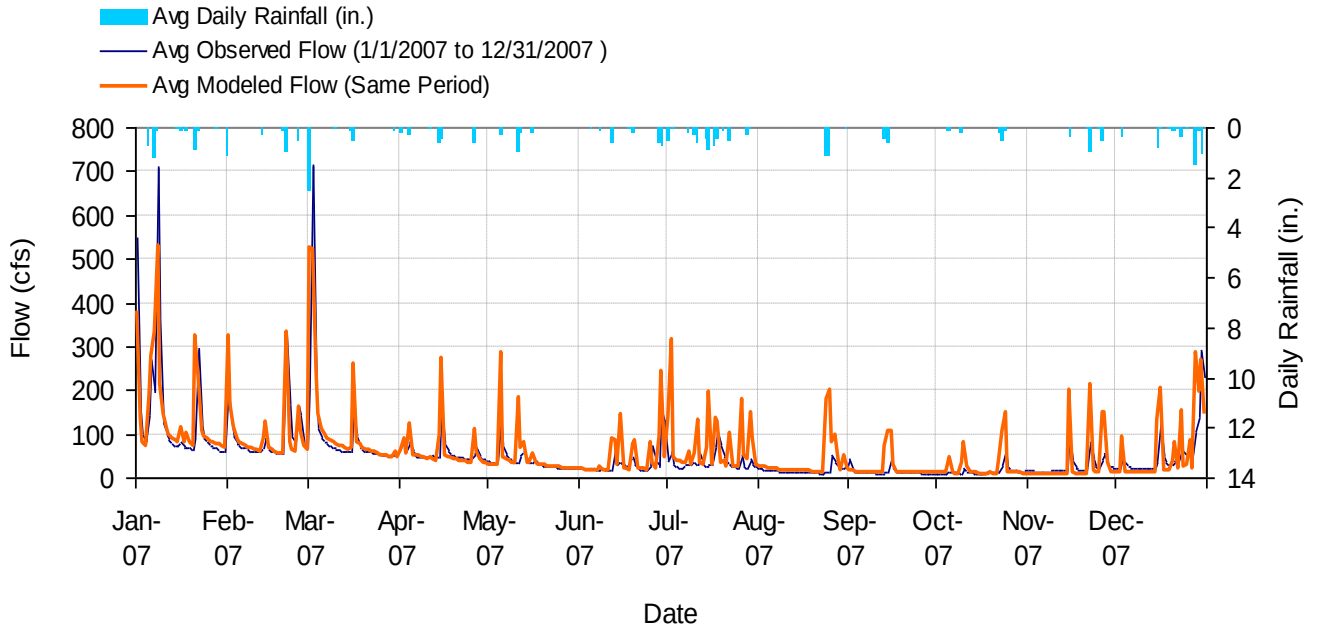

Figure 5.11 Mean daily flow for a dry year (2007): model outlet 7 vs. USGS 02335700 Big Creek near Alpharetta, GA. Experimental scenario 0100: STRM30m, field-based FTABLEs, complete land use classification and GEMN270 meteorological station.

Table 5.12 Comparative summary statistics for the scenarios with field- and digital- based FTABLES (scenarios 0000 and 0100, respectively) for a wet year (2005). Model Outlet 7 vs. USGS 02335700 Big Creek near Alpharetta, GA.

Errors in flow volumes (percent) ((Simulated-Observed)/Observed)*100)	LSPC Simulated Flow	
	Scenario 0000 Digital-based FTABLE	Scenario 0100 Field-based FTABLE
Error in total volume:	19.95	20.10
Error in 50% lowest flows:	20.02	21.46
Error in 10% highest flows:	7.52	6.90
Seasonal volume error - Summer:	48.41	48.75
Seasonal volume error - Fall:	23.79	23.88
Seasonal volume error - Winter:	-5.68	-5.72
Seasonal volume error - Spring:	7.49	7.64
Error in storm volumes:	8.90	7.16
Error in summer storm volumes:	22.15	21.27
Nash-Sutcliffe Coefficient of Efficiency	0.437	0.453

Table 5.13 Comparative summary statistics for the scenarios with field- and digital -based FTABLES (scenarios 0000 and 0100, respectively) for a dry year (2007). Model Outlet 7 vs. USGS 02335700 Big Creek near Alpharetta, GA.

Errors in flow volumes (percent) ((Simulated-Observed)/Observed)*100)	LSPC Simulated Flow	
	Scenario 0000 Digital–based FTABLE	Scenario 0100 Field-based FTABLE
Error in total volume:	21.20	21.09
Error in 50% lowest flows:	-1.92	1.72
Error in 10% highest flows:	22.13	19.51
Seasonal volume error - Summer:	96.17	95.85
Seasonal volume error - Fall:	24.99	24.14
Seasonal volume error - Winter:	5.83	6.03
Seasonal volume error - Spring:	18.09	17.85
Error in storm volumes:	63.32	59.25
Error in summer storm volumes:	298.30	283.84
Nash-Sutcliffe Coefficient of Efficiency	0.570	0.606

5.4 Meteorological data

Comparison of input parameters

Comparison of precipitation data between the baseline and experimental scenarios at the outlet USGS 235700, Big Creek near Alpharetta, GA indicated that the Atlanta airport station 090451, located south of both 092408 Cumming 1 ENE and GEMN270 station, had the lowest seasonal rainfall totals. Comparison of the average monthly precipitation values for the two scenarios from the same subbasin depicted that seasonal precipitation records from Atlanta airport station 090451 (assigned to the subbasin for the experimental scenario) were not at all congruent with values from the GEMN270 station (assigned to the subbasin for the baseline scenario) (Table 5.14). The Atlanta airport station 090451, which is located 50 km south of the Big Creek watershed, received 2.4 percent less rainfall in the spring, 2.09 percent less in the summer and 11.71 percent less in the fall season than the GEMN270 station, located 9 km from the watershed. Overall smaller amounts of precipitation recorded at the Airport station 090451 than at the GEMN270 station were consistent with a study by Diem and Mote (2004). The study was conducted within a 180 km radius of the Atlanta metropolitan area and illustrated that for previous decades southern stations experienced less precipitation than northern stations. Figure 5.12 illustrates that the difference in monthly and seasonal rainfall supply during 1998-2007 is translated into discrepancy of modeled hydrological outputs for the two scenarios. It is interesting to notice a general overprediction of the ‘low flow’ in the baseline scenario (GEMN270 station) and underprediction of high flow in the experiment scenario (Atlanta airport station 090451), which is probably caused by overall lower amount of precipitation recorded by Atlanta airport station in experiment scenario.

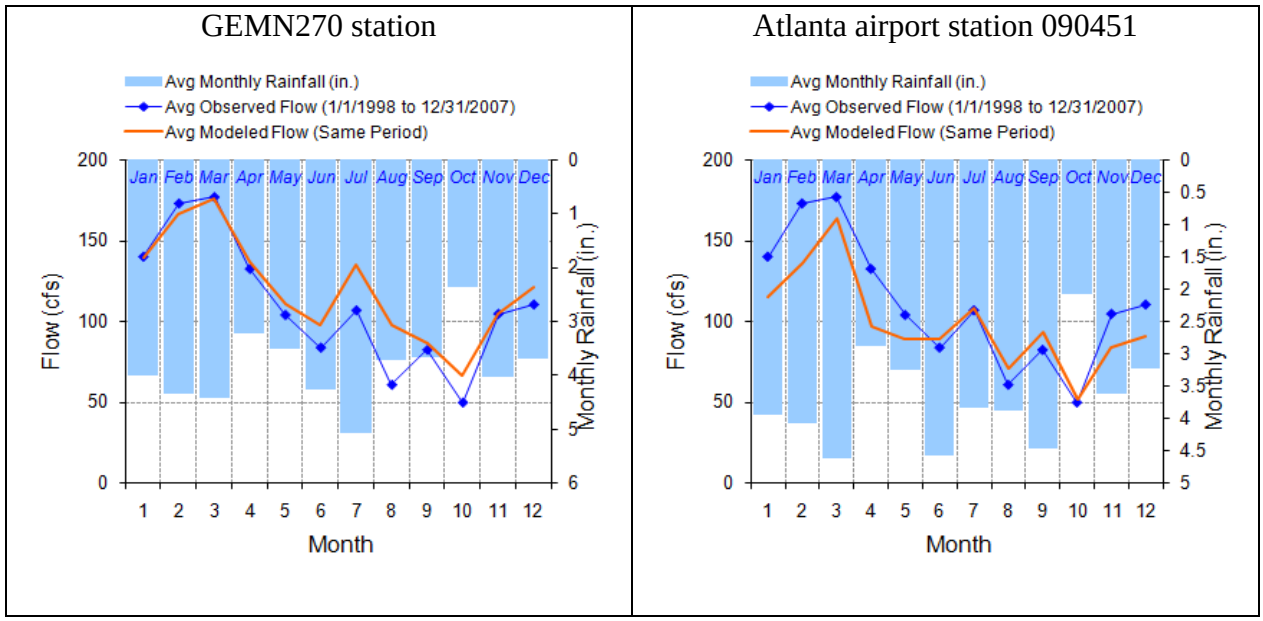

Figure 5.12 Seasonal temporal aggregate of the rainfall, observed and modeled flow at USGS 02335700 Big Creek near Alpharetta, GA

Table 5.14 Average monthly rainfall at GEMN270 and Atlanta Airport 090451 meteorological stations for the period from 1/1/1998 to 31/12/2007

Month	Average rainfall from 1/1/1998 to 31/12/2007 (inches)	
	GEMN270 station	ATL Airport 090451 station
Jan	3.99	3.93
Feb	4.33	4.07
Mar	4.42	4.6
Apr	3.2	2.88
May	3.5	3.24
Jun	4.25	4.56
Jul	5.06	3.83
Aug	3.7	3.88
Sep	3.66	4.45
Oct	2.36	2.07
Nov	4.03	3.62
Dec	3.69	3.21

LSPC Output Comparison

The 10-year streamflow predictions from the experimental scenario (Atlanta airport station 090451 only), were compared to model predictions from the baseline scenario (GEMN 270 station). Table 5.15 shows the average annual simulated flow volumes for the two scenarios, and the predictive error is summarized in Table 5.16. The total in-stream flow simulated for the 10-year period (1998-2007), based on the rainfall readings from Atlanta airport station 090451, was 4.91 inches/year (18.82%) less than the flow simulated from the GAEMN 270 station.

Table 5.15 The average annual simulated flow volumes and its components for scenarios with meteorological stations of different proximity to the Big Creek watershed: GEMN270 station, (scenario 0000) and Atlanta Airport 090451, (scenario 0001). Model Outlet 7 vs

Flow volumes inches/year	LSPC Simulated Flow	
	Scenario 0000 GEMN270	Scenario 0001 ATL Airport
Total In-stream Flow:	22.60	18.69
Highest 10% flows:	9.47	8.60
Lowest 50% flows:	3.57	2.57
Summer Flow Volume	5.08	4.33
Fall Flow Volume	4.63	3.59
Winter Flow Volume	7.47	6.46
Spring Flow Volume	5.41	4.32
Storm Volume:	9.73	8.86
Summer Storm Volume	2.53	2.54

Table 5.16 Comparative statistics for scenarios with meteorological stations of different proximity to the Big Creek watershed: GEMN270 station, (scenario 0000) and Atlanta Airport 090451, (scenario 0001). Model Outlet 7 vs. USGS 02335700 Big Creek near Alphare

Errors in flow volumes (percent) (Simulated-Observed)/Observed)*100	LSPC Simulated Flow	
	Scenario 0000 GEMN270	Scenario 0001 ATL Airport
Error in total volume:	8.76	-10.06
Error in 50% lowest flows:	9.23	-21.57
Error in 10% highest flows:	-3.13	-12.11
Seasonal volume error - Summer:	28.29	9.19
Seasonal volume error - Fall:	10.51	-14.43
Seasonal volume error - Winter:	-1.75	-15.05
Seasonal volume error - Spring:	7.80	-14.05
Error in storm volumes:	2.77	-6.40
Error in summer storm volumes:	19.81	20.36
Nash-Sutcliffe Coefficient of Efficiency	0.655	0.100

In order to explore the sensitivity of the flow to precipitation records from the Airport station 090451, a comparison of the model output for both wet (2005) and dry (2007) years was conducted; the resulting hydrographs are shown in Figures 5.1 and 5.13 for the wet year, and Figures 5.2 and 5.18 for the dry year, and the error for the two scenarios is summarized in Tables 5.17 and 5.18. While flow predictions for the experimental scenario were poor relative to both observed and predicted (baseline) discharges at the annual time scale, seasonal flow patterns generally matched the predicted (experimental) results. Specifically, average flows in February were over predicted, while flows in March, July and August were under predicted, and the timing and intensity of storms in September and October were significantly different. Overall, the accuracy of model performance according to Nash Sutcliff coefficient for the 10-year period was higher by 0.555 for the baseline scenario. The difference in meteorological conditions of Atlanta metropolitan area is responsible for poor LSPC performance at Big Creek watershed at time scales ranging from the entire period of study to annual in the experimental scenario, when rainfall data from the Atlanta airport station 090451 were used for the entire Big Creek watershed. This underscores the fact that LSPC is a precipitation-driven model and that an appropriately-detailed representation of precipitation is required to produce reliable model output. Differences in precipitation data between the stations also underscore the need of taking into consideration additional local factors that may drive precipitation in the watershed of study (local lifting mechanisms, heat island effect, etc).

A more detailed statistical analysis comparing predicted and observed values for the experimental scenario are presented in Appendix E to facilitate more detailed qualitative and quantitative evaluations.

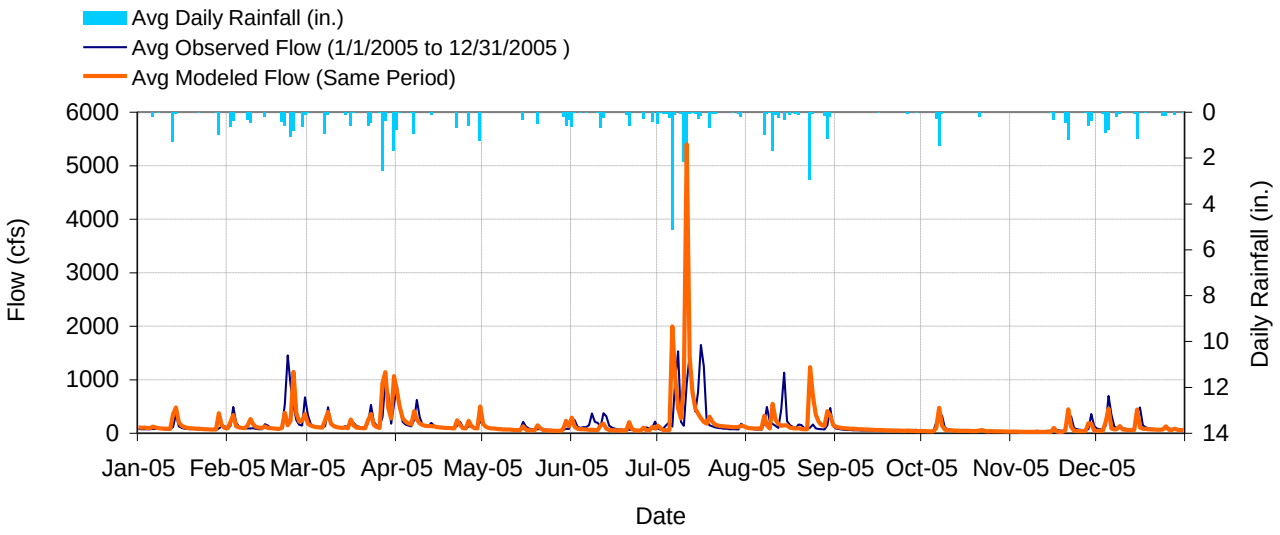

Figure 5.13 Mean daily flow for a wet year (2005): model outlet 7 vs. USGS 02335700 Big Creek near Alpharetta, GA Experimental scenario 0001: STRM30m, field-based FTABLEs, complete land use classification and Atlanta Airport 090451 meteorological station.

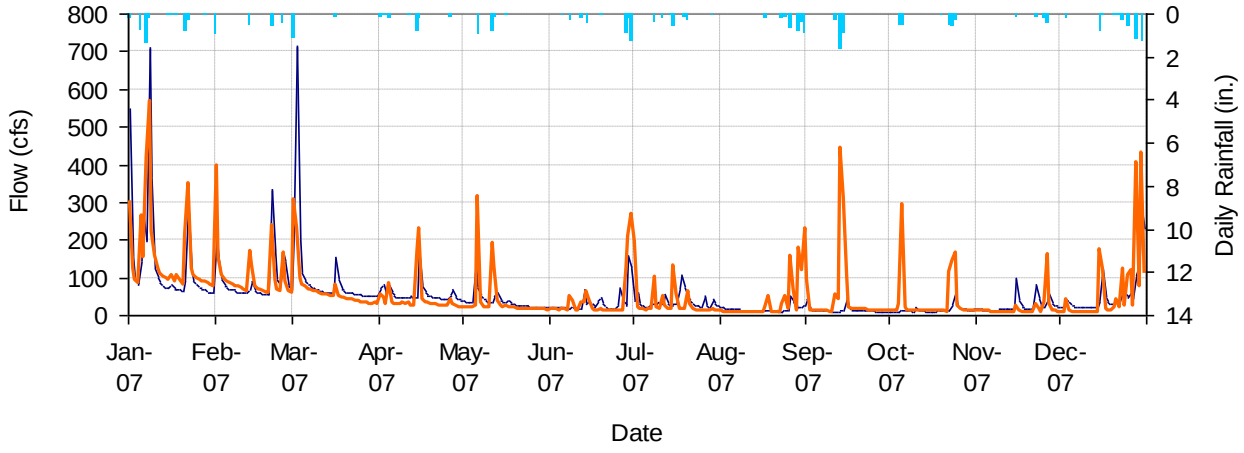

Figure 5.14 Mean daily flow for a dry year (2007): model outlet 7 vs. USGS 02335700 Big Creek near Alpharetta, GA Experimental scenario 0001: STRM30m, field-based FTABLEs, complete land use classification and Atlanta Airport 090451 meteorological station.

Table 5.17 Comparative summary statistics for the scenarios with complete and reduced assignment of meteorological stations (scenarios 0000 and 0001, respectively) for a wet year (2005).

Errors in flow volumes (percent) (Simulated-Observed)/Observed)*100	LSPC Simulated Flow	
	Scenario 0000 Complete met data	Scenario 0001 Reduced met data
Error in total volume:	20.10	2.77
Error in 50% lowest flows:	21.46	-7.31
Error in 10% highest flows:	6.90	8.81
Seasonal volume error - Summer:	48.75	25.50
Seasonal volume error - Fall:	23.88	-23.99
Seasonal volume error - Winter:	-5.72	1.92
Seasonal volume error - Spring:	7.64	-12.86
Error in storm volumes:	7.16	4.56
Error in summer storm volumes:	21.27	26.37
Nash-Sutcliffe Coefficient of Efficiency	0.453	-0.984

Table 5.18 Comparative summary statistics for the scenarios with complete and reduced assignment of meteorological stations as (scenarios 0000 and 0001, respectively) for a dry year (2007).

Errors in flow volumes (percent) (Simulated-Observed)/Observed)*100	LSPC Simulated Flow	
	Scenario 0000 Complete met data	Scenario 0001 Reduced met data
Error in total volume:	21.09	7.51
Error in 50% lowest flows:	1.72	-25.86
Error in 10% highest flows:	19.51	21.20
Seasonal volume error - Summer:	95.85	67.40
Seasonal volume error - Fall:	24.14	22.05
Seasonal volume error - Winter:	6.03	-4.16
Seasonal volume error - Spring:	17.85	-5.35
Error in storm volumes:	59.25	50.68
Error in summer storm volumes:	283.84	305.68
Nash-Sutcliffe Coefficient of Efficiency	0.606	0.263

5.5 Sensitivity analysis

In order to avoid limitations associated with the use of a single statistical index of model performance (as described in the Methods section), comparison of the accuracy of model performances was estimated by using both the Nash-Sutcliffe coefficient (NS) and the average error in the simulated total flow volumes (AE) relative to the observed flow for the 10-year study period (1997-2008). Figure 5.15 illustrates the comparative analysis of model performance for the 16

scenarios for both NS and AE; high values of NS correspond with low values of AE. The experimental scenarios that have the least error in simulated discharge (with the correspondingly highest NS coefficients) are associated with the coarser DEM resolution (scenario 1000) and the use of a surveyed cross-section for the representative reach (scenario 0100). Even when these two factors are combined in an experimental scenario (scenario 1100), the AE and NS coefficients are only 0.01 percent different than the baseline scenario (scenario 0000).

The scenario with the simplified land use classification (scenario 0010) had a fairly high degree of error in flow volume (24.12 percent). However, when combined with the simplified DEM and surveyed cross-section scenarios, the error actually decreased slightly (by 0.12 percent), thereby improving the predictive performance. The scenario with the highest average error was the experimental rainfall scenario (0001) that was associated with reduced availability of meteorological station and the use of rainfall data from the Atlanta airport station for the entire study area. The average error in predicted flow for all the other scenarios that used data from the Airport station is above 10 percent: AE (scenario 0001)=13.69 percent, AE (scenario 1001)=13.68 percent, AE (scenario 0011)=41.82 percent, AE (scenario 0101)=13.61 percent, AE (scenario 0111)=41.74 percent, AE (scenario 1101)=13.6 percent, AE (scenario 1011)=41.84 percent, AE (scenario 1111)=41.77 percent. According to the Nash-Sutcliff coefficients, the model's poorest performance is also associated with all the scenarios using data from Atlanta airport station, varying from 0.1 to 0.223. High sensitivity of the model to the resolution of meteorological data underscores that LSPC is a precipitation-driven model and suggests that representative meteorological data are a critical component of the modeling effort.

Following the goal of the study to determine the optimal data density for the input parameters of the LSPC model, these results indicate that scenarios with coarser 90 m DEM reso-

lution, and digital-derived cross-sections, most successfully predict runoff with the least error among all the scenarios; therefore data density of these two input parameters reduced according to the experimental scenarios, could potentially be the minimum data density required for prediction of the flow volume in locations similar to Big Creek watershed. As shown in Figure 5.15, the minimum resolution of the input parameters that is required to obtain less than 15 percent error in prediction of the total flow volume plus a Nash Sutcliff model efficiency greater than 0.5, is obtained using the 90 m DEM and/or digital-derived cross sections– scenarios 1000, 0100, 1100. In order to have less than 25 percent error in the prediction of total flow over a 10-year period and an accuracy higher than 0.5 for the Nash Sutcliff coefficient, a 90 m DEM, a single surveyed representative cross-section for the watershed of study, and a simplified land use classification scheme can be used. In fact, the Nash-Sutcliff coefficient was above 0.5 for each of the scenarios associated with the reduced land use classification (0010, 0110). However, an average error in total flow of 25 percent indicates a large variance in predicted flow output for the scenarios associated with the reduced land use classification. Additionally, the annual hydrograph analysis pointed out a significant difference in storm and baseflow volumes, which decreases by over 100 for the dry year in scenario 0010 (Table 5.9). Therefore, land use classification should include at least an approximate percentage of imperviousness in order to accurately predict base flow and storm flow at the annual time scale.

When a hydrologic model is used to estimate flow response for a watershed from data poor environment, every effort is taken to make a full use of input data that is available. Results of this research depict that resolution of input parameters has a significant impact on the outputs of the distributed hydrologic model that was used in the study (LSPC model). On the one side, it is desirable to have as much detailed input data as possible; on the other side – data availability

and cost of data collection defines resolution of the input parameters. A comparison of the Nash–Sutcliff model efficiency coefficient and the error in flow volume in LSPC model predictions, brought by various resolutions of DEM, land use, level of details of channel's cross-section and meteorological stations, indicated that LSPC model was the most sensitive to selection of meteorological stations and the land use classification. Difference in seasonal and monthly precipitation supply at GEMN 270 station and Atlanta airport station induced most of the difference between flow predictions in the baseline and the experiment scenarios. It suggests that selection of weather stations, which are representative of the weather condition in the watershed of study, is crucial for accurate flow predictions with the LSPC model. Simplified land use classification used in the experiment scenario had relatively high Nash–Sutcliff model efficiency coefficient and a high error in prediction of the total flow volume, which indicates that an effort should be made to provide data on percent of impervious cover to minimize errors in the model predictions. Level of data detail used to develop both channel cross sections (FTABLEs) and topography had insignificant impact on the prediction of the flow volume. Both field-measured and digitally-derived cross-section characteristics and the DEM resolutions of 30 m to 90 m produce a correspondingly small amount of error at the decadal time scale, which suggests that digital-derived channel cross-section and a 90 m DEM may be viable substitutes to the field-based cross sections and 30m DEM, when simulating flow volumes with the LSPC model in data poor environments. Overall, results of this study indicate that less effort may be made to find DEM data at a finer resolution and to survey channel cross section in order to provide efficient model predictions with the LSPC model in the watersheds similar to the Big Creek. Instead more efforts should be made to collect data on impervious cover and to find weather gages that would better represent the land use and weather conditions in the watershed.

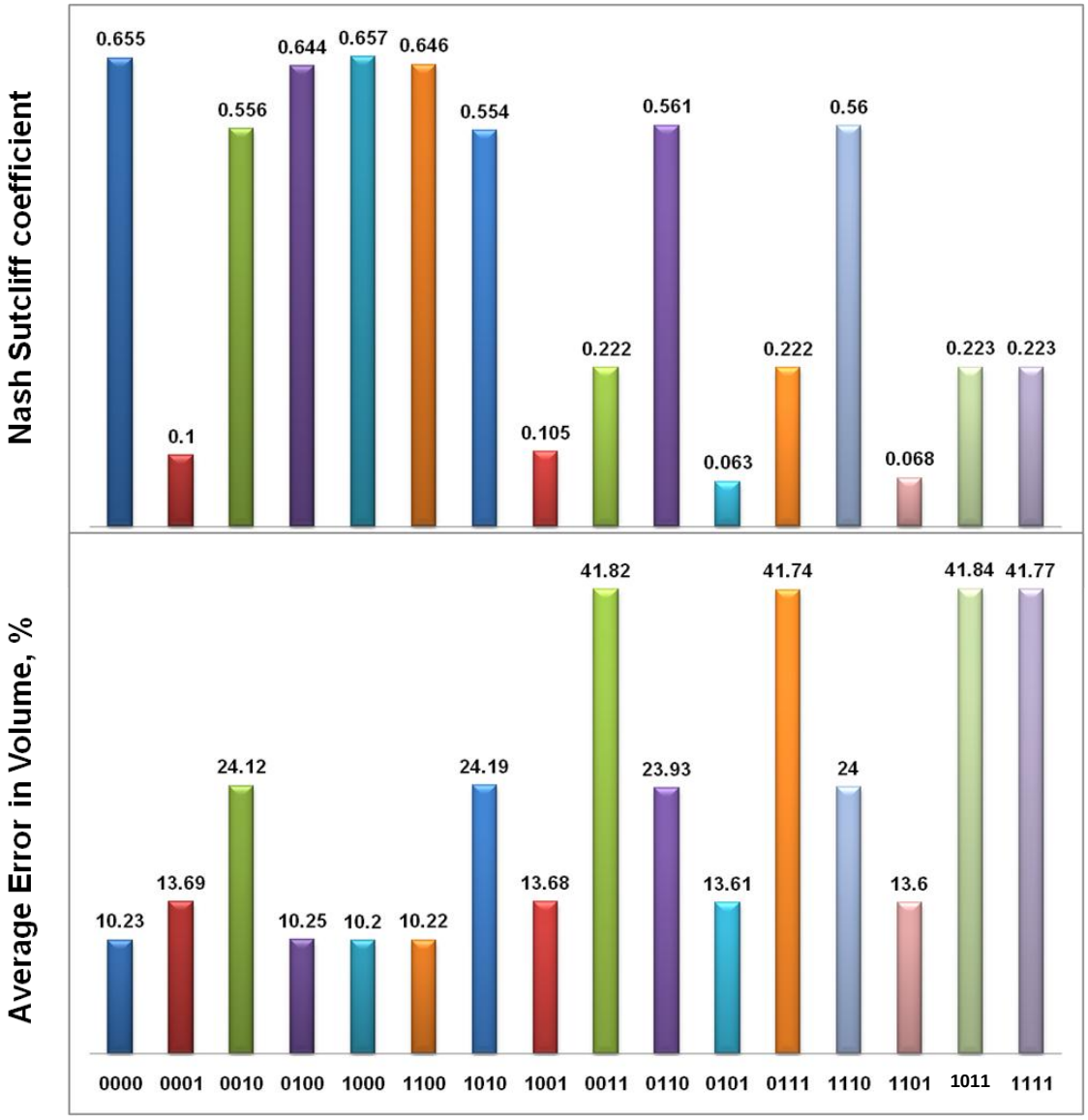

Scenarios:
0000 : NED30m, field-based FTABLES, complete land use classification, and GEMN270 station;
0001: STRM30m, field-based FTABLEs, complete land use classification, and Atlanta Airport 090451 station;
0010: STRM30m, field-based FTABLEs, simplified land use classification, and GEMN270 station;
0100: STRM30m, digital-based FTABLEs, complete land use classification, and GEMN270 station;
1000: STRM90m, field- based FTABLEs, complete land use classification, and GEMN270 station;
1100: STRM90m, digital-based FTABLEs, complete land use classification, and GEMN270 station;
1010: STRM90m, field-based FTABLES, simplified land use classification, and GEMN270 station;
1001: STRM90m, field-based FTABLES, complete land use classification, and Atlanta Airport 090451 station;
0011: NED30m, field-based FTABLES, simplified land use classification, and Atlanta Airport 090451 station;
0110: NED30m, digital-based FTABLEs, simplified land use classification, and GEMN270 station;
0101: NED30m, digital-based FTABLEs, complete land use classification, and Atlanta Airport 090451 station;
0111: NED30m, digital-based FTABLEs, simplified land use classification, and Atlanta Airport 090451 station;
1110: STRM90m, digital-based FTABLEs, simplified land use classification, and GEMN270 station;
1101: STRM90m, digital-based FTABLEs, complete land use classification, and Atlanta Airport 090451 station;
1011: STRM90m, field-based FTABLES, simplified land use classification, and Atlanta Airport 090451 station;
1111: STRM90m, digital-based FTABLEs, simplified land use classification and Atlanta Airport 090451 station.

Figure 5.15 Nash Sutcliff coefficient and the average error in total volume for the 16 scenarios run in the study

6 SUMMARY AND CONCLUSIONS

When distributed models are used to evaluate the hydrologic response of a watershed in ungaged, data poor environments, every effort must be taken to make full use of whatever available input data exists. The data available in such watersheds are often of poor spatial or temporal resolution; additionally, high costs associated with data collection preclude obtaining as much detailed data as would often be desirable. A central goal of this study was to identify ways to increase model efficiency by applying reduced resolution spatial data without sacrificing significant model reliability, and to develop a tool that may be transferable to ungaged watersheds.

The Big Creek watershed, a 186.4 km^2 urbanizing watershed near Atlanta, GA, for which all input parameters at high resolution are available (land use coverage, watershed segmentation, soils coverage, meteorological data resolution, and stream reach characteristics) was used to run the LSPC distributed hydrological model for a 10 year period (1998-2007). First, the full range of spatially-distributed input parameters at the highest available resolution, as well as the measured stream discharge at a USGS gauge to establish the baseline conditions was used. Then an output sensitivity matrix was developed by evaluating the effects of downscaling (in resolution) the four potential influential spatial input variables: land use coverage, watershed segmentation, meteorological data resolution, and stream reach characteristics. Overall, 16 permutations were required to identify which reduction of variables most successfully predicts runoff with the least error.

Results of this study indicate that resolution of some input data has more significance on model accuracy than others. The findings of this study can be summarized in following ways.

1. A comparison of the Nash Sutcliff coefficient of model efficiency and absolute error in the LSPC model predictions determined that switching from a DEM of 30 m to 90 m affected

LSPC outputs by a 0.20 percent decrease in the mean subbasin slope and a 28.39 percent decrease in the mean reach slope. These changes resulted in a minor decrease in the error for summer storm flows at the annual time scale (0. 0.008 percent) and in 0 – 0.01 percent change of the accuracy of predicting the total flow volume at the decadal time scale. The insignificant impact of coarsening the DEM resolution on flow volumes may be due to unaltered area of subbasins and reaches lengths, therefore. More research considering redeliniation of subbasins and variation of reaches lengths may be considered when evaluating the effect of DEM resolutions on LSPC outputs in the future. This study demonstrated that, at least for the Big Creek watershed, the mean slope plays a minor role in runoff output for the LSPC model, and smoothing the DEM from 30 m to 90 m resolution does not substantively affect the hydrological simulations, which suggests that a 90 m DEM may be a viable substitute when simulating annual and/or decadal flow volumes with the LSPC model.

2. Both field-measured and digitally-derived cross-section characteristics produce a correspondingly small amount of error at decadal time scales. The field-based FTABLES were developed using a surveyed cross-section data and digital based FTABLES were calculated using Rosgen method and Manning's equation; the stage-discharge relations below bankfull for both scenarios were similar. Increased topographic complexity of the surveyed cross-section in the field-based scenario had a stronger impact on the simulation of storm flow at the annual time scale. The error in summer storm volumes were higher by almost 15 percent, likely due to the floodplain not being physically surveyed but computed based on the stage-discharge relationship for bankfull elevations. Overall, the low percent error related to the data resolution incorporated in the cross-section suggests that the method used to develop FTABLEs did not have a significant effect on the prediction of total flow in a small wa-

tershed similar to Big Creek. Therefore, depending on data availability, an LSPC modeler may have flexibility to choose between digital- or field- based FTABLE while simulating total flow volume at annual and decadal time scales.

3. Flow predictions were significantly affected by land use classification. Even thought the LSPC scenario with a unique class for developed land use that neglected to incorporate the degree of imperviousness resulted in an increase in error of only 13.91 percent for total flow, the difference in error was more pronounced when estimating storm and baseflow at the annual time scales. With the simplified land use classification, the prediction error for storm flow and baseflow changed by over 100 percent, for the dry year. The large impact of land use classification on the flow predictions can be explained by the high level of urbanization in the watershed of study (Big Creek is an urbanizing watershed with 27 percent impervious cover). The demonstrated significant sensitivity of storm and base flow to the simplified land use classification schemes at the annual time scale suggests that when LSPC is used to evaluate the response of flow components (i.e. baseflow, storm flow), a full land cover classification including detailed percentage of the impervious cover may be crucial.
4. The meteorological data resolution was the most sensitive input variable and affected flow predictions at both annual and decadal time scales. Even though the difference in error of flow prediction associated with the sole use of the Atlanta airport weather station is not significant (3.46 percent), the goodness of fit of the hydrograph with the baseline scenario is extremely low (Nash Sutcliff coefficient is 0.1). A visual comparison of the hydrograph illustrated inconsistencies at both decadal and annual time frames, which suggests that the Airport station is not representative of the area and therefore, allocation of rainfall gages in

close proximity to the watershed of study is the key for an accurate flow prediction with LSPC.

5. The minimum resolution input data required to achieve 25 percent model output error (or less) and a Nash-Sutcliff coefficient higher than 0.5 in the Big Creek watershed were the following: a 90 m resolution DEM, a single surveyed representative cross section, a simplified land cover classification with combined developed land use classes, and a weather station in close proximity to the watershed.

Overall, sensitivity of the LSPC model to variations in land use classification, resolution of the digital elevation model, meteorological data resolution, and complexity of stream reach characteristics presented above indicate that if simulating total flow in data poor environment and conditions similar to the Big Creek watershed, efforts should be made to find or even add rainfall gages and collecting detailed data on land use (and impervious cover, in particular) rather than spending limited resources obtaining high resolution DEMs and transect characteristics.

7 IMPLICATIONS AND FURTHER DEVELOPMENTS

The findings of this study are important for the hydrological community since the use of LSPC models is expected to increase in the future, as it became a part of the Better Assessment Science Integrating Point and Nonpoint Sources (BASINS) modeling framework and is supported by the U.S. Environmental Protection Agency (USEPA) for TMDL development (Di Luzio et al., 2002). Given the sensitivity analysis of LSPC to the resolution of the input parameters presented in this study, it appears that this watershed management tool may be further developed and used in data poor regions of the world with inadequate hydrological monitoring capabilities. By exploring how sensitive the model is to variations in scale of topographic and

meteorological input parameters, this study illustrated that rainfall distribution is essential for reliable hydrologic prediction which indicates that our ability to predict flow volume in ungaged watersheds strongly depends on the development of rain gage networks. It's believed that findings of this study will contribute to the improvement and/or development of rain gage networks in data poor environments and will overall support our ability to estimate discharge in the ungaged watersheds.

Modelers running the LSPC model will also benefit from the sensitivity analysis presented in this study since it determined the environmental factors that significantly / insignificantly affect the variation of the model output. Knowing that, model performance may be improved by prioritizing measurements of rainfall data, whereas reducing the scale of DEM and details of cross-section characteristics is less significant.

The study can be further advanced by running similar analyses for other topographic and climatic conditions with the goal to develop an understanding the essential features of hydrological models under various environmental conditions. As earlier mentioned, more studies considering re-deliniation of subbasins may be considered in the future when evaluating the effect of DEM resolutions on LSPC outputs. Exploring sensitivity of the model to the temporal resolution of input data may be another interesting point for further research, since LSPC is commonly used for the long term time series data input. As indicated in the 'discussions', the model was sensitive to representation of impervious cover in the experiment land use scenario and, therefore, data on land use change over time may need to be incorporated in simulations to minimize the errors in flow predictions.

REFERENCES

Abbott, M.B., and J.C. Refsgaard. 1996. *Distributed hydrological modeling*. Springer.

Arnold, J.G., R. Srinivasan, R.S. Muttiah, and J.R. Williams. 1998. Large area hydrologic modeling and assessment Part I: Model development. *J. of the American Water Resource Assoc.* 34(1):73-89.

Arnold, J G, M W Van Liew, R L Bingner, R D Harmel, T L Veith, and D N Moriasi. 2007. Model evaluation guidelines for systematic quantification of accuracy in watershed simulations. *Transactions Of The Asabe* 50, no. 3: 885-900.

Arcement, G.J., Jr., and V.R.,Schneider, 1989. *Guide for selecting Manning's roughness coefficients for natural channels and flood plains.* U.S. Geological Survey Water-Supply Paper 2339. 38 p.

Bertrand-Krajewski, J.L.., S. Barraud, and B. Chocat. 2000. Need for improved methodologies and measurements for sustainable management of urban water systems. *Environmental Impact Assessment Review* 20, no. 3: 323-331. doi:10.1016/S0195-9255(00)00044-5.

Beven, K. J. 2000. *Rainfall-runoff modeling : the Primer*. Chichester, UK .

Beven, K. J, and M.J Kirkby. 1979. A physically based, variable contributing area model of basin hydrology. *Bulletin of the International Association of Scientific Hydrology* 24, no. 1: 43.

Bhaduri, B., J. Harbor, B. Engel, and M. Grove. 2000. Assessing Watershed-Scale, Long-Term Hydrologic Impacts of Land-Use Change Using a GIS-NPS Model. *Environmental Management* 26, no. 6 (12): 643-658. doi:10.1007/s002670010122.

Bicknell, B. R., J. C. Imhoff, A. S. Donigian, and R. C. Johanson. 1997. Hydrological simulation program-FORTRAN (HSPF): User's manual for release 11. EPA-600/R-97/080. Athens, GA: U.S. Environmental Protection Agency.

Blöschl, G., R. B. Grayson, and M. Sivapalan. 1995. On the representative elementary area (REA) concept and its utility for distributed rainfall-runoff modelling. *Hydrological Processes* 9, no. 3-4 (4): 313-330. doi:10.1002/hyp.3360090307.

Brashear, R., J. Santo, and T. Stanko. 2001. Development of s a sustainable water resource for the Big Creek watershed. In . University of Georgia: Hatcher K.J., 26-27 3.

Brasington, J., and K. Richards. 1998. Interactions between model predictions, parameters and DTM scales for topmodel. *Computers & Geosciences* 24, no. 4 (May 15): 299-314. doi: 10.1016/S0098-3004(97)00081-2.

Chaubey, I., A. S. Cotter, T. A. Costello, and T. S. Soerens. 2005. Effect of DEM data resolution on SWAT output uncertainty. *Hydrological Processes* 19, no. 3 (2): 621-628. doi:10.1002/hyp.5607.

Chen, X., Y.D. Chen, and C.Y. Xu. 2007. A distributed monthly hydrological model for integrating spatial variations of basin topography and rainfall. *Hydrological Processes* 21, no. 2 (1): 242-252. doi:10.1002/hyp.6187.

Cho, S-M, and M. W. Lee. 2001. Sensitivity considerations when modeling hydrologic processes with digital elevation model. *Journal of the American Water Resources Association* 37, no. 4 (8): 931-934. doi:10.1111/j.1752-1688.2001.tb05523.x.

Coon, W.F., 1998. *Estimation of roughness coefficients for natural stream channels with vegetated banks.* U.S. Geological Survey Water-Supply. Paper 2441.133 p.

Crawford N.H., and Linsley R. K. 1966. *Digital Simulation in Hydrology: The Stanford Watershed Model IV*. Tech. Rep. Palo Alto, CA: Stanford University.

Diem J.E., T.L. Mote. 2005. Interepochal changes in summer precipitation in the southeastern United States: Evidence of possible urban effects near Atlanta, Georgia. *Journal of Applied Meteorology* 44:717-73

Donigian, A.S. Jr., J.C. Imhoff, B.R. Bicknell and J.L. Kittle. 1984. *Application Guide for Hydrological Simulation Program - Fortran (HSPF)*, prepared for U.S. EPA, EPA-600/3-84-065, Environmental Research Laboratory, Athens, GA.

Fisher, P. F., and N. J. Tate. 2006. Causes and consequences of error in digital elevation models. *Progress in Physical Geography* 30, no. 4: 467 -489. doi:10.1191/0309133306pp492ra.
Göncü, S., and E. Albek. 2009. Modeling Climate Change Effects on Streams and Reservoirs with HSPF. *Water Resources Management* 24, no. 4 (6): 707-726.

Grayson, R., and G. Blöschl. 2001. *Spatial patterns in catchment hydrology: observations and modelling*. CUP Archive, August 6.

Gregory, K.J.. 2006. The human role in changing river channels. *Geomorphology* 79: 172-191.

Gupta, H. V., S. Sorooshian, and P. O. Yapo. 1999. Status of automatic calibration for hydrolog ic models: Comparison with multilevel expert calibration. *J. Hydrologic Eng.* 4(2): 135-143.

Hughes, D.A., and K. Sami. 1994. A semi-distributed, variable time interval model of catchment hydrology-structure and parameter estimation procedures. *Journal of Hydrology* 155, no. 1-2: 265-291. doi:10.1016/0022-1694(94)90169-4.

Jakeman, A. J., and G. M. Hornberger. 1993. How much complexity is warranted in a rainfall-runoff model? *Water Resources Research* 29, no. 8: PP. 2637-2649. doi:199310.1029/93WR00877.

IDRISI Klimanjaro. 2004. *Guide to GIS and Image Processing Volume 2*, Idrisi Production, Clark Labs,USA, pp.57-8

Legates, David R., and Gregory J. McCabe Jr. 1999. Evaluating the use of "goodness-of-fit" Measures in hydrologic and hydroclimatic model validation. *Water Resources Research* 35, no. 1: PP. 233-241. doi:199910.1029/1998WR900018.

Lin, S., C. Jing, V. Chaplot, X. Yu, Z. Zhang, N. Moore, and J. Wu. 2010. Effect of DEM resolution on SWAT outputs of runoff, sediment and nutrients. *Hydrology and Earth System Sciences Discussions* 7, no. 4 (7): 4411-4435. doi:10.5194/hessd-7-4411-2010.

Lumb, A.M., McCammon, R.B., and Little, J.L., Jr 1994. *Users manual for an expert system (HSPEXP) for calibration of the Hydrological Simulation Program-FORTRA.*: U.S. Geological Survey Water-Resources Investigations Report 94-4168: 102 p.

Maidment, D. 2002. *Arc Hydro: GIS for Water Resources*. Esri Press, August 1.

McDonnell, J. J., M. Sivapalan, K. Vaché, S. Dunn, G. Grant, R. Haggerty, C. Hinz, et al. 2007. Moving beyond heterogeneity and process complexity: A new vision for watershed hydrology. *Water Resources Research* 43, no. 7 (7). doi:10.1029/2006WR005467.

Mendoza, M., G. Bocco, and M. Bravo. 2002. Spatial prediction in hydrology: status and implications in the estimation of hydrological processes for applied research. *Progress in Physical Geography* 26, no. 3 (9): 319-338. doi:10.1191/0309133302pp335ra.

Mishra, A., S. Kar, and V. P. Singh. 2007. Determination of runoff and sediment yield from a small watershed in sub-humid subtropics using the HSPF model. *Hydrological Processes* 21, no. 22 (10): 3035-3045. doi:10.1002/hyp.6514.

Nash, J.E., and J.V. Sutcliffe. 1970. River flow forecasting through conceptual models part I -- A discussion of principles. *Journal of Hydrology* 10, no. 3: 282-290.
NRCS (Natural Resource Conservation Service), 2004. National Water Management Center. Regional Hydraulic Geometry Curves.
http:/wmc.ar.nrcs.usda.gov/technical/HHSWR/Geomorphic/ accessed on March 10, 2011.

Olsen, D. S., A. C. Whitaker, and D. F. Potts. 1997. Assessing stream channel stability thresholds using flow competence estimates at bankfull stage. *Journal of the American Water Resources Association* 33, no. 6 (12): 1197-1207. doi:10.1111/j.1752-1688.1997.tb03546.x.

Parrett, C., R. J. Omang, and J. A. Hull. 1983. *Mean Annual Runoff and Peak Flow Estimates Based on Channel Geometry of Streams in Northeastern and Western Montana.* USGS Open File Report 83-4046. Helena. Montana. 53 pp.

Rose, S., and N. E. Peters. 2001. Effects of urbanization on streamflow in the Atlanta area (Georgia, USA): a comparative hydrological approach. *Hydrological Processes* 15, no. 8 (6): 1441-1457.

Rosgen, D. 1994. A classification of natural rivers. *Catena* 22, no. 3: 169-199.

Ryu, J. H. 2009. Application of HSPF to the Distributed Model Intercomparison Project: Case Study. *Journal of Hydrologic Engineering* 14, no. 8: 847.

Saltelli, A., K. Chan, and M. Scott (Eds.) 2000. *Sensitivity Analysis*. Wiley Series in Probability and Statistics. New York: John Wiley and Sons.

Santhi, C, J. G. Arnold, J. R. Williams, W. A. Dugas, R. Srinivasan, and L. M. Hauck. 2001. Validation of the SWAT model on a large river basin with point and nonpoint sources. *J. American Water Resources Assoc.* 37(5): 1169-1188.

Saxe, J. G. 1963. *The Blind Men and the Elephant; John Godfrey Saxe'sVersion of the Famous Indian Legend*. Whittlesey House, New York.

Soil Conservation Service (SCS). *Urban Hydrology for Small Watersheds*. Tech. Release 55, Washington, DC. 1986. Available online at http://www.wcc.nrcs.usda.gov/water/quality/common/tr55/tr55.pdf [Accessed March 10, 2011].

Singh, V. P. 1996. *Kinematic Wave Modeling in Water Resources, Surface-Water Hydrology*. Wiley-Interscience

Sivakumar, B.. 2004. Dominant processes concept in hydrology: moving forward. *Hydrological Processes* 18, no. 12 (8): 2349-2353. doi:10.1002/hyp.5606.

———. 2008. The more things change, the more they stay the same: the state of hydrologic modelling. *Hydrological Processes* 22, no. 21 (10): 4333-4337. doi:10.1002/hyp.7140.

Sivapalan, M. 2003. Prediction in ungauged basins: a grand challenge for theoretical hydrology. *Hydrological Processes* 17, no. 15 (10): 3163-3170. doi:10.1002/hyp.5155.

Sivapalan, M., K. Takeuchi, S. W. Franks, V. K. Gupta, H. Karambiri, V. Lakshmi, X. Liang, J. J. McDonnell, E. M. Mendiondo, P. E. O'Connell, T. Oki, J. W. Pomeroy, D. Schertzer, S. Uhlenbrook, and E. Zehe. 2003. IAHS Decade on Predictions in Ungauged Basins (PUB), 2003-2012: Shaping an Exciting Future for the Hydrological Sciences, *Hydrological Sciences Journal-Journal Des Sciences Hydrologiques*. 48(6): 857-880.

Smucygz, B., J.A. Clayton, and Z. Comarova. 2010. Comparison of Changes in Runoff and Channel Cross-sectional Area as a Consequence of Urbanization for Three Chattahoochee River Subbasins, Georgia, USA. *Southeastern Geographer* 50, no. 4: 468-483.

Soil Survey Staff, Natural Resources Conservation Service, United States Department of Agriculture. Soil Survey Geographic (SSURGO) Database for [Big Creek watershed, GA]. Available at http://soildatamart.nrcs.usda.gov. Accessed [February 10, 2011].

Solomatine, D.P., and T. Wagener. 2011. Hydrological Modeling. In *Treatise on Water Science*, 435-457. Oxford: Elsevier. http://www.sciencedirect.com/science/article/B6YGP-51WFM4S-11/2/0b689a132e6a9f6200357c1c18ee7d4b.

Staley, N., T. Bright, R. W. Zeckoski, B. L. Benham, and K M. Brannan. 2007. Comparison of HSPF outputs using FTABLES generated with field survey and digital data1. *JAWRA Journal of the American Water Resources Association* 42, no. 5 (6): 1153-1162. doi:10.1111/j.1752-1688.2006.tb05291.x.

Tague, C, and M Pohl-Costello. 2008. The Potential Utility of Physically Based Hydrologic Modeling in Ungauged Urban Streams. *Annals Of The Association Of American Geographers* 98, no. 4: 818-833. doi:10.1080/00045600802099055.

Tetra Tech, Inc. 2009. *Watershed Hydrology and Water quality Modeling Report for the Upper Ocmulgee Watershed, Georgia.* Atlanta, GA.

Tetra Tech, Inc. 2010. *PEST - based Calibration and Uncertainty Analysis of the LSPC Model of the Upper Ocmulgee Watershed, Georgia*. Atlanta, GA.

US. Army Corp of Engineers. 1993. *S. Army Corp of Engineers. HEC-HMS user manual.* Davis, CA: Hydrologic Engineering Center.

U.S. Army Corp of Engineers. 2006. *HEC-HMS user manual.* Davis, CA: Hydrologic Engineering Center.

USEPA and Tetra Tech, Inc. 2007. *Modeling the Tongue River Watershed with LSPC and CE-QUAL-W2, Final Draft*. 6. http://www.epa.gov/region8/water/monitoring/Modeling%20Report%20Main%20Document%20FINAL%20DRAFT.pdf. [Accessed February 3, 2011].

USEPA. 2000. BASINS Technical Note 6. Estimating hydrology and hydraulic parameters for HSPF. EPA-823-R-00-012. U. S. Environmental Protection Agency, Office of Water. Washington, D. C. Available at http://www.epa.gov/ost/basins/tecnote6.html . [Accessed November 20, 2010].

USEPA. 2007. Loading Simulation Program in C++ (LSPC). User's Manual. Available at http://www.epa.gov/athens/wwqtsc/html/lspc.html. [Accessed November 20, 2010].

Van Liew, M. W., T. L. Veith, D. D. Bosch, and J. G. Arnold. 2007. Suitability of SWAT for the conservation effects assessment project: A comparison on USDA-ARS experimental watersheds. *J. Hydrologic Eng.* 12(2): 173-189.

Vieux, B.E. 2004. *Distributed Hydrologic Modeling Using GIS*. 2nd ed. Springer, December 20.

Walsh, C.J., Roy, A.H., Feminella, J.W., Cottingham, P.D., Groffman, P.M., and Morgan, R.P. Jr., 2005, The urban stream syndrome: current knowledge and the search for a cure. *Journal of the North American Benthological Society*, v. 24(3), p. 706-723.

Watson, F.G.R., R.B. Grayson, R.A. Vertessy and T.A. McMahon.1998. Large-scale distribution modelling and the utility of detailed ground data, *Hydrological Processes* 12:873-888.

Weiler M, J.J. McDonnell. Conceptualizing lateral preferential flow and flow networks and simulating the effects on gauged and ungauged hillslopes. *Water Resources Research., 43, W03403, doi:10.1029/ 2006WR004867*.

Weng, Q. 2001. Modeling Urban Growth Effects on Surface Runoff with the Integration of Remote Sensing and GIS. *Environmental Management* 28, no. 6 (12): 737-748.

Wolock, David M., and Curtis V. Price. 1994. Effects of digital elevation model map scale and data resolution on a topography-based watershed model. *Water Resources Research* 30, no. 11: PP. 3041-3052. doi:199410.1029/94WR01971.

Wood, E. F., J. K. Roundy, T J. Troy, L. P. H. van Beek, M. F. P. Bierkens, E. Blyth, Ad de Roo, et al. 2011. Hyperresolution global land surface modeling: Meeting a grand challenge for monitoring Earth's terrestrial water. *Water Resources Research* 47 (May 6): 10. doi:201110.1029/2010WR010090.

White, M.D., Greer, K.A., 2006. The effects of watershed urbanizationon the stream hydrology and riparian vegetation of Los Pen˜ asquitosCreek, California. *Landscape and Urban Planning* 74 (2):125–138.

Zajac, Z.B. 2010.*Global sensitivity and uncertainty analysis of spatially distributed watershed models*. PhD diss., University of Florida.

Zhan, X, and M Huang. 2004. ArcCN-Runoff: an ArcGIS tool for generating curve number and runoff maps. *Environmental Modelling & Software* 19, no. 10 (10): 875-879.

Zhang, W., and D. R. Montgomery. 1994. Digital elevation model grid size, landscape representation, and hydrologic simulations. *Water Resources Research* 30, no. 4: 1019. doi:10.1029/93WR03553.

APPENDIX A

Baseline scenario 0000: STRM30m, digital-derived FTABLEs, complete land use classification and GEMN270 meteorological station.

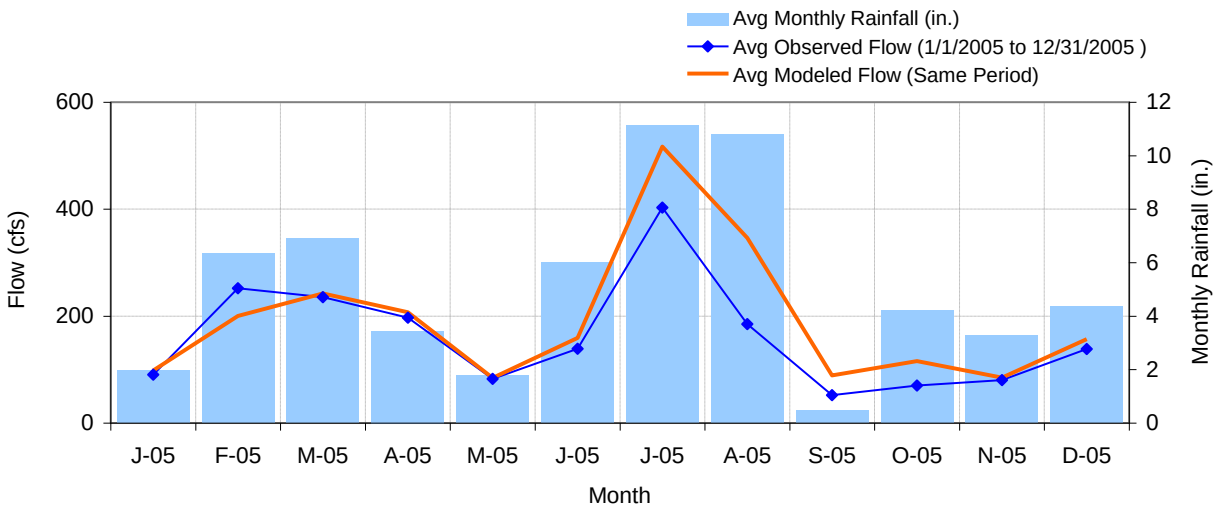

Figure A.1Baseline scenario 0000; wet year (2005). Mean monthly flow: Model Outlet 7 vs. USGS 02335700 BIG CREEK NEAR ALPHARETTA, GA

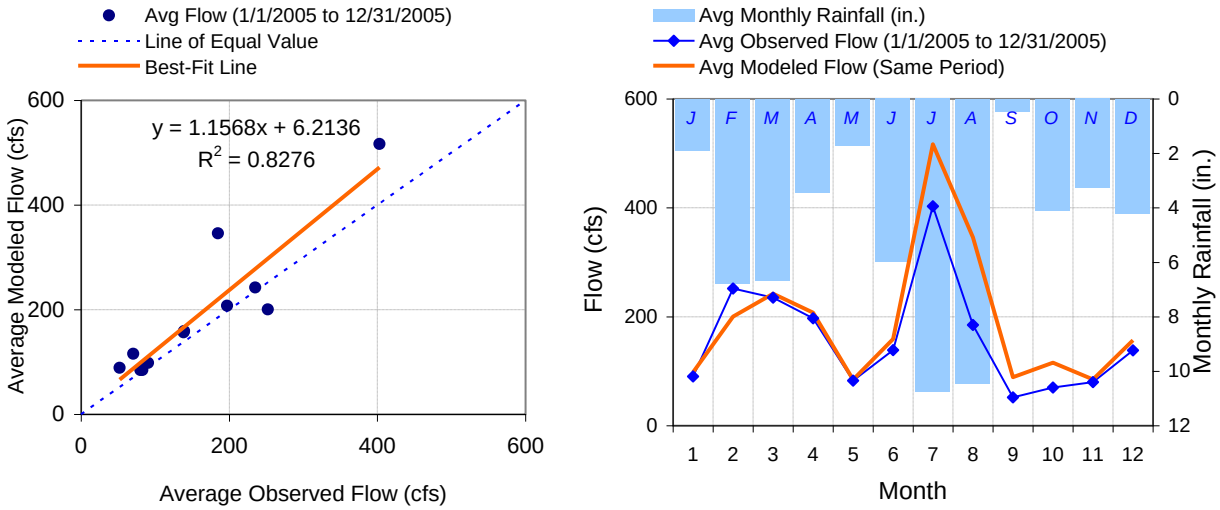

Figure A.2 Baseline scenario 0000; wet year (2005). Seasonal regression and temporal aggregate: Model Outlet 7 vs. USGS 02335700 BIG CREEK NEAR ALPHARETTA, GA

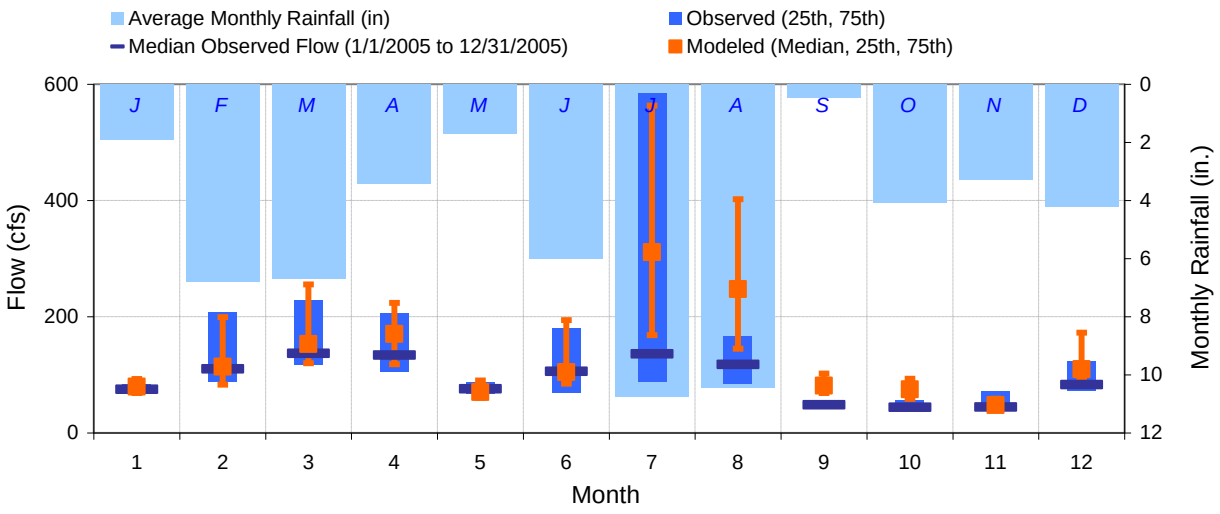

Figure A.3 Baseline scenario 0000; wet year (2005). Seasonal medians and ranges: Model Outlet 7 vs. USGS 02335700 BIG CREEK NEAR ALPHARETTA, GA

Table A.1 Baseline scenario 0000; wet year (2005). Seasonal summary: Model Outlet 7 vs. USGS 02335700 BIG CREEK NEAR ALPHARETTA, GA

MONTH	OBSERVED FLOW (CFS)				MODELED FLOW (CFS)			
	MEAN	MEDIAN	25TH	75TH	MEAN	MEDIAN	25TH	75TH
Jan	90.26	75.00	70.00	84.00	98.31	79.83	68.72	92.99
Feb	252.04	110.00	87.75	207.00	200.49	113.86	82.97	199.09
Mar	235.29	137.00	118.00	228.00	242.15	152.82	120.04	255.69
Apr	197.27	134.00	104.75	205.50	207.35	170.17	118.11	223.92
May	82.58	76.00	67.00	86.00	84.47	70.34	60.56	90.32
Jun	138.93	106.00	69.50	181.00	159.12	104.52	84.60	194.26
Jul	402.81	136.00	87.50	584.00	516.92	310.91	168.09	563.03
Aug	184.90	118.00	84.00	165.50	345.96	247.67	144.73	401.99
Sep	52.00	48.50	43.25	55.75	89.09	81.45	68.62	102.12
Oct	70.26	44.00	40.00	56.00	115.95	75.00	58.38	93.05
Nov	80.17	44.50	40.00	71.00	84.82	47.94	40.31	59.10
Dec	138.55	83.00	72.00	123.50	156.76	109.92	95.53	172.64

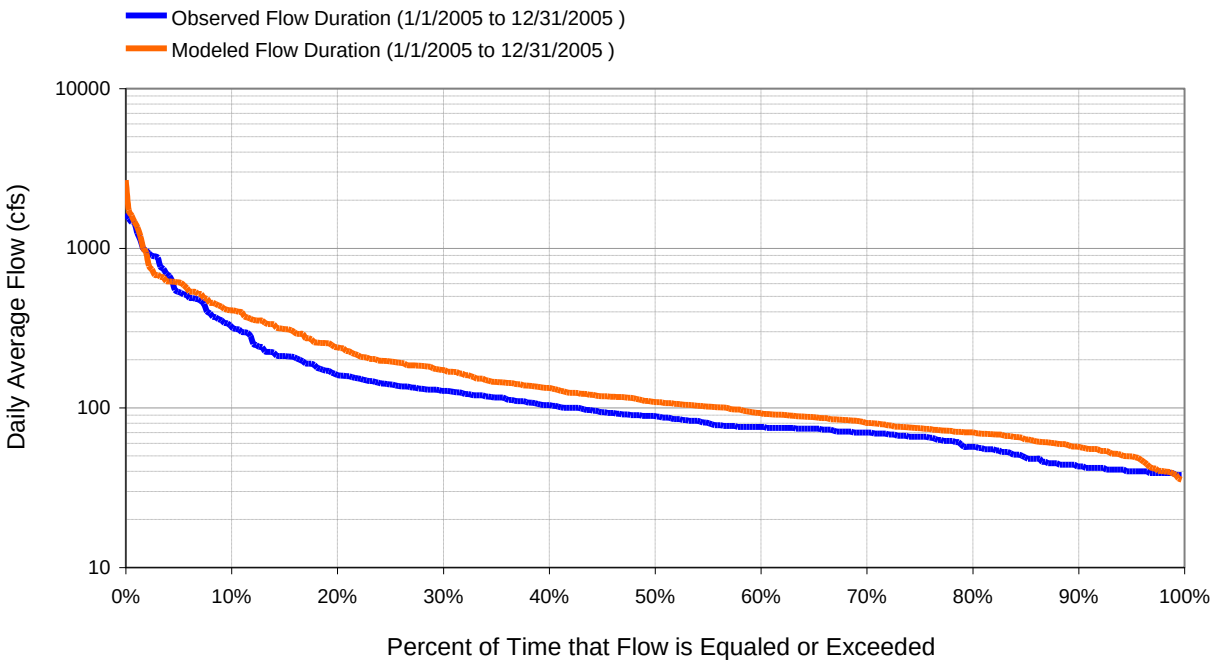

Figure A.4 Baseline scenario 0000; wet year (2005). Flow exceedence: Model Outlet 7 vs. USGS 02335700 BIG CREEK NEAR ALPHARETTA, GA

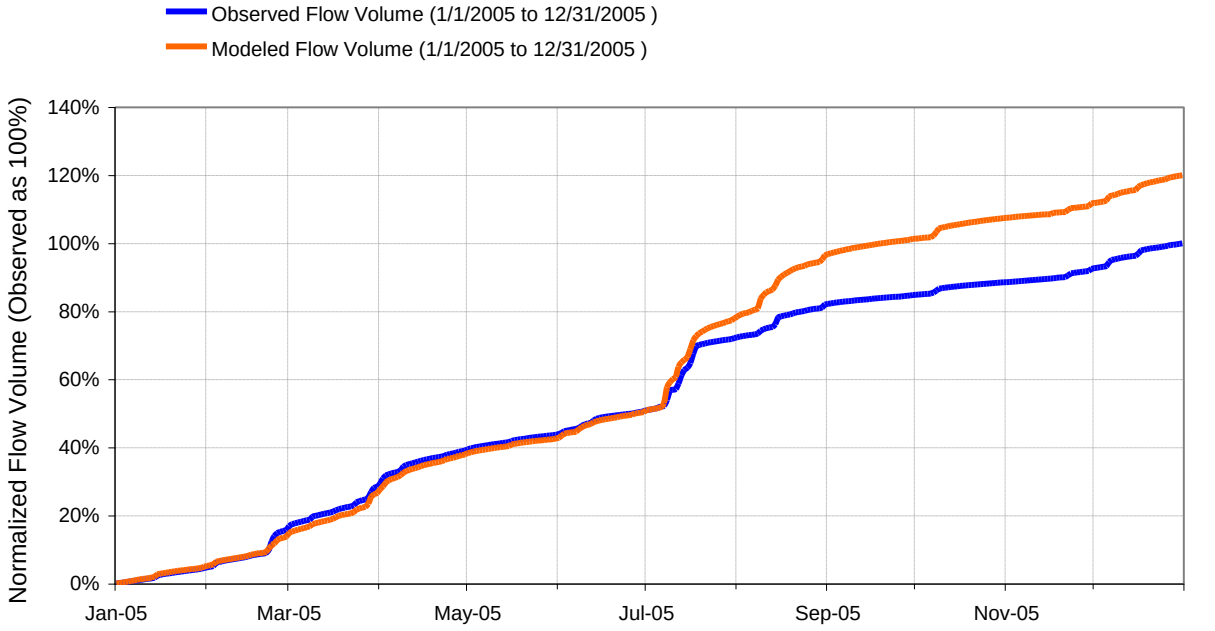

Figure A.5 Baseline scenario 0000; wet year (2005). Flow accumulation: Model Outlet 7 vs. USGS 02335700 BIG CREEK NEAR ALPHARETTA, GA

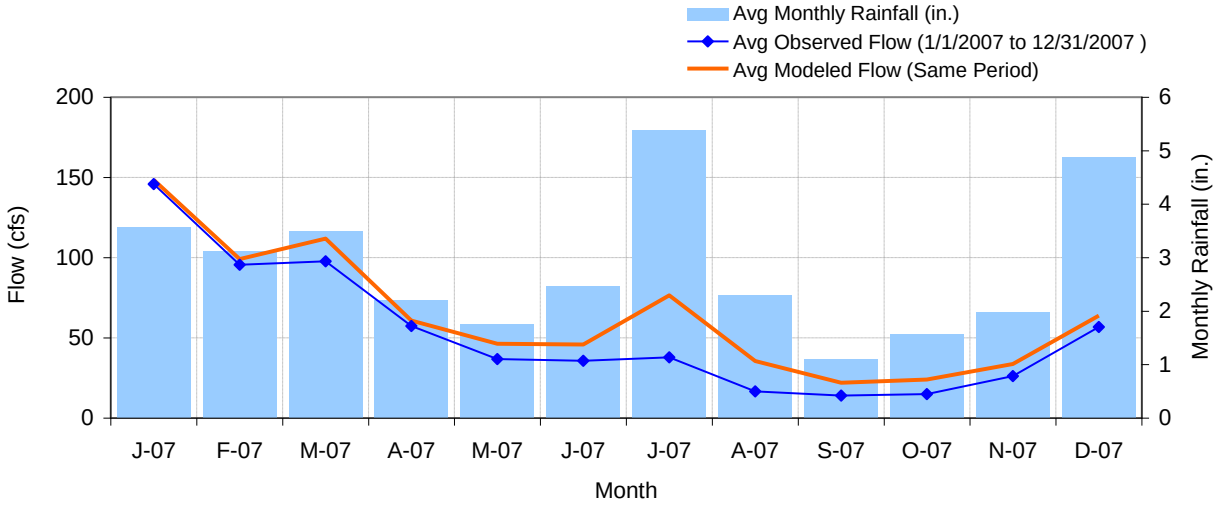

Figure A.6 Baseline scenario 0000; dry year (2007). Baseline scenario 0000; dry year (2007). Mean monthly flow: Model Outlet 7 vs. USGS 02335700 BIG CREEK NEAR ALPHARETTA, GA

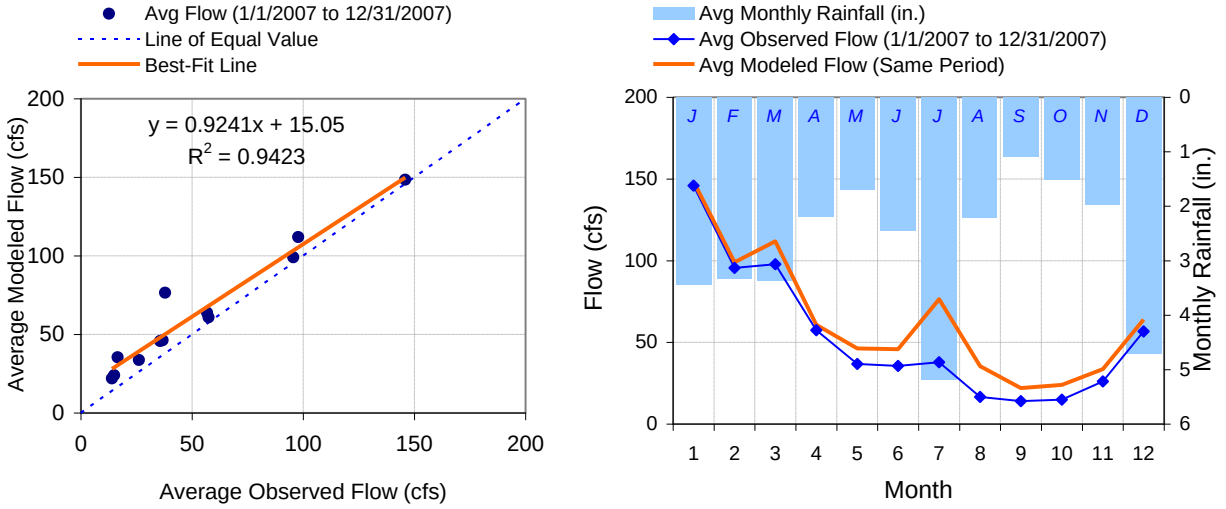

Figure A.7 Baseline scenario 0000; dry year (2007). Baseline scenario 0000; dry year (2007). Seasonal regression and temporal aggregate: Model Outlet 7 vs. USGS 02335700 BIG CREEK NEAR ALPHARETTA, GA

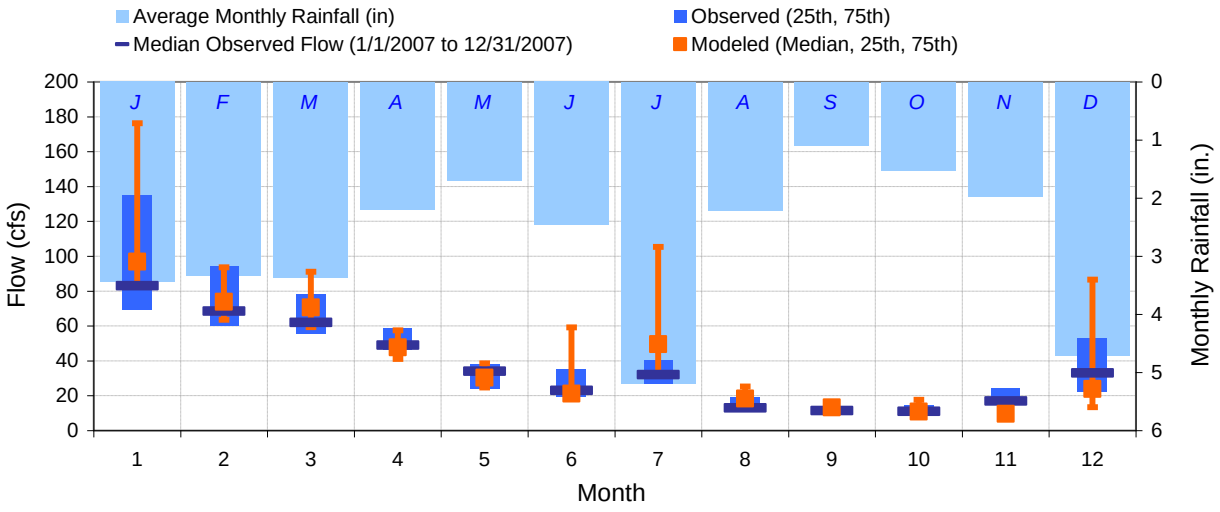

Figure A.8 Baseline scenario 0000; dry year (2007). Baseline scenario 0000; dry year (2007). Seasonal medians and ranges: Model Outlet 7 vs. USGS 02335700 BIG CREEK NEAR ALPHARETTA, GA

Table A.2 Baseline scenario 0000; dry year (2007). Seasonal summary: Model Outlet 7 vs. USGS 02335700 BIG CREEK NEAR ALPHARETTA, GA

MONTH	OBSERVED FLOW (CFS)				MODELED FLOW (CFS)			
	MEAN	MEDIAN	25TH	75TH	MEAN	MEDIAN	25TH	75TH
Jan	145.90	83.00	69.00	135.00	148.44	96.85	82.95	176.28
Feb	95.54	68.50	60.00	94.00	99.08	73.84	63.51	93.64
Mar	97.74	62.00	55.50	78.00	111.90	70.58	59.28	91.14
Apr	57.40	49.00	46.25	58.75	60.80	47.76	41.12	57.46
May	36.77	34.00	24.00	38.00	46.28	30.44	24.69	38.61
Jun	35.63	23.00	19.25	35.00	45.80	21.17	18.69	59.14
Jul	37.84	32.00	27.00	40.50	76.42	49.51	32.77	105.33
Aug	16.55	13.00	11.00	19.00	35.47	18.35	15.76	25.31
Sep	14.04	11.50	10.25	12.75	21.95	13.22	12.27	14.72
Oct	14.98	11.00	10.00	14.50	23.97	10.90	10.53	17.70
Nov	26.10	17.00	15.25	24.00	33.64	9.55	9.29	16.00
Dec	56.74	33.00	22.00	53.00	63.87	23.93	13.46	86.64

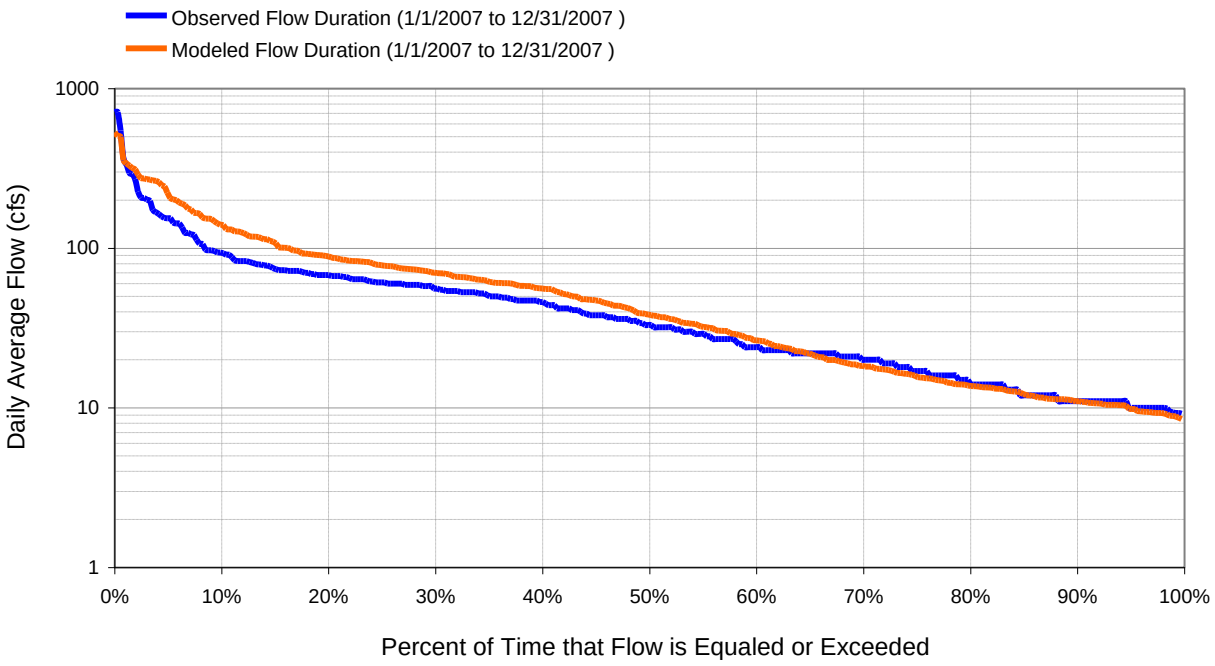

Figure A.9 Baseline scenario 0000; dry year (2007). Flow exceedence: Model Outlet 7 vs. USGS 02335700 BIG CREEK NEAR ALPHARETTA, GA

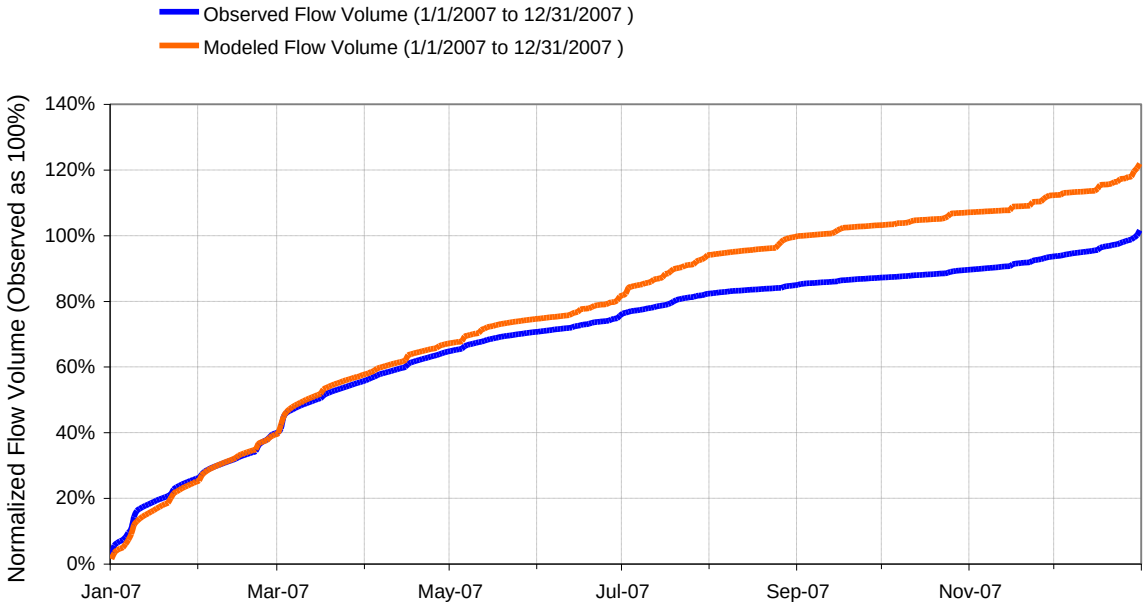

Figure A.10 Baseline scenario 0000; dry year (2007). Flow accumulation: Model Outlet 7 vs. USGS 02335700 BIG CREEK NEAR ALPHARETTA, GA

APPENDIX B

Experimental scenario 1000: STRM90m, digital-derived FTABLEs, complete land use classification and GEMN270 meteorological station.

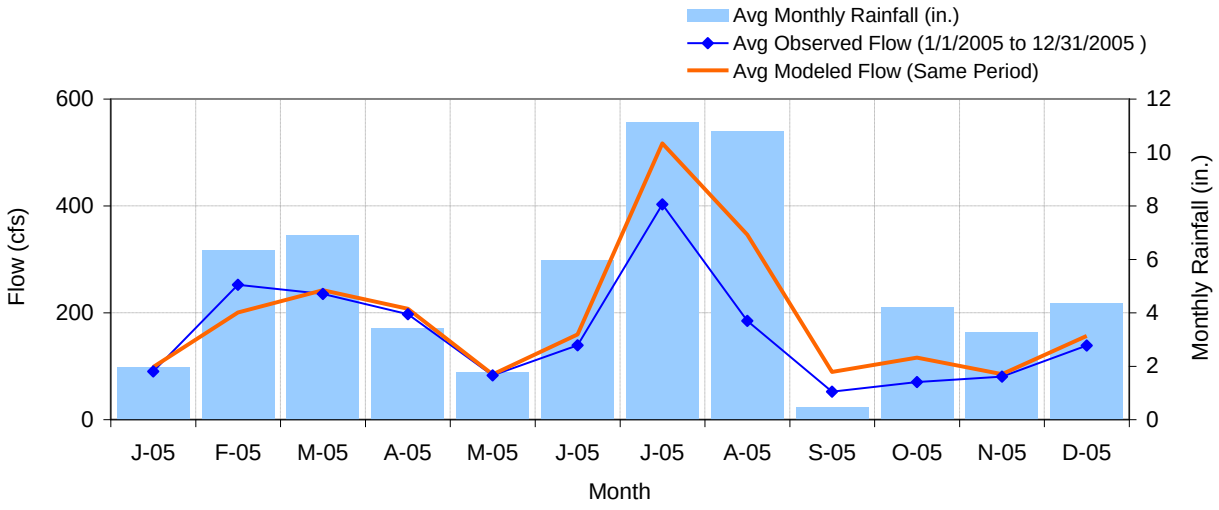

Figure B.1 Experimental scenario 1000; wet year (2005). Mean monthly flow: Model Outlet 7 vs. USGS 02335700 BIG CREEK NEAR ALPHARETTA, GA

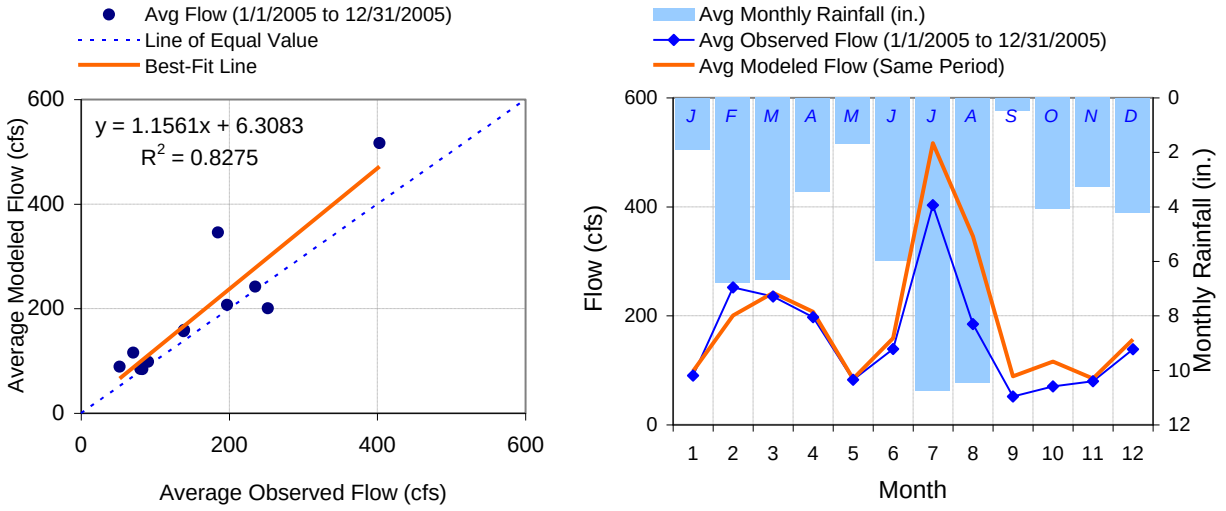

Figure B.2 Experimental scenario 1000; wet year (2005). Seasonal regression and temporal aggregate: Model Outlet 7 vs. USGS 02335700 BIG CREEK NEAR ALPHARETTA, GA

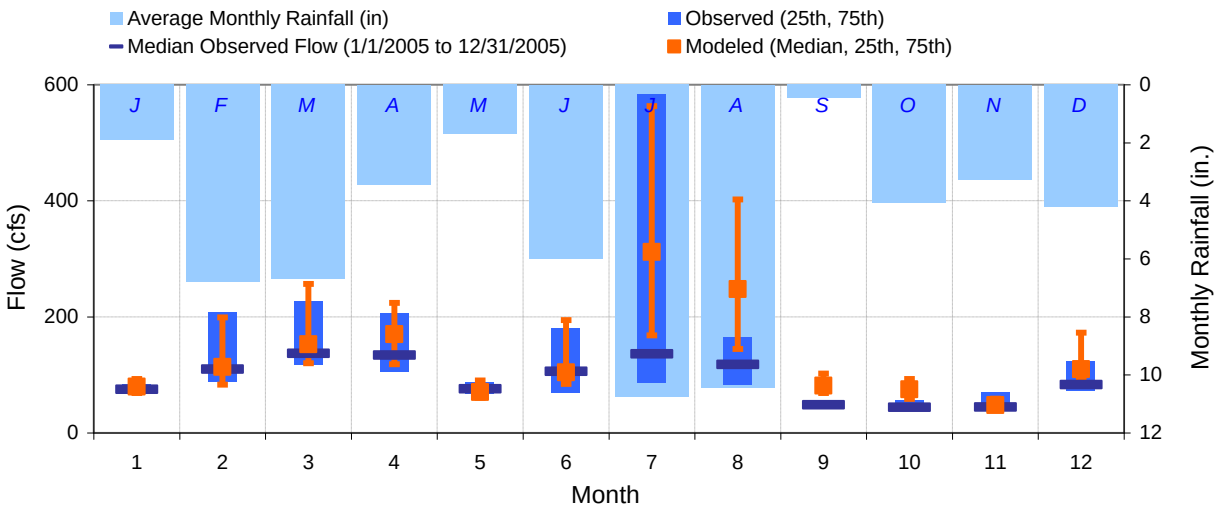

Figure B.3 Experimental scenario 1000; wet year (2005). Seasonal medians and ranges: Model Outlet 7 vs. USGS 02335700 BIG CREEK NEAR ALPHARETTA, GA

Table B.1 Experimental scenario 1000; wet year (2005). Seasonal summary: Model Outlet 7 vs. USGS 02335700 BIG CREEK NEAR ALPHARETTA, GA

MONTH	OBSERVED FLOW (CFS)				MODELED FLOW (CFS)			
	MEAN	MEDIAN	25TH	75TH	MEAN	MEDIAN	25TH	75TH
Jan	90.26	75.00	70.00	84.00	98.33	79.86	68.75	93.03
Feb	252.04	110.00	87.75	207.00	200.42	113.91	83.00	199.00
Mar	235.29	137.00	118.00	228.00	242.04	152.80	120.17	256.88
Apr	197.27	134.00	104.75	205.50	207.42	170.30	118.19	223.95
May	82.58	76.00	67.00	86.00	84.49	70.37	60.60	90.34
Jun	138.93	106.00	69.50	181.00	159.14	104.55	84.58	194.21
Jul	402.81	136.00	87.50	584.00	516.71	311.77	168.02	563.12
Aug	184.90	118.00	84.00	165.50	345.86	247.74	144.89	402.20
Sep	52.00	48.50	43.25	55.75	89.17	81.52	68.66	102.21
Oct	70.26	44.00	40.00	56.00	115.98	75.00	58.41	93.09
Nov	80.17	44.50	40.00	71.00	84.81	47.96	40.33	59.12
Dec	138.55	83.00	72.00	123.50	156.79	109.96	95.58	172.83

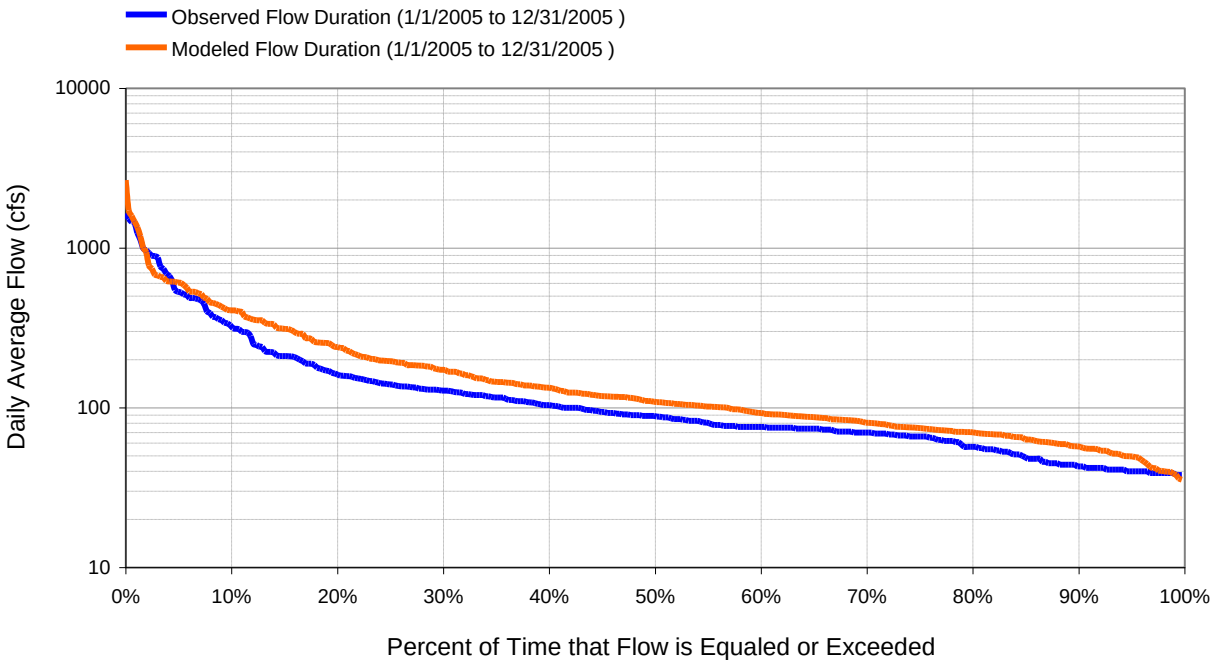

Figure B.4 Experimental scenario 1000; wet year (2005). Flow exceedence: Model Outlet 7 vs. USGS 02335700 BIG CREEK NEAR ALPHARETTA, GA

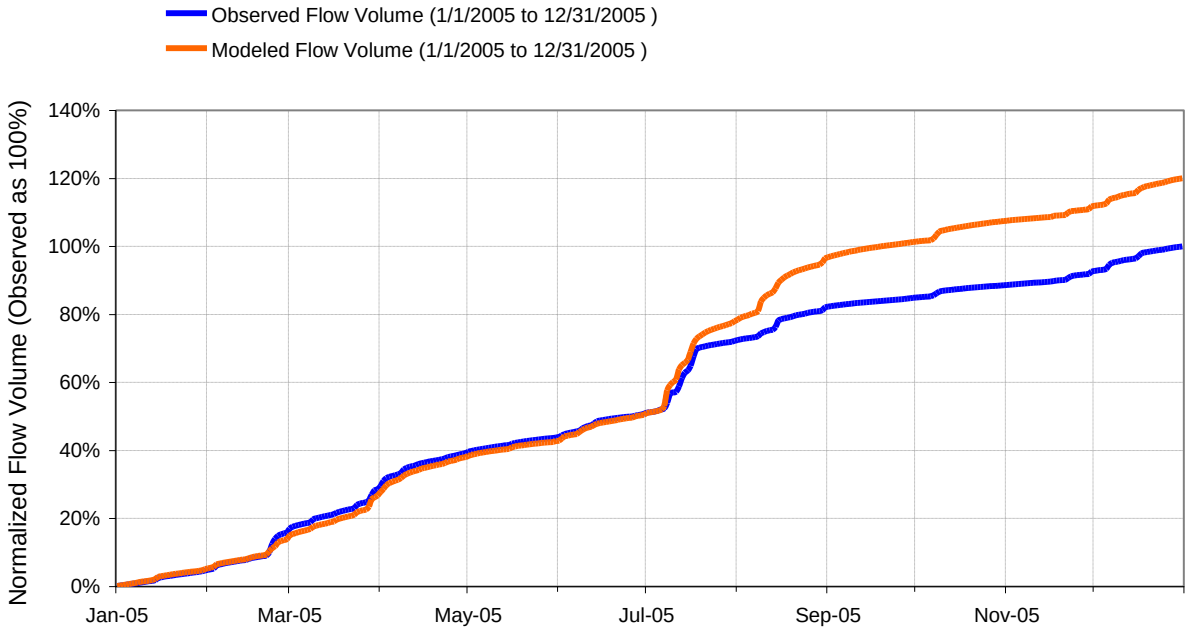

Figure B.5 Experimental scenario 1000; wet year (2005). Flow accumulation: Model Outlet 7 vs. USGS 02335700 BIG CREEK NEAR ALPHARETTA, GA

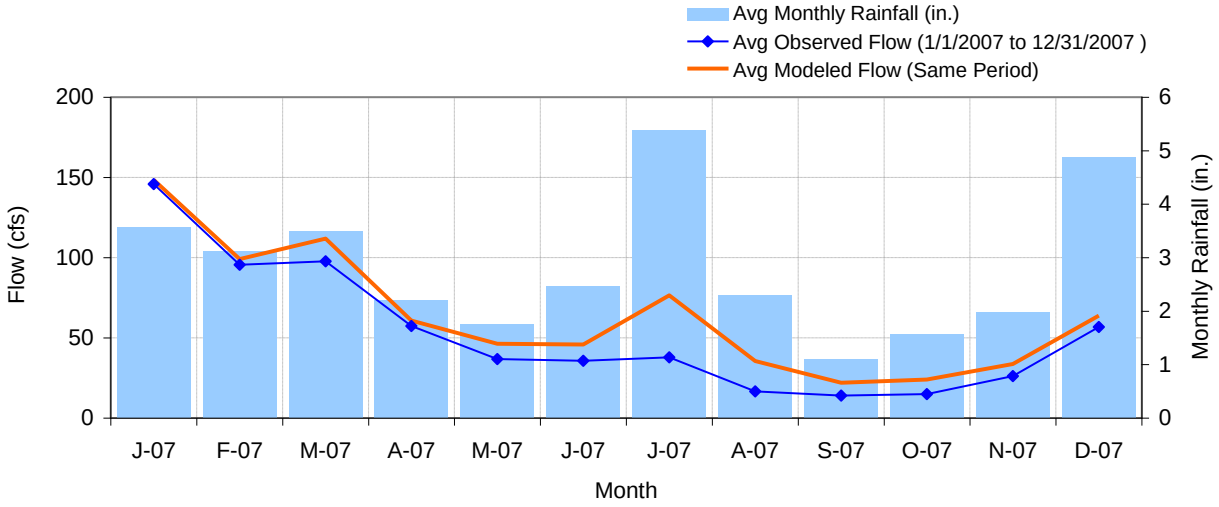

Figure B.6 Experimental scenario 1000; dry year (2007). Mean monthly flow: Model Outlet 7 vs. USGS 02335700 BIG CREEK NEAR ALPHARETTA, GA

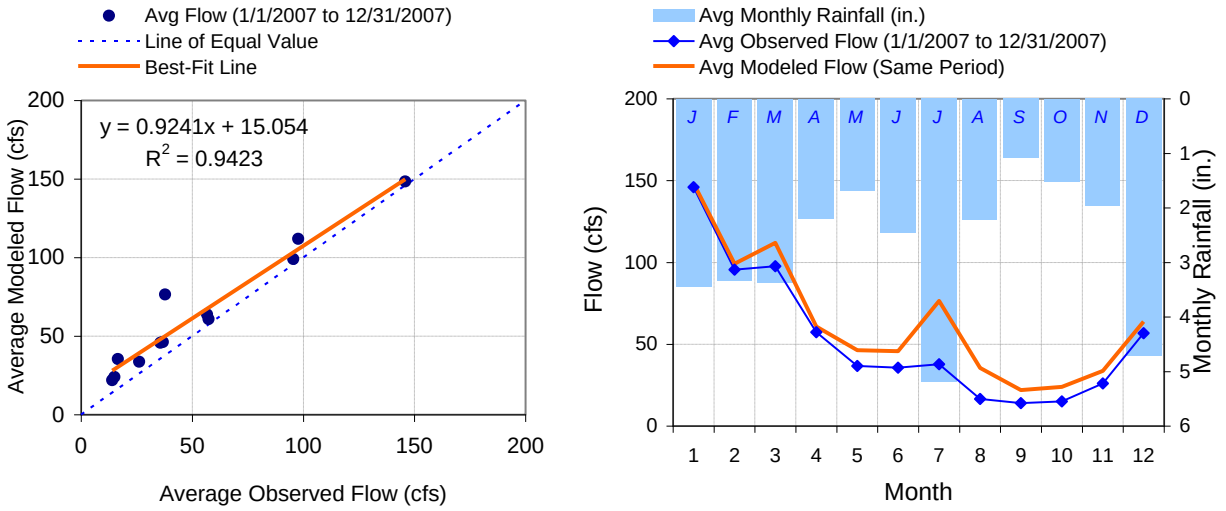

Figure B.7 Experimental scenario 1000; dry year (2007). Seasonal regression and temporal aggregate: Model Outlet 7 vs. USGS 02335700 BIG CREEK NEAR ALPHARETTA, GA

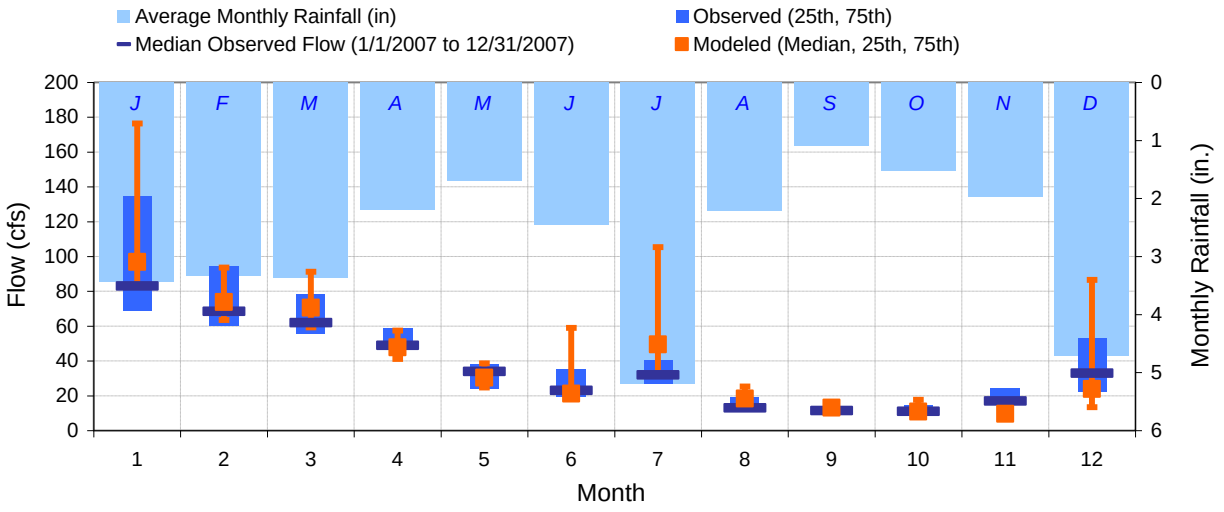

Figure B.8 Experimental scenario 1000; dry year (2007). Seasonal medians and ranges: Model Outlet 7 vs. USGS 02335700 BIG CREEK NEAR ALPHARETTA, GA

Table B.2 Experimental scenario 1000; dry year (2007). Seasonal summary: Model Outlet 7 vs. USGS 02335700 BIG CREEK NEAR ALPHARETTA, GA

MONTH	OBSERVED FLOW (CFS)				MODELED FLOW (CFS)			
	MEAN	MEDIAN	25TH	75TH	MEAN	MEDIAN	25TH	75TH
Jan	145.90	83.00	69.00	135.00	148.43	96.93	83.02	176.38
Feb	95.54	68.50	60.00	94.00	99.12	73.89	63.55	93.70
Mar	97.74	62.00	55.50	78.00	111.89	70.61	59.25	91.21
Apr	57.40	49.00	46.25	58.75	60.81	47.77	41.13	57.43
May	36.77	34.00	24.00	38.00	46.29	30.45	24.70	38.62
Jun	35.63	23.00	19.25	35.00	45.80	21.18	18.69	58.95
Jul	37.84	32.00	27.00	40.50	76.43	49.52	32.78	105.34
Aug	16.55	13.00	11.00	19.00	35.47	18.35	15.76	25.32
Sep	14.04	11.50	10.25	12.75	21.95	13.22	12.27	14.72
Oct	14.98	11.00	10.00	14.50	23.97	10.91	10.53	17.75
Nov	26.10	17.00	15.25	24.00	33.64	9.55	9.29	16.03
Dec	56.74	33.00	22.00	53.00	63.85	23.89	13.46	86.63

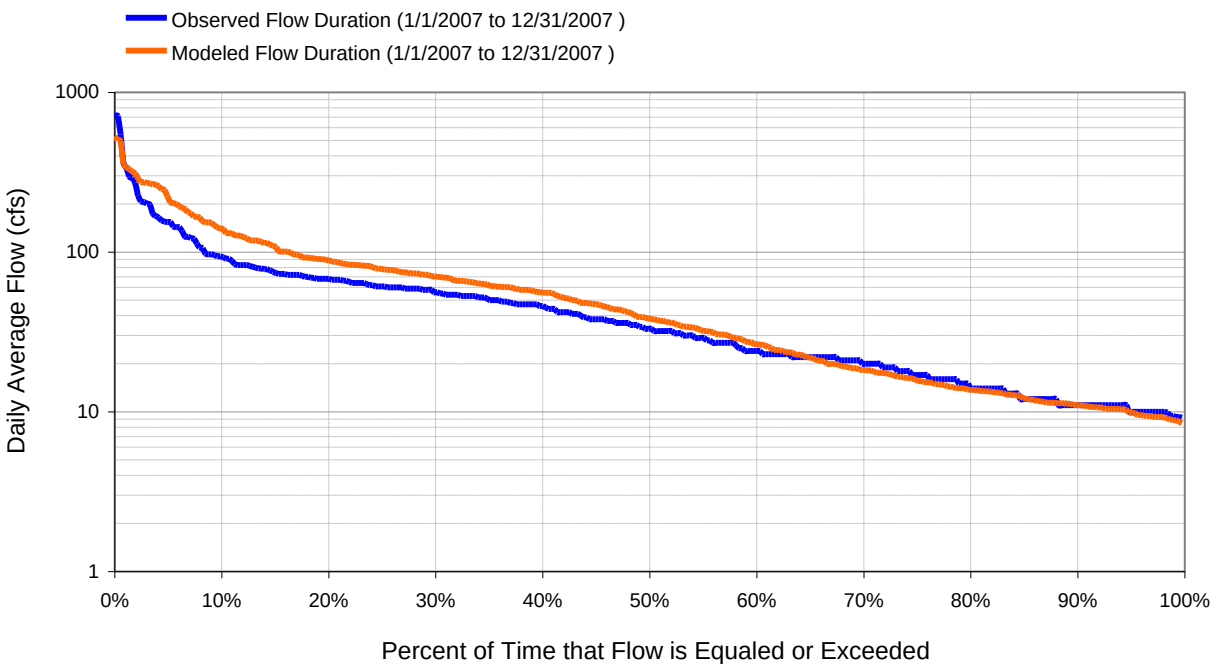

Figure B.9 Experimental scenario 1000; dry year (2007). Flow exceedence: Model Outlet 7 vs. USGS 02335700 BIG CREEK NEAR ALPHARETTA, GA

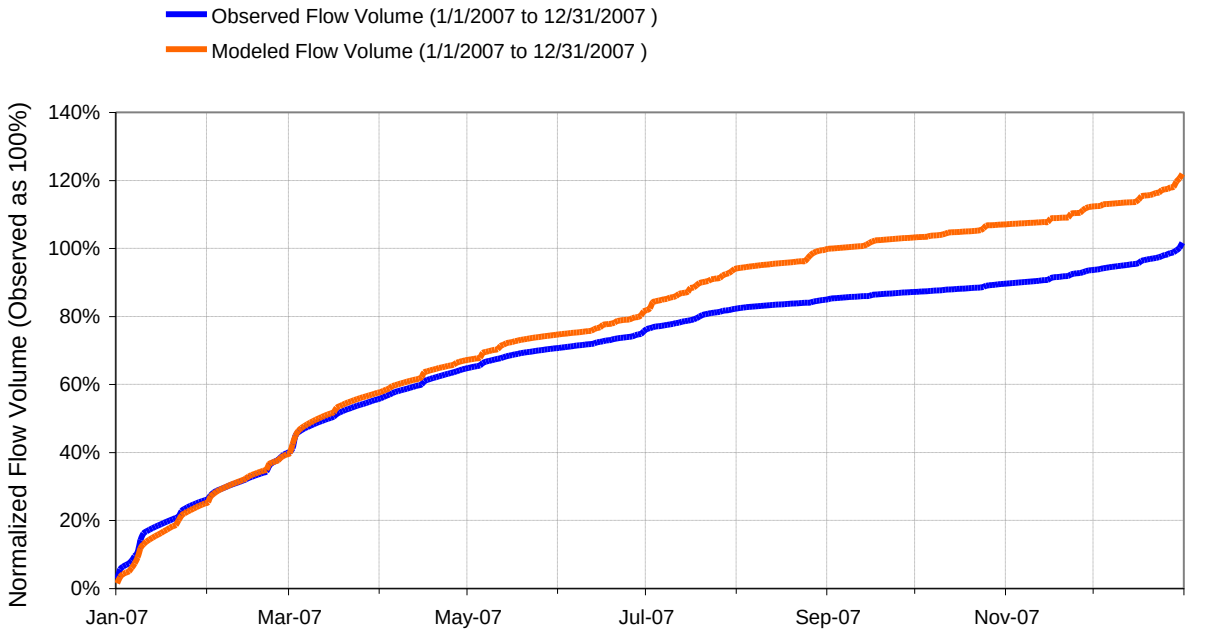

Figure B.10 Experimental scenario 1000; dry year (2007). Flow accumulation: Model Outlet 7 vs. USGS 02335700 BIG CREEK NEAR ALPHARETTA, GA

APPENDIX C

Experimental scenario 0010: STRM30m, digital-derived FTABLEs, simplified land use classification and GEMN270 meteorological station.

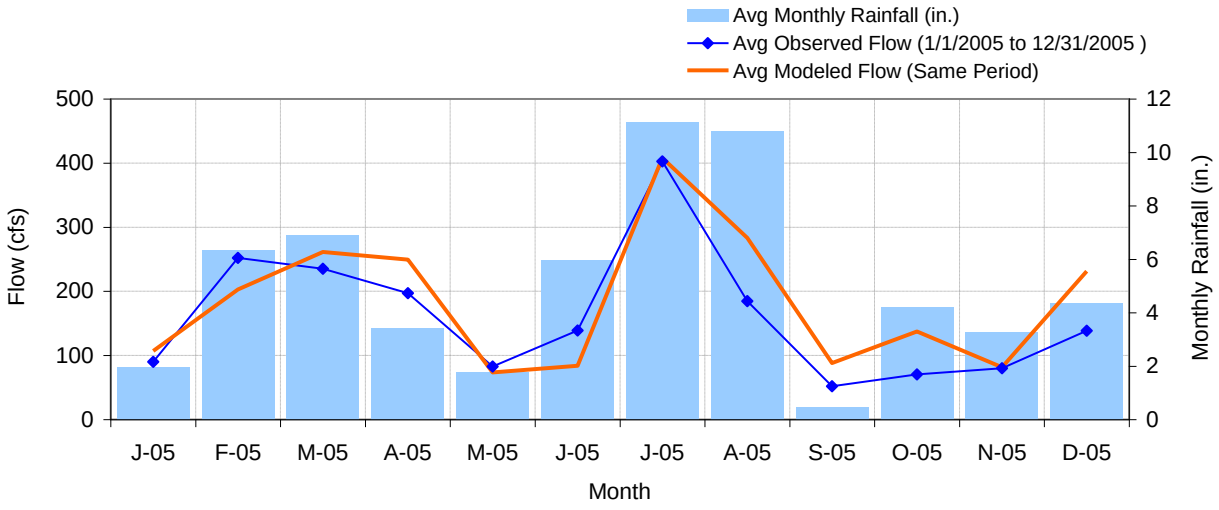

Figure C.1 Experimental scenario 0010; wet year (2005). Mean monthly flow: Model Outlet 7 vs. USGS 02335700 BIG CREEK NEAR ALPHARETTA, GA

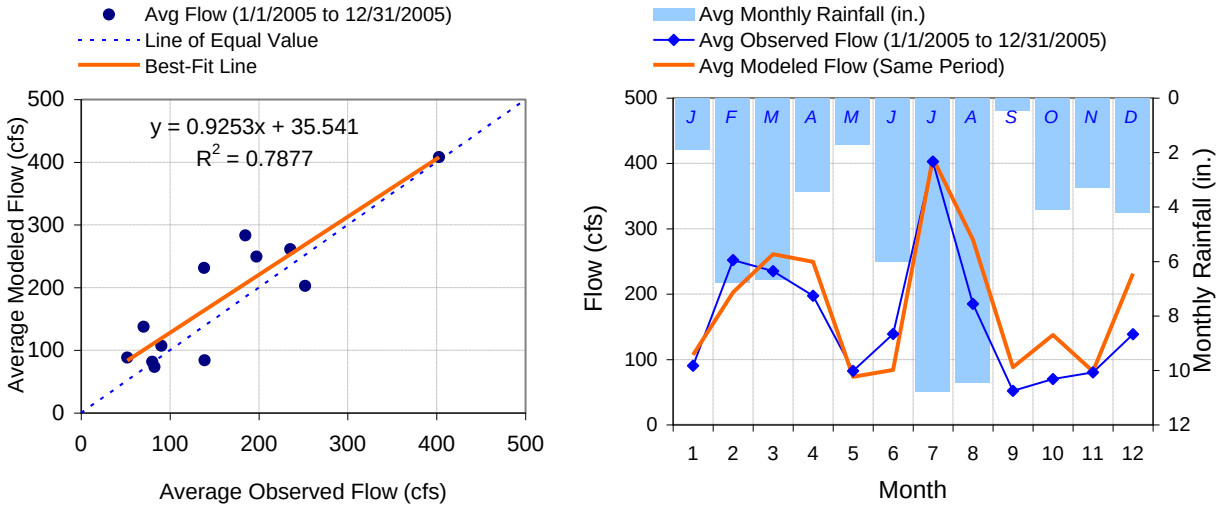

Figure C.2 Experimental scenario 0010; wet year (2005). Seasonal regression and temporal aggregate: Model Outlet 7 vs. USGS 02335700 BIG CREEK NEAR ALPHARETTA, GA

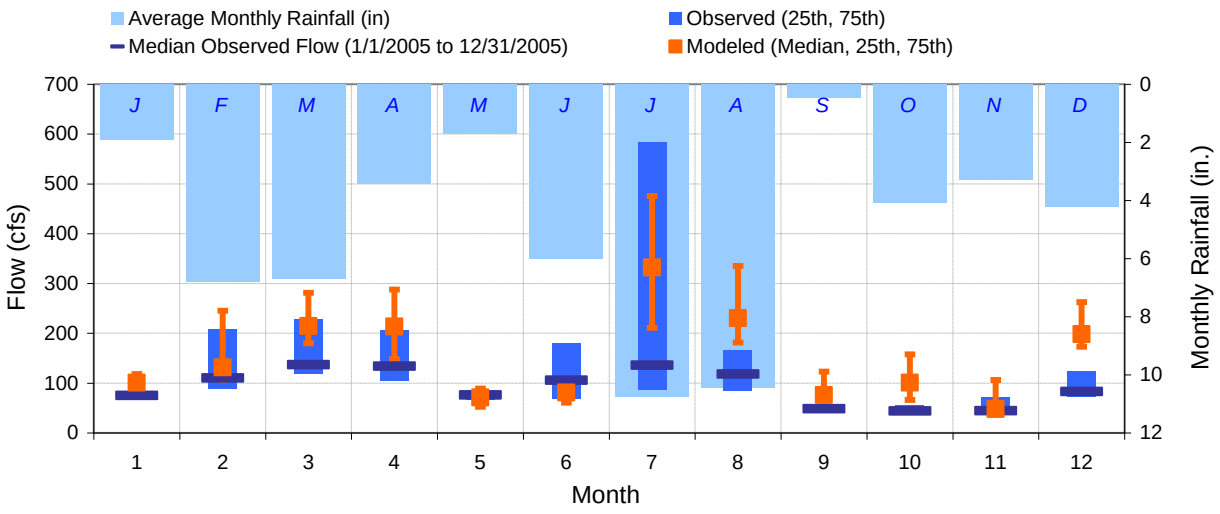

Figure C.3 Experimental scenario 0010; wet year (2005). Seasonal medians and ranges: Model Outlet 7 vs. USGS 02335700 BIG CREEK NEAR ALPHARETTA, GA

Table C.1 Experimental scenario 0010; wet year (2005). Seasonal summary: Model Outlet 7 vs. USGS 02335700 BIG CREEK NEAR ALPHARETTA, GA

MONTH	OBSERVED FLOW (CFS)				MODELED FLOW (CFS)			
	MEAN	MEDIAN	25TH	75TH	MEAN	MEDIAN	25TH	75TH
Jan	90.26	75.00	70.00	84.00	107.04	100.96	85.16	118.00
Feb	252.04	110.00	87.75	207.00	202.70	131.46	106.42	245.35
Mar	235.29	137.00	118.00	228.00	261.23	214.53	179.77	281.48
Apr	197.27	134.00	104.75	205.50	249.35	213.55	147.93	287.78
May	82.58	76.00	67.00	86.00	73.58	71.03	52.27	89.11
Jun	138.93	106.00	69.50	181.00	84.02	80.96	61.04	105.88
Jul	402.81	136.00	87.50	584.00	407.93	332.06	210.98	475.74
Aug	184.90	118.00	84.00	165.50	283.26	230.52	181.67	334.97
Sep	52.00	48.50	43.25	55.75	88.19	76.37	48.52	123.11
Oct	70.26	44.00	40.00	56.00	137.42	100.68	66.05	157.93
Nov	80.17	44.50	40.00	71.00	81.60	48.13	37.57	106.06
Dec	138.55	83.00	72.00	123.50	231.50	198.06	173.06	262.43

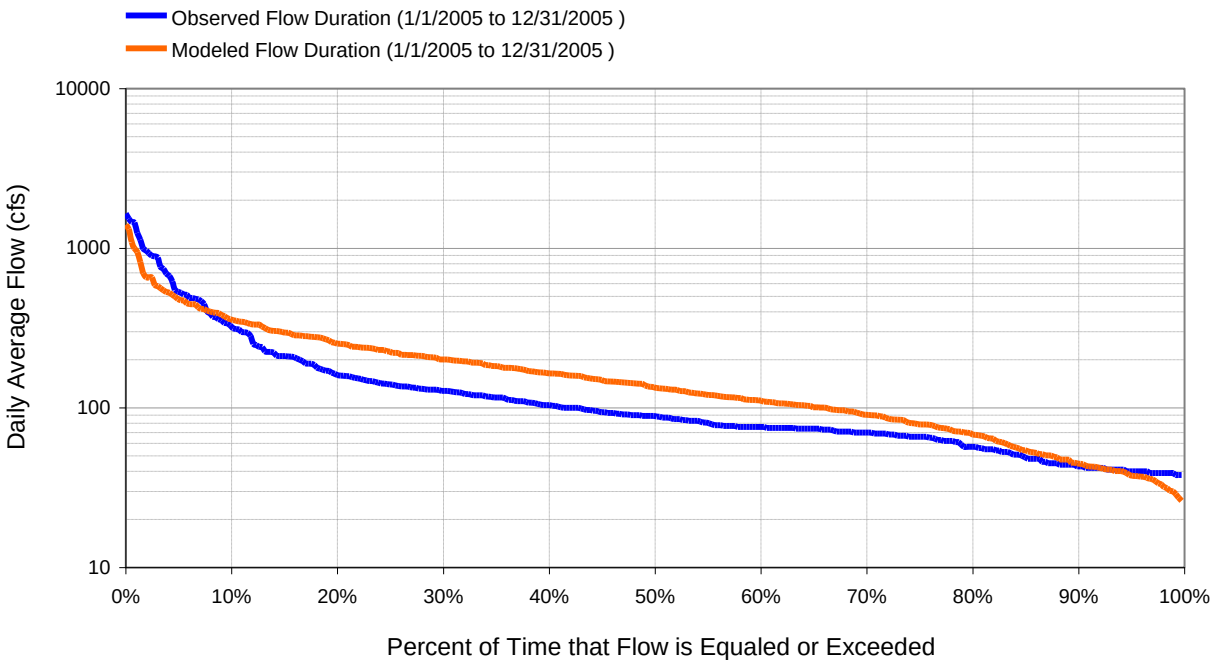

Figure C.4 Experimental scenario 0010; wet year (2005). Flow exceedence: Model Outlet 7 vs. USGS 02335700 BIG CREEK NEAR ALPHARETTA, GA

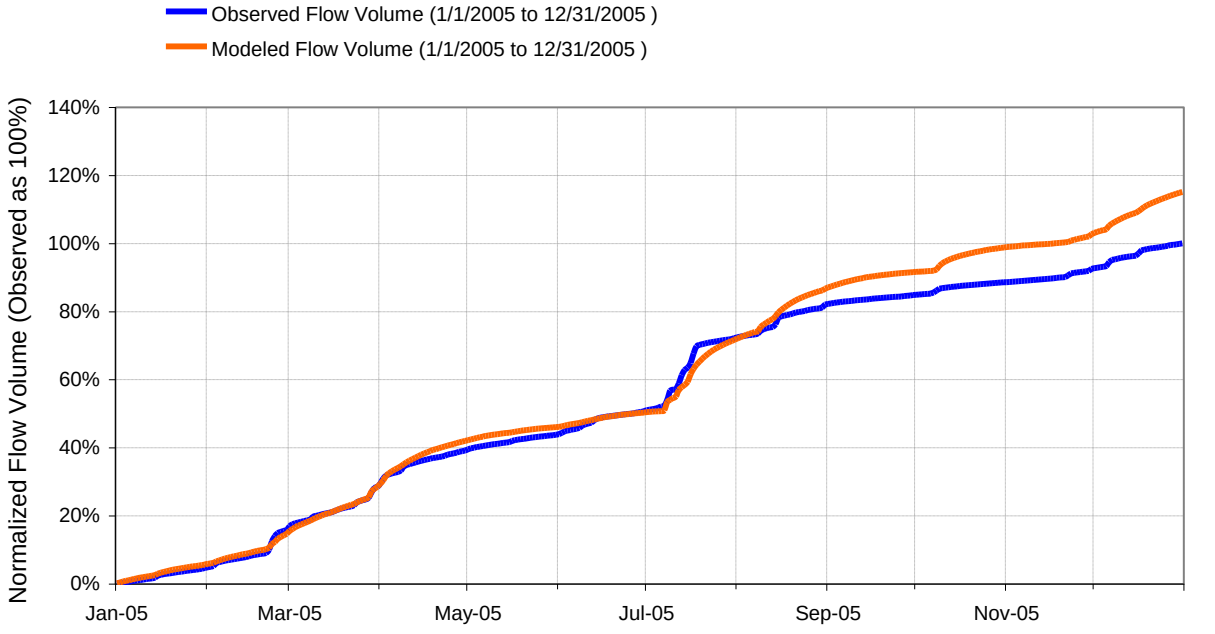

Figure C.5 Experimental scenario 0010; wet year (2005). Flow accumulation: Model Outlet 7 vs. USGS 02335700 BIG CREEK NEAR ALPHARETTA, GA

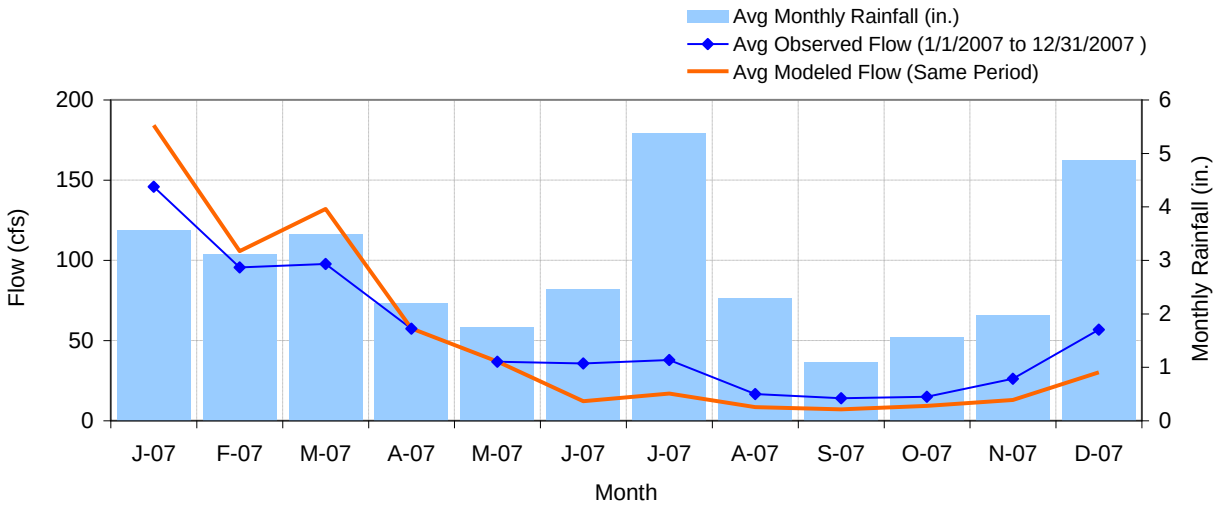

Figure C.6 Experimental scenario 0010; dry year (2007). Mean monthly flow: Model Outlet 7 vs. USGS 02335700 BIG CREEK NEAR ALPHARETTA, GA

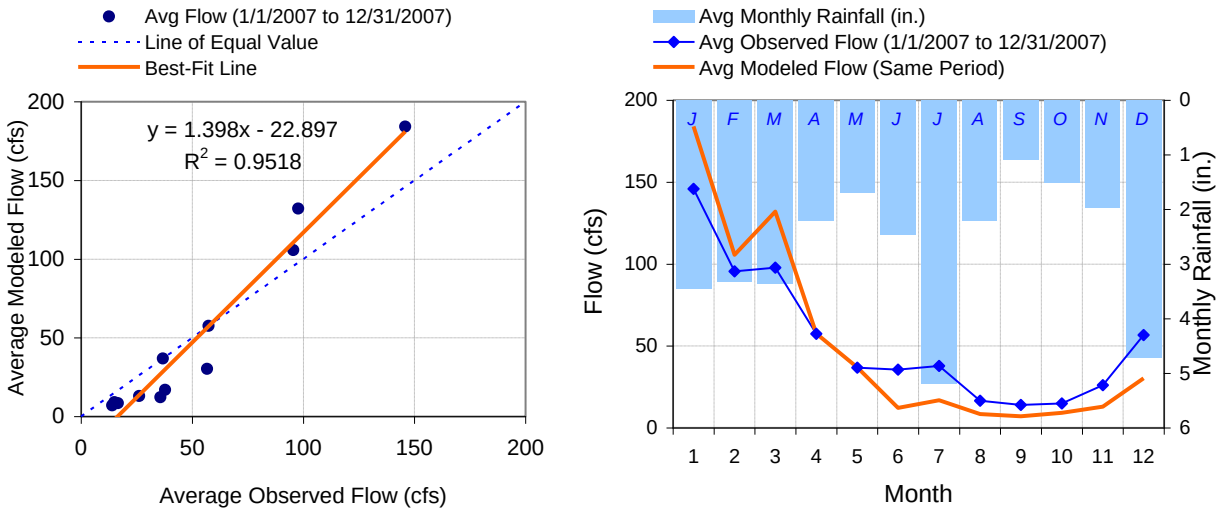

Figure C.7 Experimental scenario 0010; dry year (2007). Seasonal regression and temporal aggregate: Model Outlet 7 vs. USGS 02335700 BIG CREEK NEAR ALPHARETTA, GA

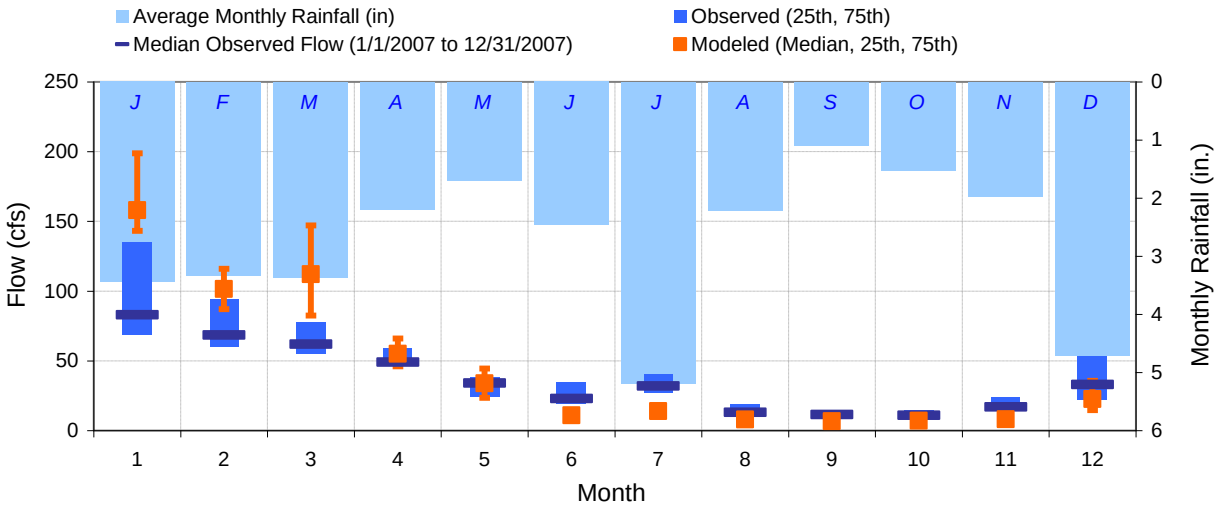

Figure C.8 Experimental scenario 0010; dry year (2007). Seasonal medians and ranges: Model Outlet 7 vs. USGS 02335700 BIG CREEK NEAR ALPHARETTA, GA

Table C.2 Experimental scenario 0010; dry year (2007). Seasonal summary: Model Outlet 7 vs. USGS 02335700 BIG CREEK NEAR ALPHARETTA, GA

MONTH	OBSERVED FLOW (CFS)				MODELED FLOW (CFS)			
	MEAN	MEDIAN	25TH	75TH	MEAN	MEDIAN	25TH	75TH
Jan	145.90	83.00	69.00	135.00	184.09	158.05	143.25	198.86
Feb	95.54	68.50	60.00	94.00	105.71	101.52	87.09	116.06
Mar	97.74	62.00	55.50	78.00	132.04	112.06	82.51	147.09
Apr	57.40	49.00	46.25	58.75	57.51	55.06	46.11	66.07
May	36.77	34.00	24.00	38.00	36.92	33.93	23.48	44.41
Jun	35.63	23.00	19.25	35.00	12.18	10.93	10.22	12.42
Jul	37.84	32.00	27.00	40.50	16.94	13.88	11.68	16.78
Aug	16.55	13.00	11.00	19.00	8.44	7.89	7.32	9.42
Sep	14.04	11.50	10.25	12.75	7.07	6.73	6.54	6.83
Oct	14.98	11.00	10.00	14.50	9.17	7.01	6.81	7.86
Nov	26.10	17.00	15.25	24.00	12.98	8.07	6.64	12.87
Dec	56.74	33.00	22.00	53.00	30.23	22.63	14.63	35.60

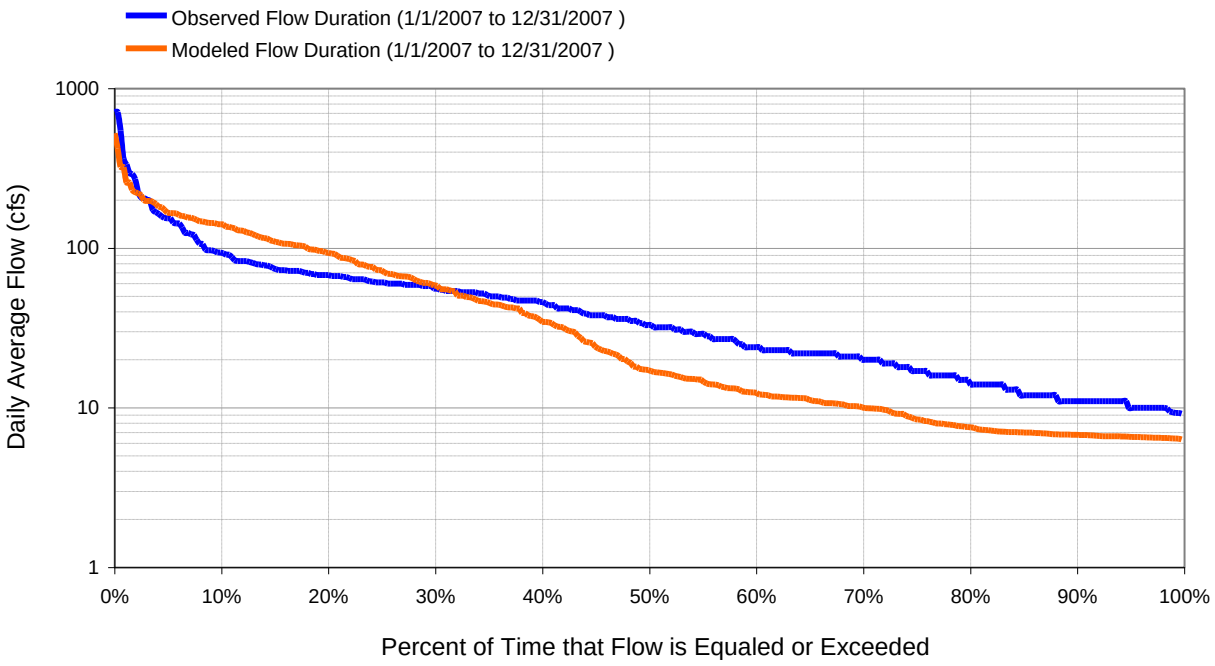

Figure C.9 Experimental scenario 0010; dry year (2007). Flow exceedence: Model Outlet 7 vs. USGS 02335700 BIG CREEK NEAR ALPHARETTA, GA

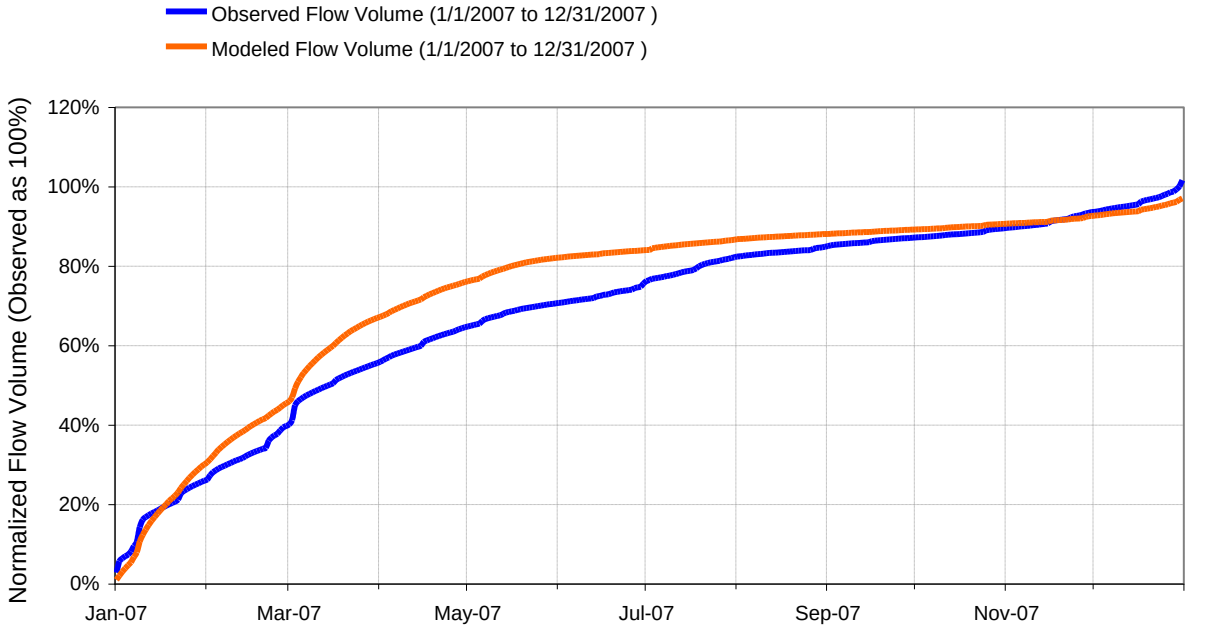

Figure C.10 Experimental scenario 0010; dry year (2007). Flow accumulation: Model Outlet 7 vs. USGS 02335700 BIG CREEK NEAR ALPHARETTA, GA

APPENDIX D

Experimental scenario 0100: STRM30m, field-based FTABLEs, complete land use classification and GEMN270 meteorological station.

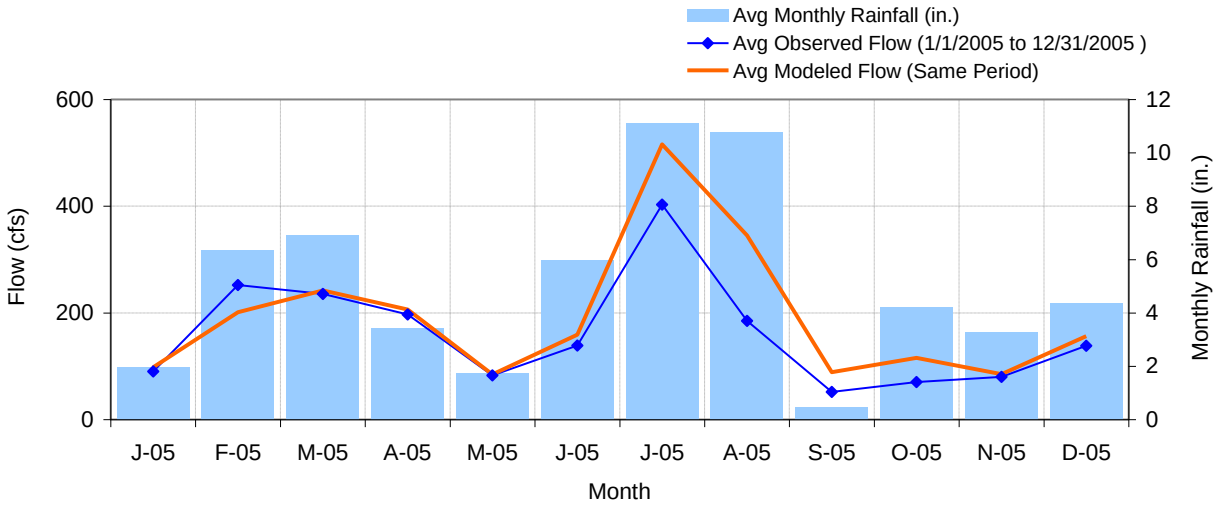

Figure D.1 Experimental scenario 0100; wet year (2005). Mean monthly flow: Model Outlet 7 vs. USGS 02335700 BIG CREEK NEAR ALPHARETTA, GA

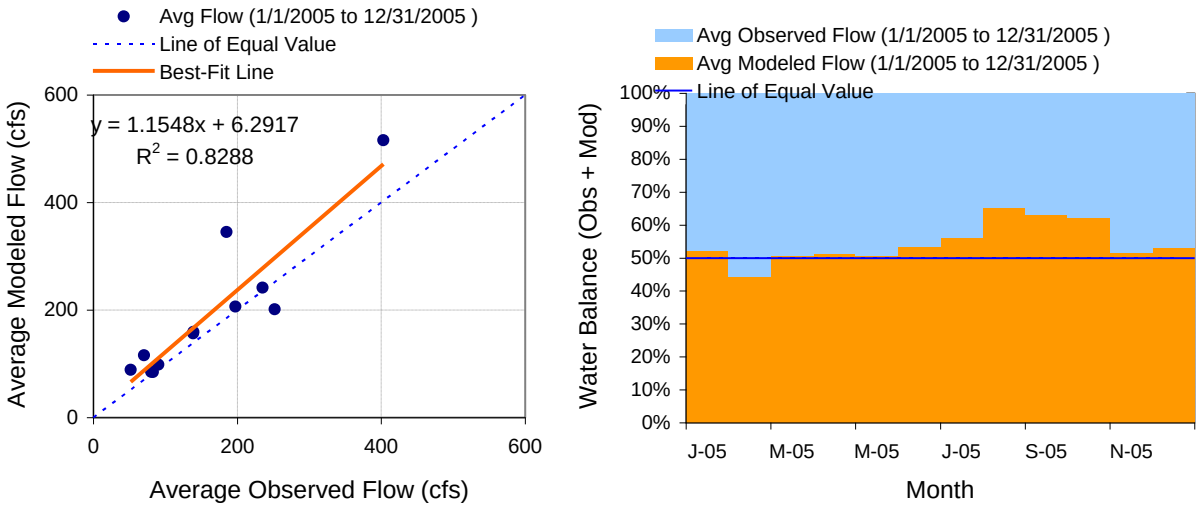

Figure D.2 Experimental scenario 0100; wet year (2005). Monthly flow regression and temporal variation: Model Outlet 7 vs. USGS 02335700 BIG CREEK NEAR ALPHARETTA, GA

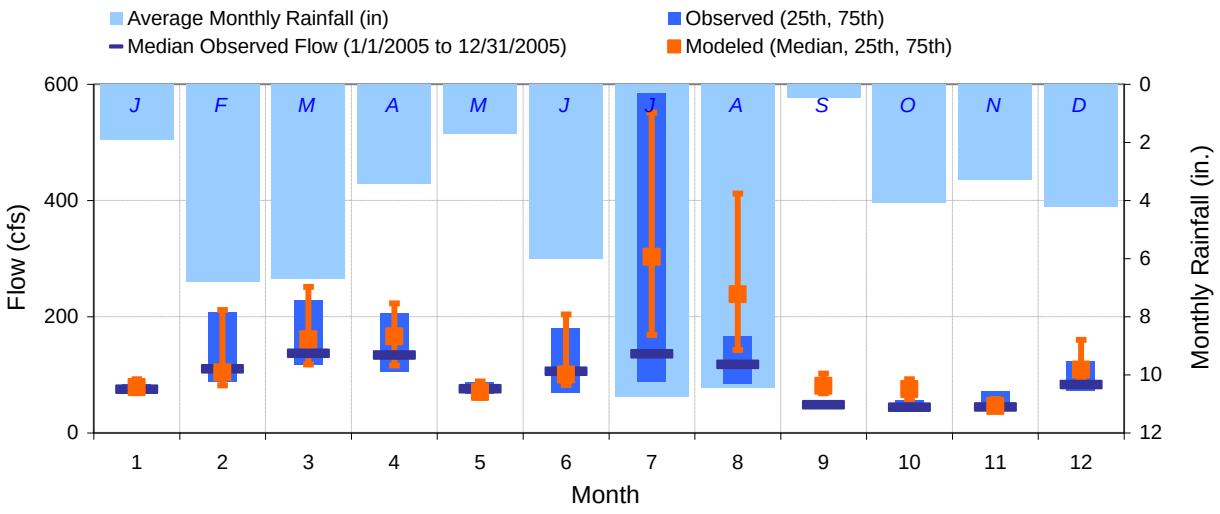

Figure D.3 Experimental scenario 0100; wet year (2005). Seasonal medians and ranges: Model Outlet 7 vs. USGS 02335700 BIG CREEK NEAR ALPHARETTA, GA

Table D.1 Experimental scenario 0100; wet year (2005). Seasonal summary: Model Outlet 7 vs. USGS 02335700 BIG CREEK NEAR ALPHARETTA, GA

MONTH	OBSERVED FLOW (CFS)				MODELED FLOW (CFS)			
	MEAN	MEDIAN	25TH	75TH	MEAN	MEDIAN	25TH	75TH
Jan	90.26	75.00	70.00	84.00	98.22	78.90	68.30	92.44
Feb	252.04	110.00	87.75	207.00	201.17	104.21	81.98	211.61
Mar	235.29	137.00	118.00	228.00	241.84	161.11	117.85	251.39
Apr	197.27	134.00	104.75	205.50	206.51	166.03	116.15	222.75
May	82.58	76.00	67.00	86.00	84.48	70.20	60.51	88.73
Jun	138.93	106.00	69.50	181.00	159.30	100.48	82.83	203.61
Jul	402.81	136.00	87.50	584.00	515.80	302.92	168.46	551.24
Aug	184.90	118.00	84.00	165.50	345.30	238.44	142.86	411.66
Sep	52.00	48.50	43.25	55.75	88.64	81.12	68.42	102.01
Oct	70.26	44.00	40.00	56.00	115.80	75.32	58.18	92.47
Nov	80.17	44.50	40.00	71.00	84.99	46.36	40.20	58.49
Dec	138.55	83.00	72.00	123.50	156.48	109.00	94.70	160.04

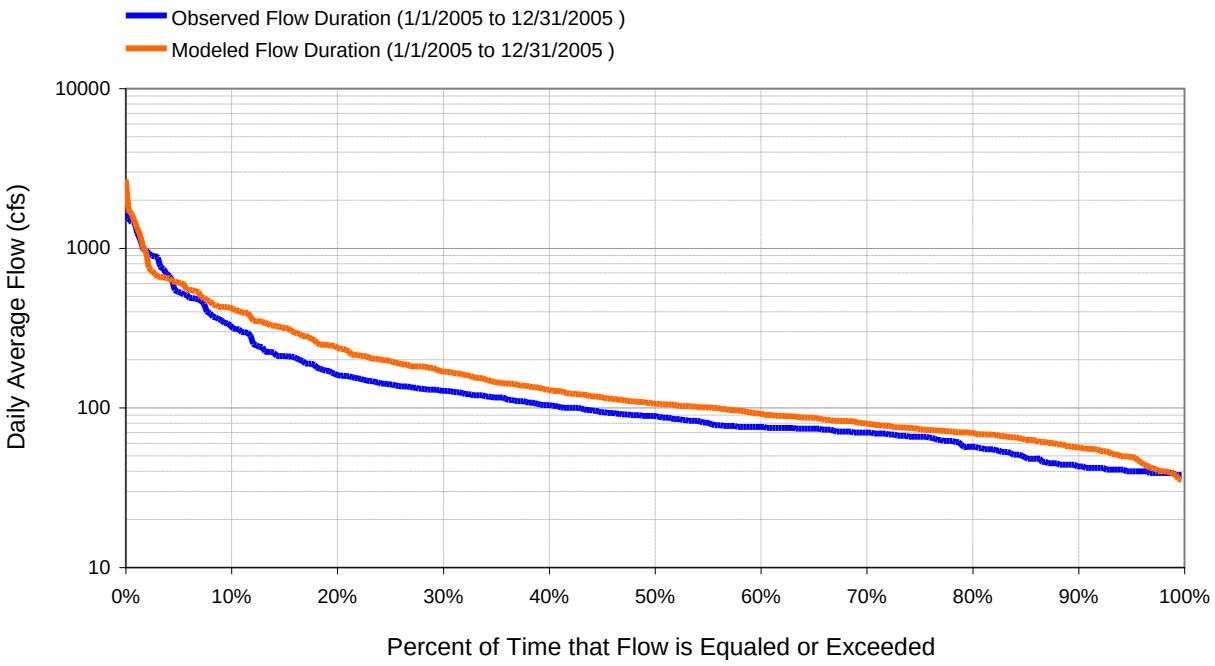

Figure D.4 Experimental scenario 0100; wet year (2005). Flow exceedence: Model Outlet 7 vs. USGS 02335700 BIG CREEK NEAR ALPHARETTA, GA

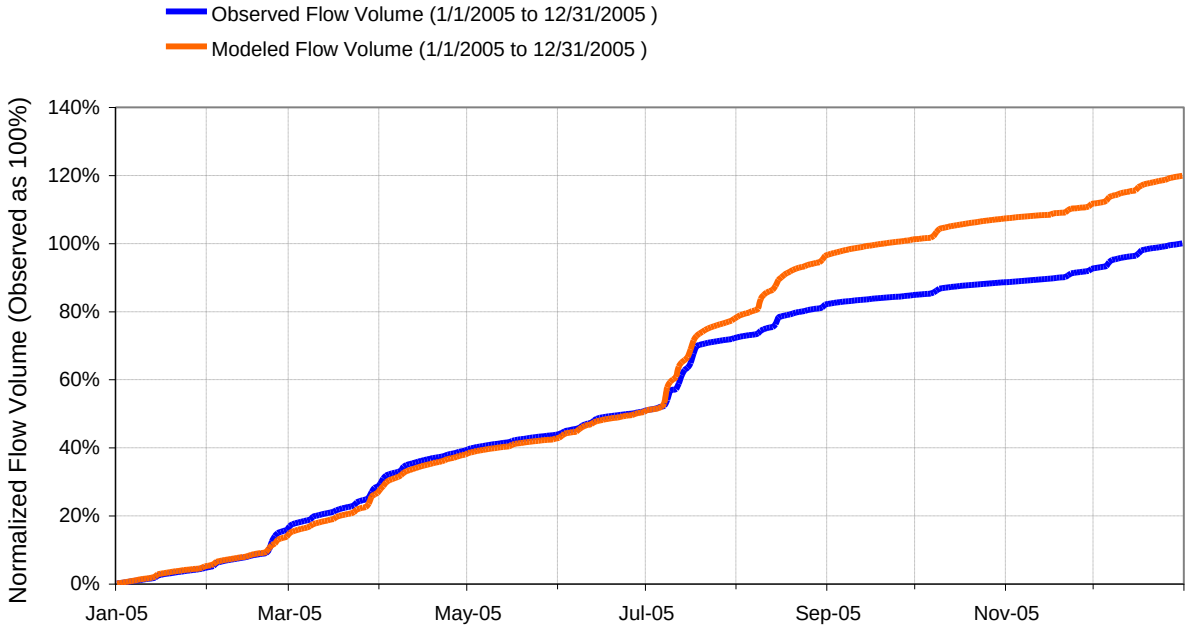

Figure D.5 Experimental scenario 0100; wet year (2005). Flow accumulation: Model Outlet 7 vs. USGS 02335700 BIG CREEK NEAR ALPHARETTA, GA

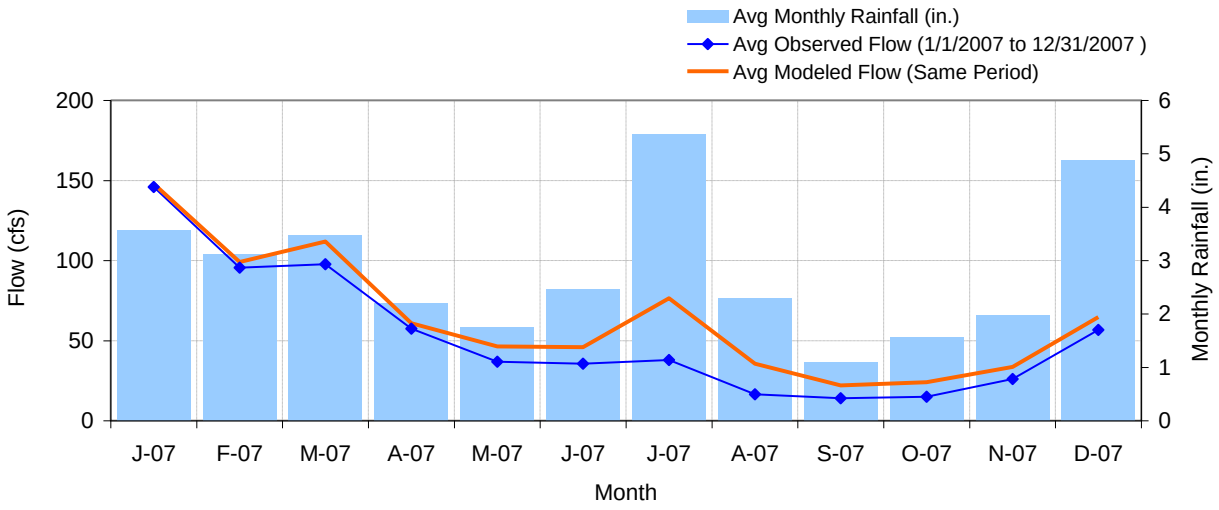

Figure D.6 Experimental scenario 0100; dry year (2007). Mean monthly flow: Model Outlet 7 vs. USGS 02335700 BIG CREEK NEAR ALPHARETTA, GA

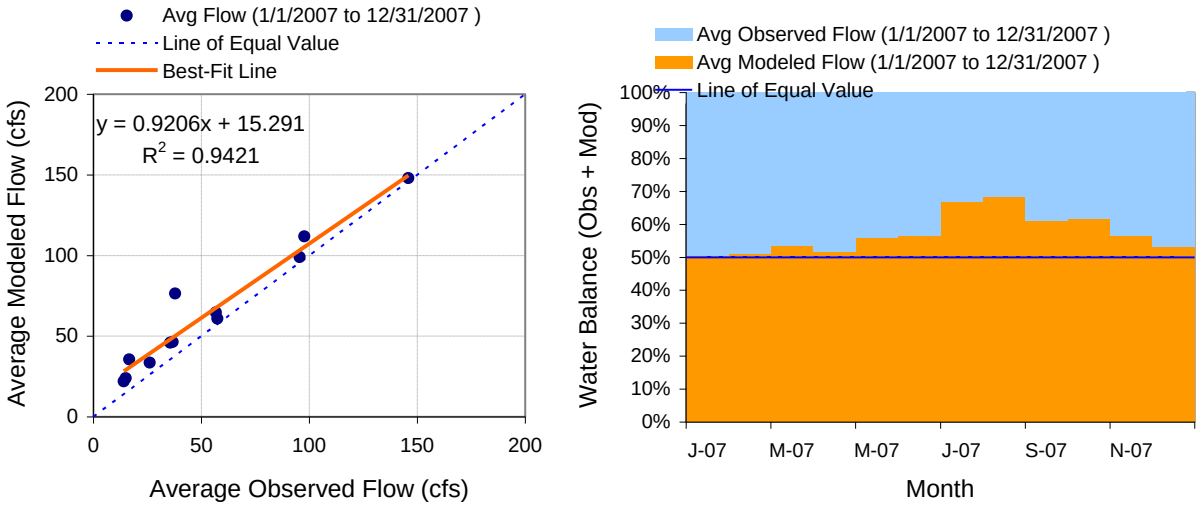

Figure D.7 Experimental scenario 0100; dry year (2007). Monthly flow regression and temporal variation: Model Outlet 7 vs. USGS 02335700 BIG CREEK NEAR ALPHARETTA, GA

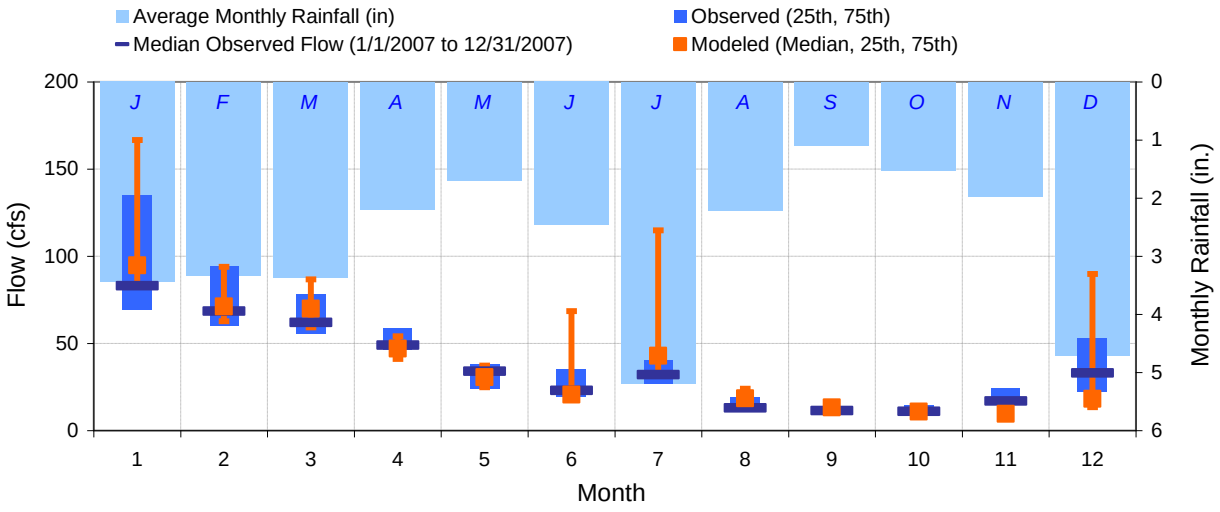

Figure D.8 Experimental scenario 0100; dry year (2007). Seasonal medians and ranges: Model Outlet 7 vs. USGS 02335700 BIG CREEK NEAR ALPHARETTA, GA

Table D.2 Experimental scenario 0100; dry year (2007). Seasonal summary: Model Outlet 7 vs. USGS 02335700 BIG CREEK NEAR ALPHARETTA, GA

MONTH	OBSERVED FLOW (CFS)				MODELED FLOW (CFS)			
	MEAN	MEDIAN	25TH	75TH	MEAN	MEDIAN	25TH	75TH
Jan	145.90	83.00	69.00	135.00	147.93	94.72	82.66	166.62
Feb	95.54	68.50	60.00	94.00	99.01	71.25	62.67	93.91
Mar	97.74	62.00	55.50	78.00	111.82	69.87	59.18	86.71
Apr	57.40	49.00	46.25	58.75	60.85	47.02	41.09	54.14
May	36.77	34.00	24.00	38.00	46.39	30.69	24.85	37.29
Jun	35.63	23.00	19.25	35.00	45.95	20.66	18.82	68.47
Jul	37.84	32.00	27.00	40.50	76.44	42.99	31.78	114.88
Aug	16.55	13.00	11.00	19.00	35.61	18.55	15.94	24.07
Sep	14.04	11.50	10.25	12.75	22.01	13.34	12.35	14.47
Oct	14.98	11.00	10.00	14.50	24.00	10.93	10.58	12.43
Nov	26.10	17.00	15.25	24.00	33.62	9.57	9.31	14.45
Dec	56.74	33.00	22.00	53.00	64.68	18.29	13.41	89.85

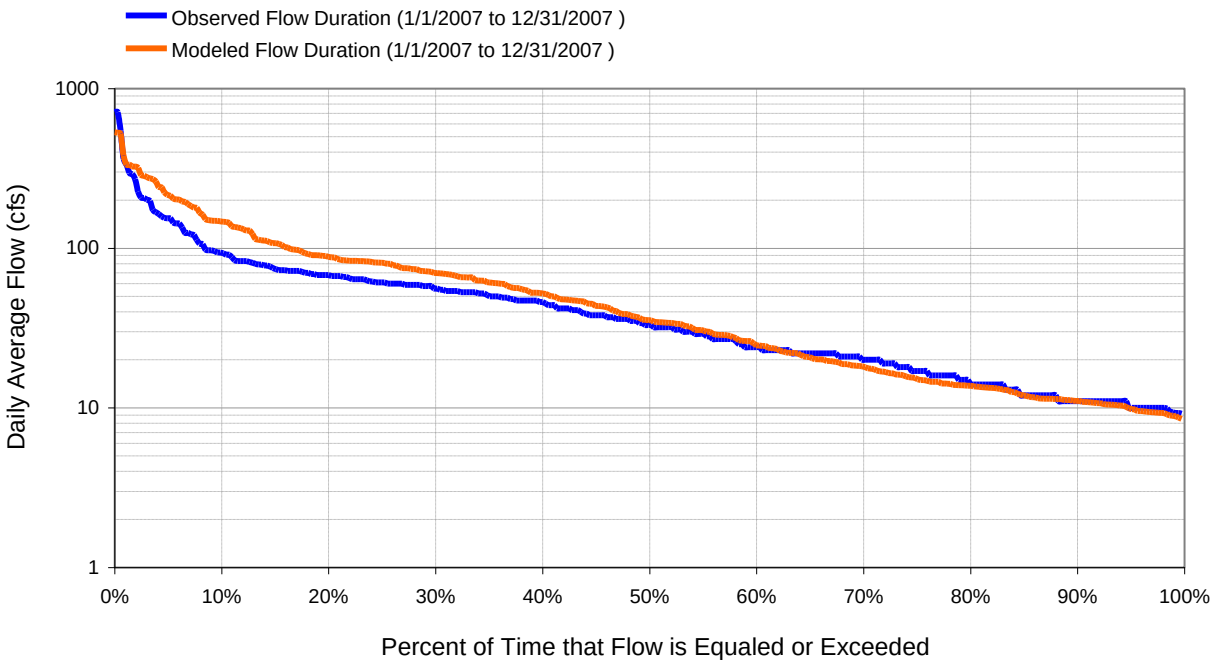

Figure D.9 Experimental scenario 0100; dry year (2007). Flow exceedence: Model Outlet 7 vs. USGS 02335700 BIG CREEK NEAR ALPHARETTA, GA

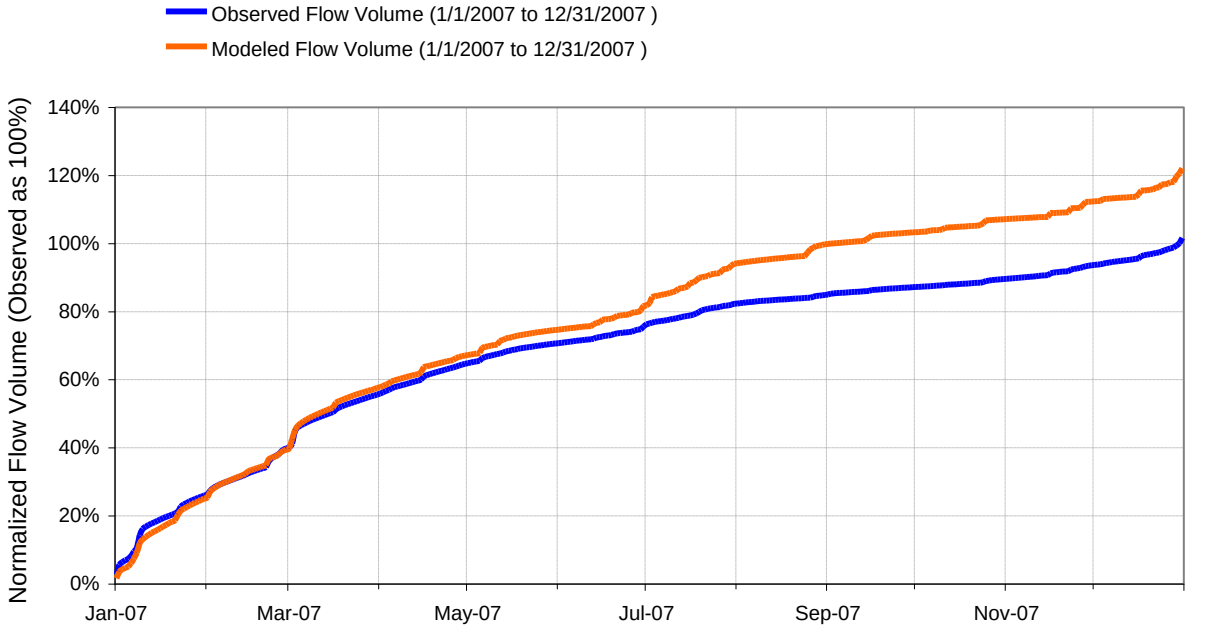

Figure D.10 Experimental scenario 0100; dry year (2007). Flow accumulation: Model Outlet 7 vs. USGS 02335700 BIG CREEK NEAR ALPHARETTA, GA

APPENDIX E

Experimental scenario 0001: STRM30m, digital -based FTABLEs, complete land use classification and Atlanta Airport 090451 meteorological station.

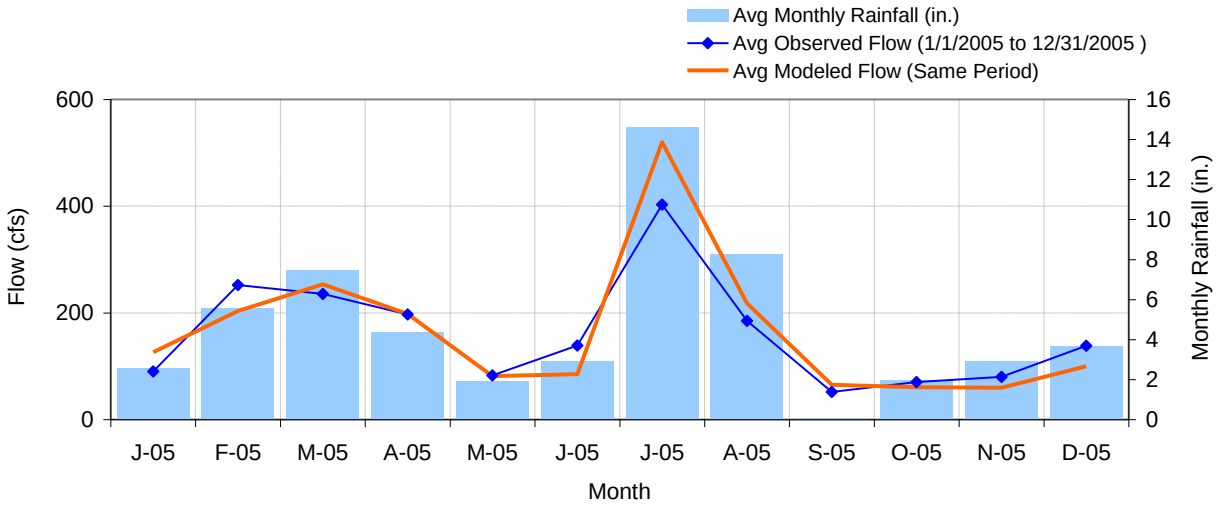

Figure E.1 Experimental scenario 0001; wet year (2005). Mean monthly flow: Model Outlet 7 vs. USGS 02335700 BIG CREEK NEAR ALPHARETTA, GA

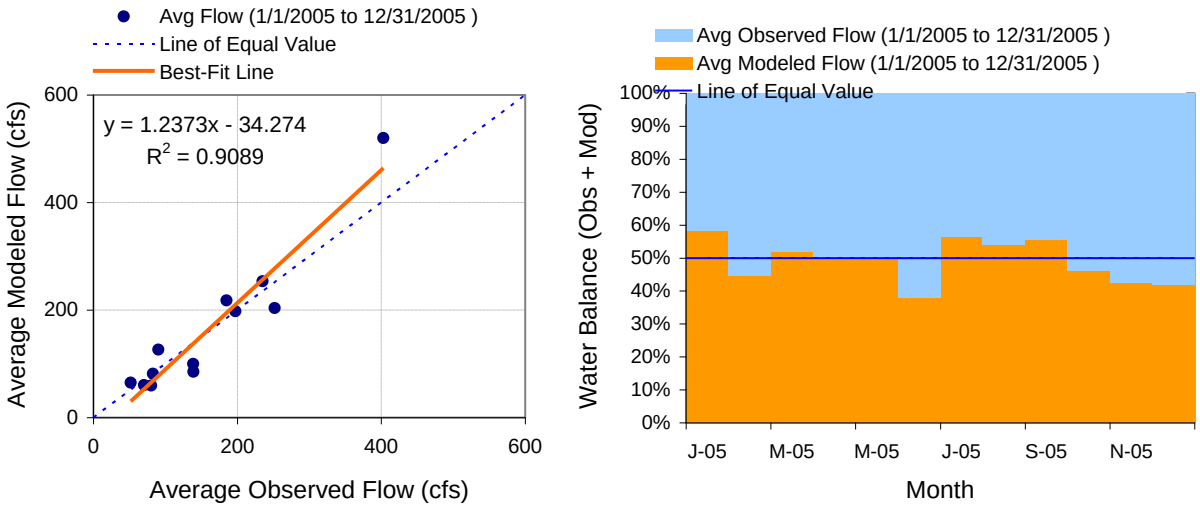

Figure E.2 Experimental scenario 0001; wet year (2005). Monthly flow regression and temporal variation: Model Outlet 7 vs. USGS 02335700 BIG CREEK NEAR ALPHARETTA, GA

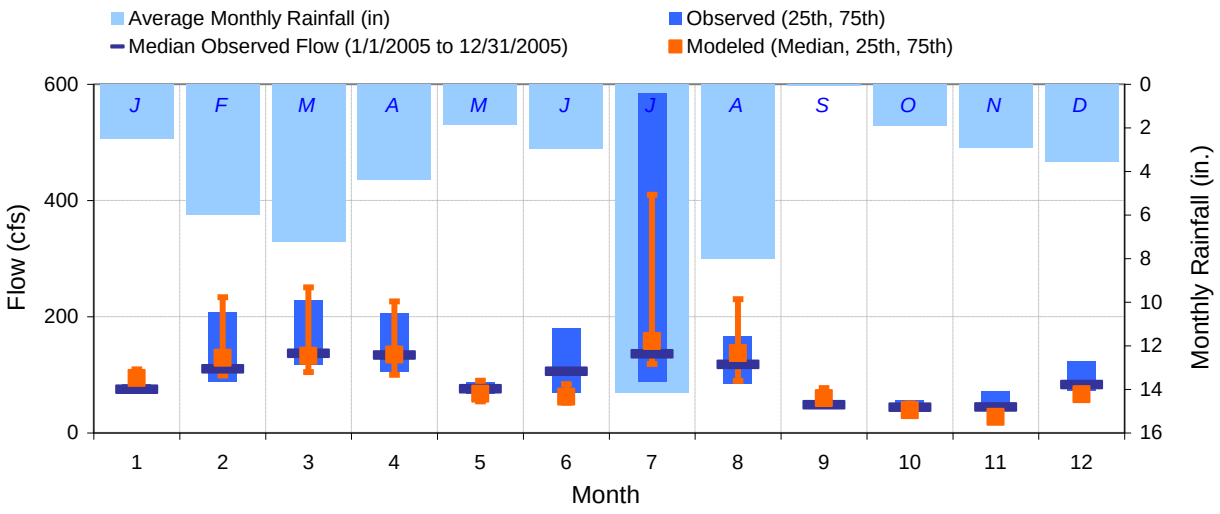

Figure E.3 Experimental scenario 0001; wet year (2005). Seasonal medians and ranges: Model Outlet 7 vs. USGS 02335700 BIG CREEK NEAR ALPHARETTA, GA

Table E.1 Experimental scenario 0001; wet year (2005). Seasonal summary: Model Outlet 7 vs. USGS 02335700 BIG CREEK NEAR ALPHARETTA, GA

MONTH	OBSERVED FLOW (CFS)				MODELED FLOW (CFS)			
	MEAN	MEDIAN	25TH	75TH	MEAN	MEDIAN	25TH	75TH
Jan	90.26	75.00	70.00	84.00	126.37	94.38	81.68	109.14
Feb	252.04	110.00	87.75	207.00	203.47	129.16	98.81	233.39
Mar	235.29	137.00	118.00	228.00	253.65	132.53	104.54	250.34
Apr	197.27	134.00	104.75	205.50	197.94	134.57	100.05	226.18
May	82.58	76.00	67.00	86.00	81.43	67.51	54.43	89.87
Jun	138.93	106.00	69.50	181.00	85.24	62.45	52.23	83.91
Jul	402.81	136.00	87.50	584.00	519.77	157.87	118.60	409.61
Aug	184.90	118.00	84.00	165.50	218.02	137.14	89.33	230.05
Sep	52.00	48.50	43.25	55.75	65.06	59.84	48.56	77.05
Oct	70.26	44.00	40.00	56.00	60.37	39.16	35.21	50.67
Nov	80.17	44.50	40.00	71.00	59.50	27.69	23.77	41.88
Dec	138.55	83.00	72.00	123.50	99.73	66.74	60.81	80.91

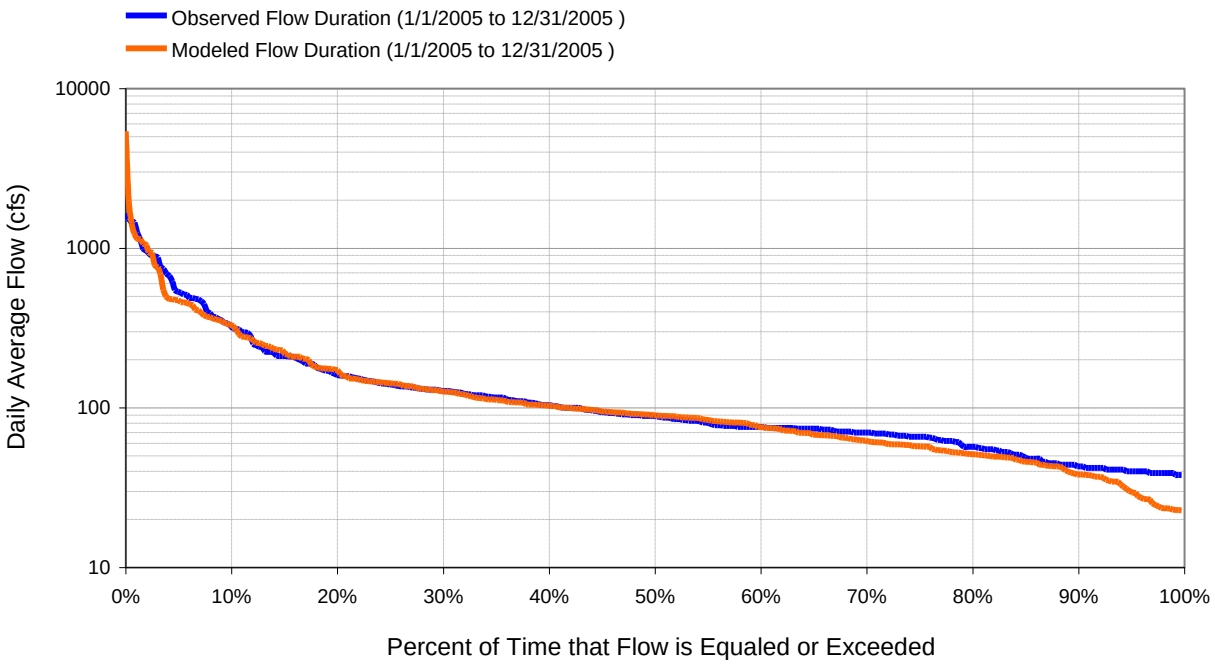

Figure E.4 Experimental scenario 0001; wet year (2005). Flow exceedence: Model Outlet 7 vs. USGS 02335700 BIG CREEK NEAR ALPHARETTA, GA

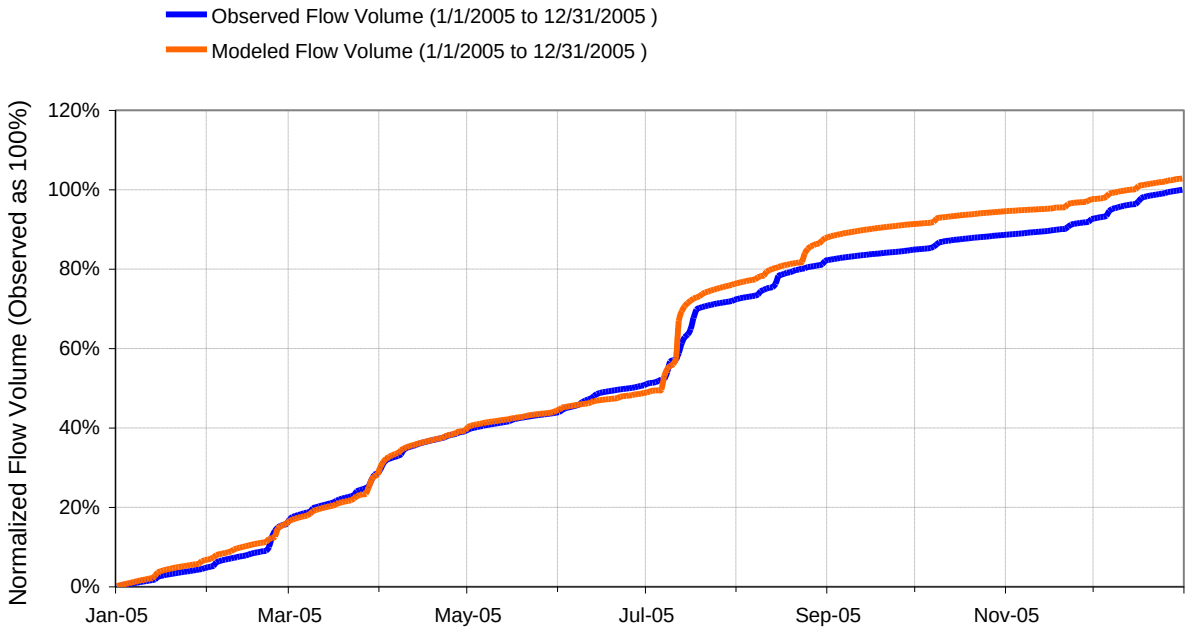

Figure E.5 Experimental scenario 0001; wet year (2005). Flow accumulation: Model Outlet 7 vs. USGS 02335700 BIG CREEK NEAR ALPHARETTA, GA

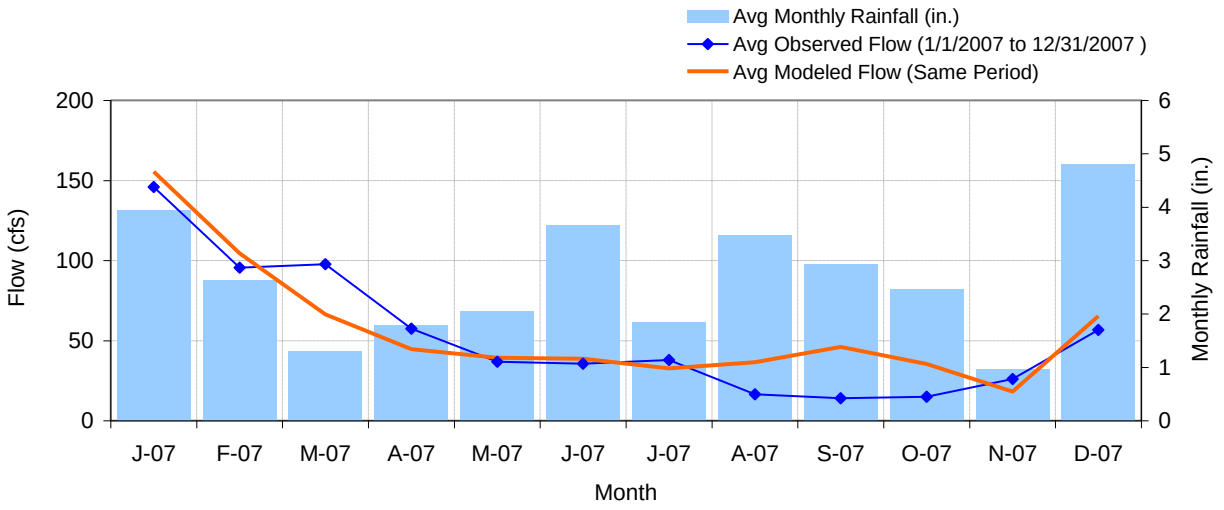

Figure E.6 Experimental scenario 0001; dry year (2007). Mean monthly flow: Model Outlet 7 vs. USGS 02335700 BIG CREEK NEAR ALPHARETTA, GA

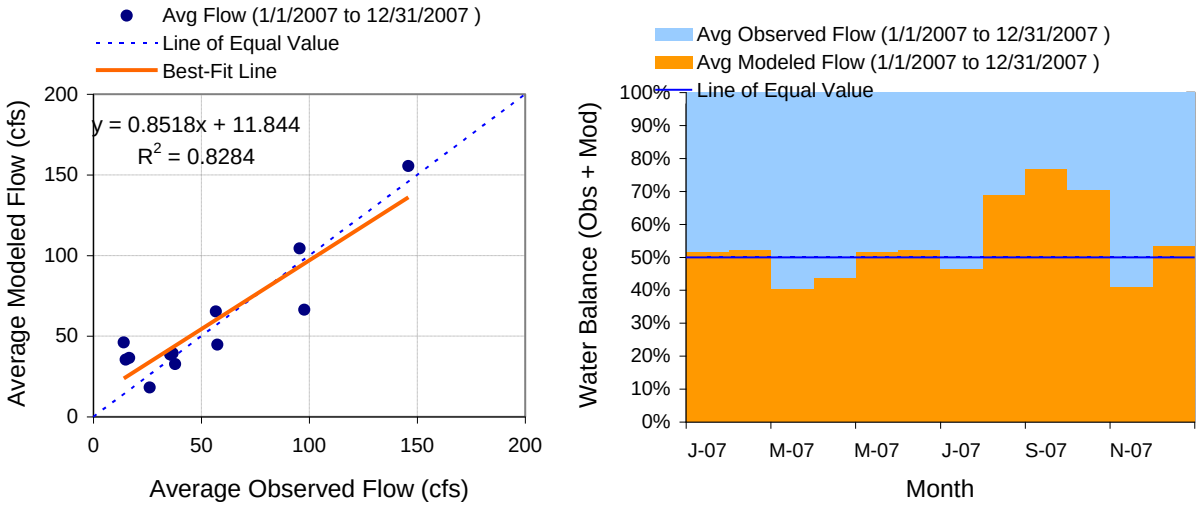

Figure E.7 Experimental scenario 0001; dry year (2007). Monthly flow regression and temporal variation: Model Outlet 7 vs. USGS 02335700 BIG CREEK NEAR ALPHARETTA, GA

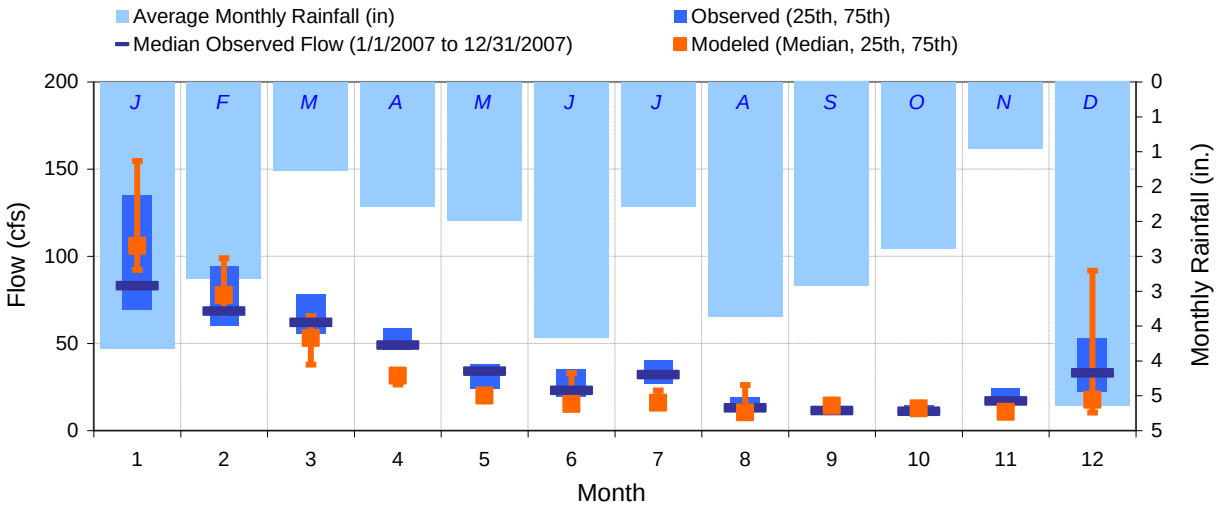

Figure E.8 Experimental scenario 0001; dry year (2007). Seasonal medians and ranges: Model Outlet 7 vs. USGS 02335700 BIG CREEK NEAR ALPHARETTA, GA

Table E.2 Experimental scenario 0001; dry year (2007). Seasonal summary: Model Outlet 7 vs. USGS 02335700 BIG CREEK NEAR ALPHARETTA, GA

MONTH	OBSERVED FLOW (CFS)				MODELED FLOW (CFS)			
	MEAN	MEDIAN	25TH	75TH	MEAN	MEDIAN	25TH	75TH
Jan	145.90	83.00	69.00	135.00	155.52	105.94	92.09	154.71
Feb	95.54	68.50	60.00	94.00	104.42	77.69	67.47	98.89
Mar	97.74	62.00	55.50	78.00	66.38	53.10	37.83	65.63
Apr	57.40	49.00	46.25	58.75	44.73	31.54	26.43	34.73
May	36.77	34.00	24.00	38.00	39.33	20.09	17.47	23.48
Jun	35.63	23.00	19.25	35.00	38.64	15.25	13.53	33.11
Jul	37.84	32.00	27.00	40.50	32.63	15.94	14.62	23.01
Aug	16.55	13.00	11.00	19.00	36.51	10.52	9.39	26.14
Sep	14.04	11.50	10.25	12.75	46.14	14.20	12.00	17.69
Oct	14.98	11.00	10.00	14.50	35.44	12.67	11.88	14.98
Nov	26.10	17.00	15.25	24.00	18.15	10.68	9.85	11.78
Dec	56.74	33.00	22.00	53.00	65.36	17.64	10.34	91.61

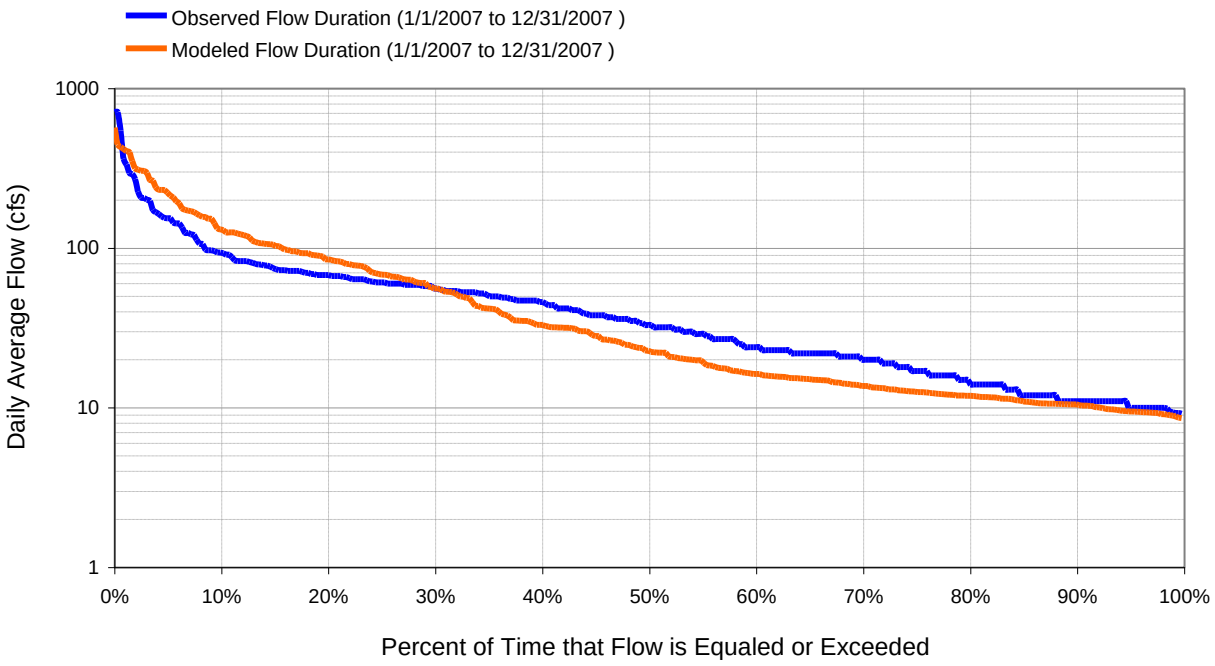

Figure E.9 Experimental scenario 0001; dry year (2007). Flow exceedence: Model Outlet 7 vs. USGS 02335700 BIG CREEK NEAR ALPHARETTA, GA

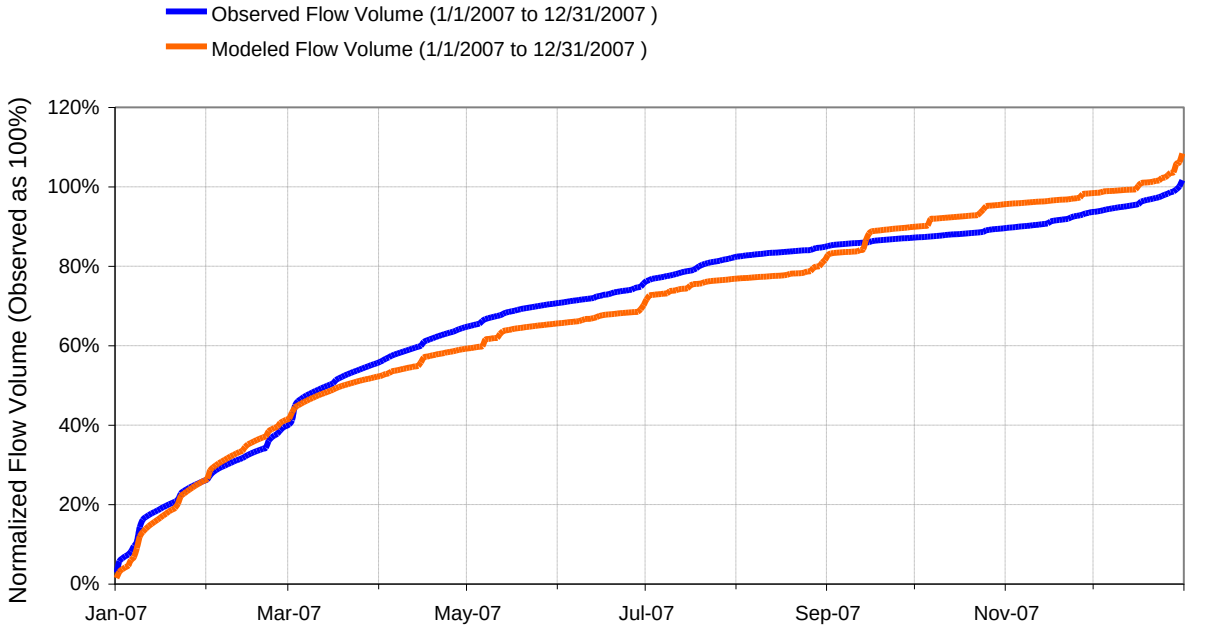

Figure E.10 Experimental scenario 0001; dry year (2007). Flow accumulation: Model Outlet 7 vs. USGS 02335700 BIG CREEK NEAR ALPHARETTA, GA